# THE COMPARATIVE PETROLOGY OF BLUESCHISTS AND GREENSCHISTS IN THE BROOKS RANGE AND KODIAK-SELDOVIA SCHIST BELTS

A

THESIS

Presented to the Faculty of the
University of Alaska in partial fulfillment
of the Requirements
for the Degree of

DOCTOR OF PHILOSOPHY

By

John R. Carden, B.S., M.S.

Fairbanks, Alaska

May 1978

THE COMPARATIVE PETROLOGY OF BLUESCHISTS

AND GREENSCHISTS IN THE BROOKS RANGE

AND KODIAK-SELDOVIA SCHIST BELTS

RECOMMENDED:

Chairman, Advisory Committee

APPROVED:

Dean of the College of Environmental Sciences

March 17, 1978
Date

Vice Chancellor for Research and Advanced Study

March 20, 1978
Date

ABSTRACT

Although several authors have noted the close relationship of intercalated blueschists and greenschists, there has been no detailed study of their space-time association.

A comparative study of the petrology and geochronology of the blueschist-greenschist facies rocks of the Seldovia-Kodiak Islands and Brooks Range metamorphic terranes shows blueschists within each terrane recrystallized under different pressure-temperature conditions and in dissimilar tectonic environments.

The Seldovia-Kodiak Islands schist belt formed along a subduction zone approximately 190 m.y. ago. Intercalated blueschist-greenschist layers in the Seldovia-Port Graham area are coeval and recrystallized at a temperature between about 350° and 470° C. Pressures that accompanied this recrystallization event were between 5.5 and 7 kb. The protolith for the blueschist-greenschist sequence was a distal tuff which had undergone spilitic degradation. Compositional layers with higher $Na_2O$ and $SiO_2$ and low CaO and $Al_2O_3$ concentrations produced epidote-crossite schist and those with low $Na_2O$-$SiO_2$ and high CaO-$Al_2O_3$ concentrations formed chlorite-albite schist upon metamorphism at the boundary between blueschist and greenschist facies P-T conditions.

Glaucophane bearing metabasites of the Brooks Range metamorphic belt recrystallized in the Late Precambrian. Although petrographic evidence indicates the possible attainment of eclogite facies P-T conditions in some segments of the belt, initial blueschist facies recrystallization took place at a temperature between 200-325° C and a minimum pressure of about 8 kb. A greenschist facies dynamo-thermal event occurred in mid-Cretaceous time which isochemically retrograded many blueschist metabasites to greenschist facies assemblages and produced polymetamorphic fabrics. The chemistry and relict mineral fabrics of the Brooks Range blueschist metabasites indicates an intrusive continental tholeiitic protolith. The Brooks Range blueschist facies event is not compatible with a classic subduction model.

ACKNOWLEDGEMENTS

I would like to acknowledge with sincere gratitude and indebtedness the continual guidance and support of Dr. Robert B. Forbes who suggested this project and for his many enthusiastic suggestions and discussions in all aspects of this study both in the field and in the laboratory.

My thanks to Dr. Richard Allison, Dr. Wyatt Gilbert, Dr. Daniel Hawkins and Dr. Donald Turner for the generous way in which they offered their time for valuable discussions, helpful comments and constructive suggestions.

I would also like to thank Dr. William Connelly, John Decker, Dr. J. Casey Moore and Dr. George Plafker for stimulating discussions on the tectonics of the southern Alaska margin.

Douglas J. Lalla and J. Mark Zdepski gave many helpful suggestions and support for the computer oriented aspects of this research. Also, my special thanks to Diane Duvall for technical assistance with mineral separations and K-Ar determinations.

It is my pleasure to acknowledge Roman J. Motyka and my wife Barbara Carden, who served as able field assistants and boat hands in Seldovia Bay and Port Graham. I am also indebted to the U.S. Geological Survey and the Alaska Division of Geological and Geophysical Surveys for their

logistics and analytical support of the Brooks Range phase of the work. I would also like to thank Leon Francisco and Cora Darling for the hospitality and courtesy they extended to me during the work on Kodiak Island.

Special appreciation is due my wife Barbara, who assisted in the proof reading, and the typing of the various drafts of this dissertation, and to Sandi Moseley who typed the final copy.

This research was supported primarily by the National Science Foundation (Grant GA-43004). I would also like to acknowledge a Penrose Bequest Grant from the Geological Society of America, and a grant-in-aid of research from the Society of Sigma-XI.

TABLE OF CONTENTS

## LIST OF FIGURES

LIST OF TABLES

# INTRODUCTION

## GLAUCOPHANE SCHISTS AND THE BLUESCHIST FACIES CONCEPT

Escola (1929) first proposed the establishment of the "glaucophane schist facies" of metamorphism which is characterized by crystallization under conditions of high pressure and low to intermediate temperatures. For many years, the validity of Escola's glaucophane schist facies was debated by many petrologists who claimed that this type of metamorphism was anomalous and unimportant.

During the last fifty years, two fundamentally contrasting concepts concerning the genesis of glaucophane schists have been expressed in the literature. One view is that the formation of these schists is linked to special conditions of high soda content, either inherent in the rock (Harker, 1932) or metasomatically introduced during the emplacement and serpentization of alpine peridotites (Taliferro, 1943; Crittenden, 1951; Brothers, 1954; Essene and others, 1965; Gresens, 1969).

The second view is that glaucophane schists result from special physical conditions imposed during metamorphism. Although a rock deficient in sodium will not form glaucophane, several workers (Washington, 1901; Smith, 1906; Ernst, 1963a; Coleman and Lee, 1963; Ghent, 1965) have found that some glaucophane schists are chemically identical to greenschists and amphibolites. In such cases, the sodium

which would enter glaucophane is contained in the plagioclase (Miyashiro and Banno, 1958). Several authors, including Ernst (1971b), doubt that there is any genetic link between the serpentinization of ultramafic masses and the genesis of glaucophane schists. The association of these two lithologies is considered fortuitous because both are associated with active continental margins. It is generally believed that high grade blueschists are brought up along faults which are commonly serpentinized (Coleman, 1971).

By comparing naturally occurring mineral assemblages from glaucophane schist terranes (i.e. aragonite, glaucophane-crossite, jadeite, and lawsonite bearing assemblages) with experimentally determined phase equilibria (Fig. 1) and oxygen isotope ratios of coexisting minerals in blueschist assemblages (Taylor and Coleman, 1968), it is evident that rocks of the blueschist facies have formed under unique conditions of relatively high pressure (5-8 or more kb) and low temperatures (150-300 degrees centigrade). Furthermore, the existence of prograde metamorphic sequences along continental margins (zeolitized rocks → prehnite-pumpellyite bearing rocks → glaucophane schists → greenschists → epidote-amphibolites) presents compelling evidence that these terranes can be regional in scope and are not always the product of local metamorphic events (Ernst, 1971a; Miyashiro, 1967).

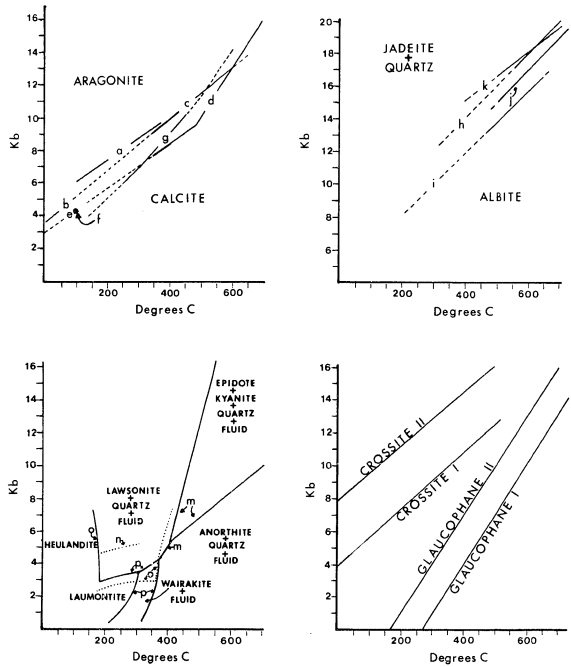


Figure 1. Experimentally determined phase equilibria diagrams of minerals common to the blueschist facies; solid where experimentally confirmed and dashed where extrapolated. a) Zimmerman, 1971; b) Jamieson, 1953; c) Clark, 1957; d) Boettcher and Wyllie, 1967a; e) Crawford and Hoersh, 1972; f) Crawford and Fyfe, 1964; g) Johannes and Puhan, 1971; h) Birch and LeComte, 1960; i) Newton and Smith, 1967; j) Boettcher and Wyllie, 1968b; k) Newton and Kennedy, 1968; m) Newton and Kennedy, 1963; n) Crawford and Fyfe, 1965; o) Nitsch, 1968; p) Liou, 1971; crossite and glaucophane stability curves after Ernst, 1963b.

In the framework of plate tectonics (Isacks and others, 1968; Le Pichon, 1968; Morgan, 1968; Dewey and Bird, 1970), the foregoing P-T conditions are usually generated when an oceanic plate is consumed in a subduction zone. If the plate is subducted rapidly, a severe downbowing of the isotherms will occur within the downgoing slab and adjacent sedimentary prism, as calculated by Hasabe and others (1970), Tokoz and others (1971), and Oxburgh and Turcotte (1971). The increase in lithostatic pressure in such an environment is relatively rapid while temperature equilibration depends on the slower process of conductive heating. Therefore, a relatively high lithostatic pressure is generated in the subducted materials while low temperatures are maintained within the descending slab; these conditions are conducive to the formation of blueschist facies assemblages. Similar conditions could also be developed in a rapidly subsiding rift or fault bounded basin.

Accelerated tectonic emergence is equally important to rapid tectonic burial if the high pressure-low temperature mineral assemblage crystallized at depth is to be preserved at the surface (Ernst, 1971a). If the blueschist assemblage remains in the same tectonic position following the cessation of lithospheric underflow, the isotherms will gradually re-establish a normal geothermal gradient (i.e. higher temperatures), erasing the characteristic blueschist mineral

assemblages and upgrading the former blueschist to greenschist or epidote amphibolite facies.

## TECTONIC IMPLICATIONS

The global geometry of blueschist belts indicates that they are generally circum-oceanic and the oceanward side of high temperature-low pressure metamorphic + igneous complexes (Miyashiro, 1961, 1972, 1973; Takeuchi and Uyeda, 1965). The belts are narrow, somewhat arcuate and commonly associated with ophiolites and melange complexes (Coleman, 1971). Thus blueschist belts, including those that are now intracontinental, may represent former subduction zones (Dewey and Bird, 1970; Ernst, 1972b; Hamilton, 1970; Forbes and others, 1971) and may be used as tectonic markers for unraveling the geometry of ancient plate boundaries.

Until a few years ago, world-wide blueschist belts were considered to be chiefly of Mesozoic or younger age (Ernst, 1972). Recent work indicates that blueschist belts range in age from Cenozoic to Precambrian (Ernst, 1972b) and the younger belts lie closer to modern oceanic basins.

The systematic progression of older to younger blueschist belts toward the margin of the circum-Pacific continental plates suggests that the blueschist-making mechanism is a recurrent tectonic process and that blueschist

terranes have been progressively accreted to, and/or imbricated onto the leading edges of continental plates during successive subduction or plate collision events (Ernst, 1973a).

## THE GLAUCOPHANE SCHIST PROBLEM

Currently, there is little argument concerning the validity of a glaucophane schist facies concept for mineral assemblages which contain aragonite, lawsonite, and/or jadeite. There is, however, widespread disagreement about the facies assignment and physico-chemical significance of sodic amphibole-bearing assemblages which do not contain one or more of those three phases. Naming the facies after the sodic amphibole glaucophane was an unfortunate choice because Ernst (1961) found that glaucophane is stable over a wide range of physical conditions, certainly into the greenschist facies; and under suitable chemical conditions, a high temperature polymorph (glaucophane I) is stable at magmatic temperatures. For this reason, there is some confusion on how the facies should be defined in the absence of aragonite, jadeite, and lawsonite, as is the case in the Shuksan belt of north-central Washington (Misch, 1966); the southwestern Washington blueschist terrane (Hawkins, 1967; Vance, 1968); the Seldovia terrane, Alaska (Forbes and Lanphere, 1973); the Seward Peninsula (Sainsbury and others,

1971); Kamchatka, USSR (Dobretsov, 1975); central Kyushu, Japan (Hayase and Ishizaka, 1967); northwestern Honshu, Japan (Banno, 1958); Taiwan (Yen, 1966; Liou and others, 1975); several localities in Turkey (Kaaden, 1966); southeastern Spain (de Roever and Nijhuis, 1963); Scotland (Bloxam, 1958); and Spitsbergen (Horsfield, 1972). Therefore, it became necessary to sub-divide the facies on the basis of minerals which are stable in portions of the facies.

Winkler (1967) proposed the series (1) lawsonite-albite facies, (2) lawsonite-glaucophane-jadeite facies (formerly glaucophane schist facies), and (3) glaucophanitic greenschist facies. The entrance of the glaucophanitic greenschist facies is signalled by the disappearance of aragonite and lawsonite, although sodic pyroxene and sodic amphibole remain stable. Winkler believes that this transition takes place at temperatures between 400-450 degrees centigrade, even though pressures may remain at (5-10 kb).

Taylor and Coleman (1968) attacked this same problem in a quantitative fashion by examining the $O^{18}/O^{16}$ ratios of coexisting mineral phases in various blueschist assemblages. They recognized (1) a low temperature group corresponding to the type II and type III blueschists from Cazadero, California (Coleman and Lee, 1963) which they named the lawsonite-aragonite blueschist facies and (2) a higher temperature

group corresponding to the type IV blueschists of Cazadero which they named the epidote-rutile blueschist facies. The low temperature group is characterized by the presence of lawsonite (rather than epidote), jadeite + quartz (rather than albite), aragonite (rather than calcite), sphene (rather than rutile), and blue amphibole. Temperature conditions in this realm of the blueschist facies range between 200 and 300 degrees centigrade, along with pressures of 6 to 7 kb. The higher temperature group is characterized by epidote-zoisite, calcite, rutile, garnet, and glaucophane. Crystallization temperatures range between 400 and 550 degrees centigrade and pressures are in excess of 7 kb. The total absence of biotite in the high temperature blueschist facies is an aid to separating it from the greenschist facies with which it may be closely associated (Taylor and Coleman, 1968).

Rocks of the high temperature blueschist facies are commonly intercalated with rocks containing greenschist facies mineral assemblages (chlorite, epidote, albite, $\pm$ actinolite); for example, in northwestern Washington (Misch, 1966); Shikoku, Japan (Ernst and others, 1967); Seldovia, Alaska (Forbes and Lanphere, 1973); Seward Peninsula, Alaska (Sainsbury and others, 1970); and in the Baird Mountains, Alaska (Forbes and others, 1974).

As previously mentioned, Ernst (1971a) has shown that a progressive increase in metamorphic grade across many high

pressure-low temperature belts results in a transitional zone between metamorphic facies. Iwasaki (1963) expressed the belief that such transitional P-T conditions between blueschist and greenschist facies explain the occurrence of intercalated blueschist facies and greenschist facies rocks. Other workers have suggested that intercalated blueschists and greenschists result from differences in the accessibility to water during metamorphism (Ernst, 1973b).

Although several authors have noted the close relationship of high temperature blueschist facies (i.e. the epidote-rutile blueschist facies of Taylor and Coleman, 1968) and greenschist facies assemblages, there has been no detailed geochemical, petrologic, and geochronologic study of their space-time association. Clearly, a study of the physicochemical conditions governing the formation of intercalated blueschist and greenschist assemblages should further understanding of the blueschist facies and is critical to the establishment of the boundary conditions which separate the two facies. Furthermore, a detailed study of blueschist facies rocks in Alaska will facilitate the tectonic understanding of the paleo-continental margins and tectonics of the state.

## OBJECTIVES OF THE STUDY

Alaska has several blueschist terranes (Fig. 2) offering a unique opportunity to study blueschist facies assemblages in belts of differing tectonic styles and settings.

The objectives of this study are to:

(1) ascertain the areal relationships and tectonic significance of the two Alaska blueschist-greenschist terranes.

(2) determine the radiogenic age constraints of the blueschist versus greenschist assemblages in order to establish whether the assemblages are coeval in time as well as in space.

(3) describe the metamorphic assemblages, phase compositions, and mineral paragenesis of the two terranes.

(4) and define the comparative physico-chemical condidions and constraints of metamorphism of the two terranes through interpretation of the coexisting mineral assemblages and oxygen isotope data.

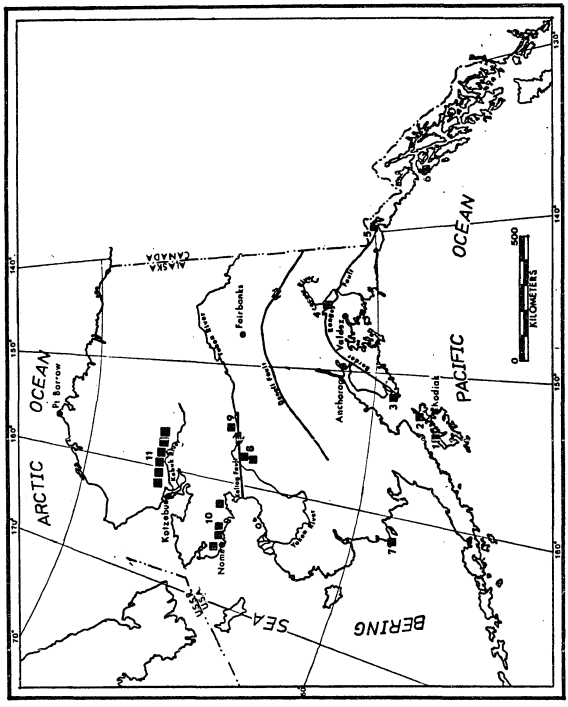


Figure 2. Blueschist localities of Alaska; Study areas are localities 1, 3, and 11. Numbered localities are described in the text.

## DISTRIBUTION OF BLUESCHIST FACIES IN SOUTHERN ALASKA

The existence of metamorphic rocks on the southwest Kenai Peninsula has been known since the early 1900's when Martin and others (1915) described the crystalline schists of Seldovia Bay and Port Graham in their reconnaissance mapping of the geology of the Kenai Peninsula. In his description of the petrology, Martin makes brief mention of a glaucophane-epidote schist that he collected near Seldovia Point. At that time, however, nothing was known of the tectonic implications of glaucophane schists.

Based on this reference, Forbes and Lanphere (1973) confirmed the presence of blueschist facies metamorphic rocks occurring with what they consider to be a dismembered ophiolite sequence cropping out in and near the fishing village of Seldovia (Fig. 2, Loc. 3). This study shows that this occurrence is part of a belt of blueschist facies metamorphic rocks extending at least 16 km southwestward toward Port Graham (Fig. 3).

Martin (1912), Maddren (1917), and Capps (1937) described rocks similar to those occurring at Seldovia (without reference to glaucophane) on the northwest shore of Kodiak Island between the old village site of Uyak and Seven Mile Beach, near the mouth of Uyak Bay (Fig. 3). Forbes and Lanphere (1973) predicted that the southwest extension of the Seldovia blueschist terrane would be found on the north-

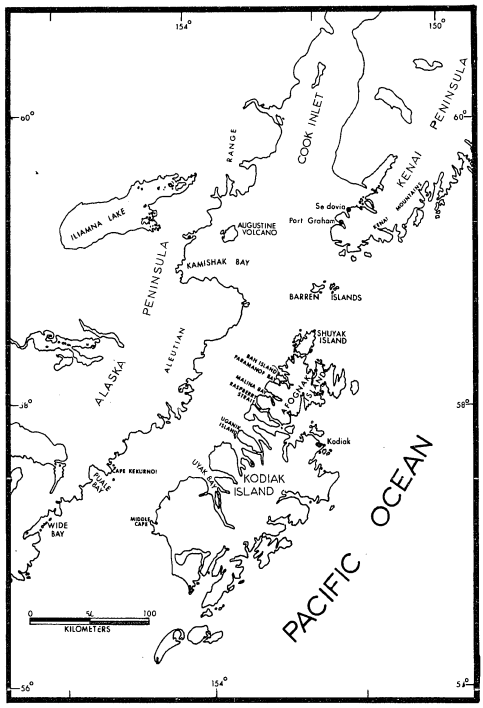


Figure 3. Location map of the Kenai Peninsula, Kodiak Islands, and Alaska Peninsula showing localities mentioned in this study.

west coast of Kodiak Island. During a short reconnaissance visit in the summer of 1975, Carden discovered rocks of the blueschist facies near Seven Mile Beach (Carden and Forbes, 1976). Later that summer, Wm. Connelly and M. Hill, from the University of California at Santa Cruz, discovered blueschists in their mapped extension of the Uyak Complex in Malina and Paramanof Bays, in Raspberry Strait on Afognak Island, and on Ban Island (Fig. 3). Carden and others (1977b) believe that the blueschist facies metamorphic rocks from Kodiak and Afognak Islands are correlative with those in the Seldovia terrane based on similar lithologies, associated rock types, structural style, and radiometric age relationships, thus delineating a belt at least 260 km long.

Forbes and others (1976, 1977) and Carden and others (1977) list other blueschist terranes which appear to be on trend with the Kodiak-Seldovia blueschist belt including: (1) blue amphibole-bearing metabasite amd metasediments from the central portion of the Valdez C-2 quadrangle near Chitna (Metz, 1975, 1976) (Fig. 2, Loc. 4), (2) blueschist float recovered from the vicinity of the Hubbard Glacier east of Yakatat by G. Plafker (1975, personal communication) (Fig. 2, Loc. 5), and (3) crossite and glaucophane assemblages described by Reed and Coats (1941) and by Carden and Connelly (1976, unpublished field notes) on Chichagof Island (Fig. 2, Loc. 6) in the metabasites of the Kelp Bay group (see Loney and others, 1975).

## DISTRIBUTION OF BLUESCHISTS IN NORTHERN AND SOUTHWESTERN ALASKA

The earliest known references to glaucophane-bearing rocks in northern Alaska are from the works of Mendenhall (1901), Smith (1910), and Moffit (1913) in the Solomon District of the Seward Peninsula (Fig. 2, Loc. 10). Sainsbury and others (1970) studied the glaucophane schists of that area in greater detail and concluded that they belong to the high temperature subdivision of the blueschist facies. Based on stratigraphic relationships, the rocks may be as old as Precambrian.

Rocks of the blueschist facies of the Kaiyuh Hills (Fig. 2, Loc. 8) have been described by Forbes and others (1971) based on the work of Mertie (1936) and the discovery of chloritoid-sodic amphibole assemblages collected by W. Patton and R. Tagg of the United States Geological Survey (Forbes and others, 1974). This terrane is also found in the Kokrine Hills north of the Yukon River, where it is believed to be offset from the Kaiyuh Hills by the Kaltag fault (Fig. 2, Loc. 9). Blueschist facies rocks also occur with an ophiolite sequence near Cape Peirce (Fig. 2, Loc. 7) (J. Hoare, personal communication).

The possible existence of rocks of the blueschist facies on the south flank of the Brooks Range in the Ambler River quadrangle was first indicated by float, collected

by T. Hamilton of the University of Alaska, in terrace gravels of the Ambler River valley. Subsequent identification of blueschist assemblages in the U. S. G. S. collections of I. Tailleur and W. Patton by R. Forbes (Forbes and others, 1971), suggested that the cobbles collected by Hamilton had a nearby source in the Baird Mountains crystalline schist terrane. Further field work by W. Brosge, G. Pessel, I. Tailleur, R. Forbes, and J. Carden indicates that the metamorphic belt containing the blueschist assemblages is discontinuously exposed from the Chandalar District to the hills north of Kiana near Kotzebue Sound, a distance of about 550 km (Fig. 2, Loc. 11).

## STUDY AREA

The main areas chosen for this study are those containing intercalated blueschists and greenschists in (1) the northern part of the Seldovia B-5 quadrangle between Seldovia Bay and Port Graham and (2) the southeastern one-quarter of the Ambler River quadrangle in the vicinity of Ruby Ridge.

The Seldovia area was chosen for its accessibility and because preliminary work had been done there by Forbes and Lanphere (1973). In addition to the Seldovia occurrences, several localities were also studied on Kodiak Island near the vicinity of Uyak Bay (Fig. 3).

The schists of the southeastern Ambler River quadrangle were studied as a cooperative effort with the U.S. Geological Survey and the Alaska Division of Geological and Geophysical Surveys to obtain petrologic, structural, and geochronologic data for the south flank of the Brooks Range between the Survey Pass quadrangle and Kotzebue Sound. The program included helicopter and logistic support for the Ambler River study as well as similar support for study areas in the western Brooks Range above Kiana and in the Cosmos Hills.

## GEOLOGIC SETTING

### KODIAK ISLAND

#### Regional Geology

The Kodiak Islands are located near the mouth of Cook Inlet about 250 km southwest of the Kenai Peninsula. The rocks exposed on the Islands are typical of those seen elsewhere on the southern Alaska margin.

The Islands are bordered on the south by the Shumagin-Kodiak shelf edge and adjacent Aleutian Trench. To the north and northwest lie the Cenozoic volcanic rocks and Cenozoic-Mesozoic plutons of the Alaska Peninsula (Detterman and Hartsock, 1966; Reed and Lanphere, 1973). The rocks exposed on Kodiak, the largest island in the group, are characterized by a series of progressively accreted marine rocks which generally become younger and less metamorphosed southeastward toward the present continental edge (Plafker, 1972; Moore, 1974).

The Kodiak Islands schist represents the oldest and most highly metamorphosed of these accretionary belts and is discontinuously exposed along the northwest side of the Island (Capps, 1937; Carden and others, 1977a,b) (Fig. 4). These rocks mark the southeastern extent of early Mesozoic subduction on the southwestern Alaska margin and are described in detail below.

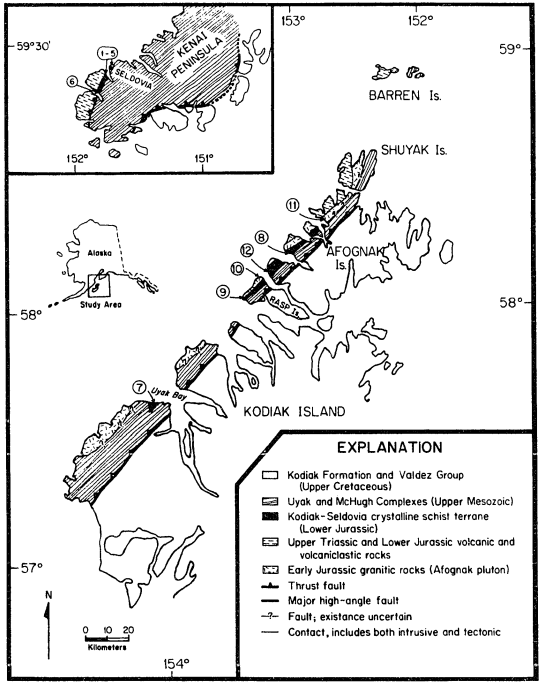


Figure 4. Generalized geologic map of the northwest Kodiak Islands and southeast Kenai Peninsula after Martin (1915), Moore (1967), Connelly and Moore (1976), Cowan and Boss (1977), and Carden and others (1977). Numbers refer to K-Ar samples listed in Table 2.

To the northwest, the Upper Triassic Shuyak Formation structurally overlies the Kodiak Islands schist along the inferred Shuyak fault (Connelly, 1976). This fault is now intruded by the Afognak pluton, which serves to separate the Kodiak Islands schist from the Shuyak Formation in most areas. Similar relations have been observed on the Barren Islands (Cowan and Boss, 1977).

The Shuyak Formation consists of a lower member containing pillowed tholeiitic basalt of volcanic arc affinities (Hill and Gill, 1976) and an upper sedimentary member consisting of volcanic turbidites and conglomerate. These rocks are characterized by broad open folding and dip to the southeast. They have been interpreted (Connelly, 1976) to represent a forearc sequence deposited in an arc-trench gap. The age of the Shuyak is considered to be Upper Triassic (lower to middle Norian).

On the southeast the Kodiak schists are tectonically juxtaposed against the Uyak Formation (Moore, 1969) which is now referred to as the Uyak Complex (Connelly, 1976) because of its structural complexity. The Uyak Complex is a severely disrupted late Mesozoic tectonic melange composed of slabs and phacoids of dunite, clinopyroxenite, layered gabbro, pillowed greenstone, radiolarian chert, wacke, and small amounts of limestone suspended in a matrix of tuffaceous argillite and recrystallized gray chert (Connelly and others,

1976). These authors suggest that the ultramafic rocks and greenstone represent oceanic crust upon which radiolarian chert was deposited on the abyssal ocean floor and that tuffaceous argillite and wacke were deposited as the plate entered the oceanic trench. As these lithologies were subducted, they were broken into blocks and phacoids of all dimensions and suspended in the less competent gray chert and argillite. Consequent with subduction, metamorphism took place to the prehnite-pumpellyite facies indicating burial or underthrusting to a depth of at least 9 km (Turner, 1968).

Chert and pillow lavas on Sanak Island (Moore, 1973a) and the occurrence of a peridotite on St. George Island, the southernmost Pribilof Island (Barth, 1956), indicate that the Uyak Complex may continue southwestward and then turn upward along the Bering Shelf edge (Scholl and others, 1975). Additional evidence supporting this hypothesis is discussed later.

The age of the Uyak Complex is poorly known owing to the paucity of fossils in it. Connelly (1976) reports a phacoid of limestone containing mid-Permian (Guadalupian) fusulinids of Tethyan affinities. He believes that the limestone was deposited on the cap of a seamount which had a large component of northerly transport prior to its subduction and subsequent incorporation in the Uyak melange. The minimum emplacement age of the complex is based on radiolaria

collected from chert which are Valanginian, or possibly Aptian age (Connelly, 1976).

Similarities in lithology, degree of metamorphism, and tectonic setting suggest a correlation between the Uyak Complex and similar rocks on the Barren Islands and southern Kenai Peninsula which are presumed to be an extension of the McHugh Complex of the Anchorage Area (Clark, 1973; Moore and Connelly, 1976; Magoon and others, 1976; Cowan and Boss, 1977).

The Uyak Complex is underthrust by a younger turbidite sequence named the Kodiak Formation. This formation was originally called the "slate and graywacke" unit by Martin (1912). Capps (1937) described the rocks of this unit in detail, recognizing graded beds and slaty cleavage to be characteristic of the unit. Moore (1969) gave the unit a formational name. The Kodiak Formation is approximately 30 km thick at the type section on the west shore of Uyak Bay. The lithologies of the exposed rocks are dominantly sandstone, siltstone, mudstone, and slate.

Capps (1937) assigned Late Cretaceous age to the formation based on Inoceramya concentrica described by Ulrich (1904) which were collected near the town of Kodiak. Jones and Clark (1975) have reported finding Inoceramus kusiroensis (Maestrichtian age) on Woody Island, near the town of Kodiak.

This same species has also been identified in the Valdez Group of the Kenai Peninsula at Turnagain Arm. Identical species have also been recovered from rocks on the Shumagin Islands and on Nagai Island, west of Kodiak Island (Jones and Clark, 1975). Moore (1972, 1973b) surmises that the Kodiak and Shumagin Formations are correlative based on lithology and internal structure in addition to faunal assemblages (also see Burk, 1965). Clark (1973) believes that the Valdez Group rocks are similar to the Kodiak Formation.

Burk (1965) noted that the trend of flysch deposits of the Kodiak-Shumagin Formation departs radically from the shelf edge on Sanak Island and intersects the trend of the younger volcanic rocks of the Aleutian Island-Alaska Peninsula near Unimak Island. Hopkins and others (1969) reported dredging flysch-type sandstone, siltstone, and mudstone from rocks just under the acoustic basement in the Pribilof Canyon on the Bering Shelf edge. The rocks there have been assigned a Late Cretaceous age based on the identification of an abundant Campanian foraminiferal population.

I. kusiroensis has also been identified in turbidites of the Koryak Range of the eastern U. S. S. R. by Vereschagin and others (1965). It is likely that the Upper Cretaceous flysch deposits of the Valdez-Kodiak-Shumagin Formations follow the Bering Shelf edge and connect with the upper Mesozoic sedimentary and volcanic sequences of the Koryak

mountains of eastern Siberia (Burk, 1965; Moore, 1972; Scholl and others, 1975).

Southeast of the Kodiak Formation, the Ghost Rocks Formation, a Tertiary subduction complex (J. C. Moore, 1975, personal communication) has been accreted oceanward of the Kodiak rocks and even younger sequences occur oceanward of these rocks (Von Heune, 1972; Stewart, 1976). Thus, this region has been a site of almost continual continental accretion from early Mesozoic to Recent time.

The Kodiak Islands Schist

The Kodiak Islands schist terrane is the oldest accretionary melange outcropping discontinuously along the northwestern part of the Kodiak Islands. It is distinguishable from the Uyak Complex by its higher degree of metamorphism and fold style. The metamorphic rocks of the schist terrane are characterized by tight isoclinal overturned folds with fold axes trending northeast. Some chlorite-white mica schists display a well developed axial plane schistosity although compositional layering is commonly preserved (Fig. 6).

Lithologies include chlorite schist, garnetiferous quartz-mica schist, ferruginous meta-chert, marble, crossite, and epidote amphibolite, with metamorphic grade increasing toward the continental plate. Blueschist mineral assemblages include crossite-epidote-albite-sphene and crossite-lawsonite-sphene $\pm$ stilpnomelane. The detailed petrography of

these schists is discussed in the next chapter. The blueschists on Kodiak Island are intimately intercalated with greenschists facies assemblages on a scale ranging from centimeters to meters as is the case at Seldovia. The contacts are often razor sharp on both the macro and microscopic scale. There is no evidence to indicate that the greenschist layers were produced by thermal upgrading of former blueschist facies assemblages.

Based on the earlier observations of Martin (1912), Maddren (1917), and Capps (1937) who described schists along the northwest shore of the Islands, Forbes and Lanphere (1973) predicted that the southwestern extension of the Seldovia blueschist terrane would be found on the northwest coast of Kodiak Island. In the summer of 1975, J. Carden discovered blueschist assemblages in the metamorphic terrane at the mouth of Uyak Bay (Fig. 5) (Carden and Forbes, 1976). Wm. Connelly and M. Hill located additional localities to the northeast on Afognak Island (Carden and others, 1977a,b) (Fig. 4).

The metamorphic rocks at the mouth of Uyak Bay appear to be a large tectonic block which is either in tectonic contact with Uyak melange or is incorporated within it. The most complete sections of metamorphic rocks occur on Afognak Island at Malina Bay in a 2 to 3 km wide belt extending for at least 40 km along the northwest side of the Island (Fig. 4). Limited sampling of the area indicates that the grade

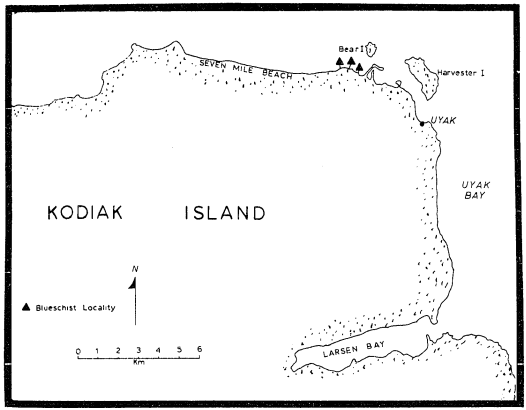


Figure 5. Location map of blueschist localities on the west side of Uyak Bay, Kodiak Island. Triangles represent crossite schists.

of metamorphism increases toward the northwest from blueschist facies to the southeast to epidote-amphibolite facies adjacent to the Early Jurassic Afognak pluton (Fig. 4). The pluton is composed of hornblende diorite bounded by migmatic gneisses along its south margin. Adjacent to the pluton, pillowed greenstone of the Shuyak Formation are commonly upgraded to amphibolite (hornblende-plagioclase $\pm$ epidote) and the interpillow limestone has been metamorphosed to calc-silicate assemblages (calcite-garnet $\pm$ diopside $\pm$ talc). The migmatic gneisses may genetically related to the emplacement of the pluton into the metamorphic terrane and the amphibolite facies assemblages in the migmatites and adjacent rocks are probably related to late synkinematic upgrading near the margin of the pluton (Wm. Connelly, personal communication).

The proximity of the Afognak pluton to the blueschist terrane is an apparent paradox since blueschist assemblages are generally thought to form at relatively low temperatures and are not associated with plutonism. This relationship is not completely understood but it may be due to tectonic juxtaposition. An alternate explanation is that the plutonism represents the near trench type described by Marshak and Karig (1977). The relationship of the Late Jurassic ages of the pluton to similar ages determined for the schist belt is discussed later.

## KENAI PENINSULA

Near Seldovia Bay, Kenai Peninsula, the Seldovia schist terrane occupies an equivalent structural position to that of the Kodiak Islands schists (Fig. 4). It is in tectonic contact with a forearc sequence on the northwest and is underthrust on the southeast by younger trench turbidites containing slices of dismembered ophiolite (Fig. 8).

### Shelf and Forearc Deposits

A series of shallow water tuff, limestone, siltstone, mudstone, shale, and minor amounts of volcanic agglomerate and conglomerate (Fig. 4) are exposed on the tip of the Kenai Peninsula between Seldovia Inlet and Koyuktolik Bay. Martin (1915) assigned a Late Triassic to Early Jurassic age to this group of rocks based on well preserved faunal assemblages he collected near the mouth of Port Graham and at Seldovia Bay.

Halobia superba and Monotis subcircularis of Karnian to late Norian age were collected on the north shore of Port Graham in a gently folded sequence of black siltstone, shale, mudstone, calcareous siltstone, and sparse limestone (Martin, 1915; and this study). These rocks are in fault contact with coarse-grained volcaniclastic rocks which are in turn interbedded with shallow water limestone and well indurated tuff. This fault will be referred to here as the

Selanie Lagoon fault (Fig. 7). The limestone contains a Lower Jurassic pelecypod assemblage (Martin, 1915) collected near Point Naskowhak at the mouth of Seldovia Bay. The tuffaceous agglomerate at Port Graham (particularly on the south shore) contains clasts of volcanic fragments several meters across suggesting that the sequence was deposited near a volcanic source.

These forearc deposits probably correlate with Norian rocks of the Barren Islands and the Shuyak Formation (Cowan and Boss, 1977; Connelly, 1976). Across the Cook Inlet, M. subcircularis has been reported by Burk (1965) in interbedded limestone and shale at the tip of Cape Kekurmoi between Puale and Alinchak Bays (Fig. 3). These rocks are in turn overlain by a coarse-grained Lower Jurassic volcaniclastic sequence similar to that at Port Graham.

Similar lithologies and biostratigraphy are observed in the Lake Iliamna-Kamishak Bay area (Detterman and Hartsock, 1966). Detterman and Jones (1974) suggest that rocks uplifted during the formation of Augustine volcano (Fig. 3) indicate that the neritic rocks exposed on the Alaska Peninsula continue under the Tertiary and Quaternary deposits filling the Cook Inlet. Subsurface information (Kirschner and Lyon, 1973) tends to confirm this hypothesis. The geometry of correlative rocks which disappear under the west side of the Cook Inlet and reappear on its eastern side on

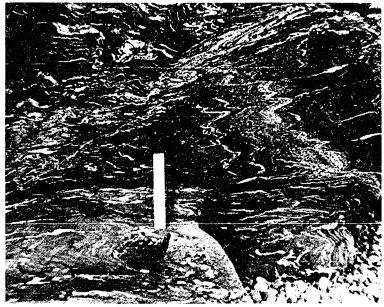

Figure 6. A typical outcrop of chlorite schist on Kodiak Island showing compositional layering and axial plane schistosity.

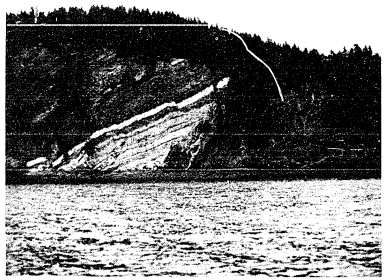

Figure 7. Selanie Lagoon fault at Port Graham which juxtaposes Lower Jurassic volcaniclastic rock and tuff (left) against Upper Triassic siltstone and shale (right).

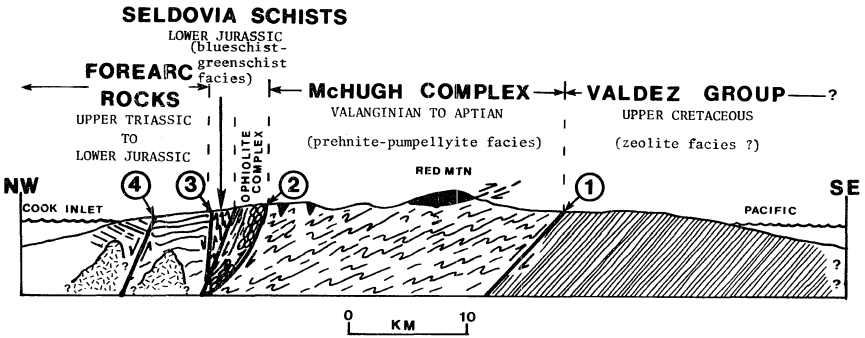


Figure 8. Generalized geologic cross section across the southern Kenai Peninsula illustrating the relationship between the schists, forearc rocks and accretionary turbidites of the McHugh and Valdez Formations. Numbers refer to faults: (1) Eagle River Thrust; (2) Border Ranges Fault; (3) Port Graham Fault (Fig. 10, this study); (4) Selanie Lagoon Fault (Fig. 7, this study).

the Kenai Peninsula, Barren Islands, and Shuyak Islands are best represented by a synclinal or graben structure which has been filled with Tertiary and younger sediments now flooring the Cook Inlet. The large angular clasts in the agglomeratic tuff of Port Graham are puzzling since they suggest that the unit was deposited adjacent to a volcanic source. The nearest source is now many kilometers distant suggesting the need for a rifting mechanism to explain their present position. However, no data suggesting that this may be a realistic hypothesis are presently available.

The contact between the forearc deposits and the Seldovia schist terrane is tectonic; although no pluton separates the forearc rocks from the metamorphic sequence as it does on the Barren and Shuyak Islands (Cowan and Boss, 1977; Connelly, in prep.). Martin (1915) has mapped several small diorite bodies intruding the forearc sequence near Pt. Bede and Turner (1978) has shown that these diorites may represent an extension of the Afognak pluton (Late Triassic-Early Jurassic).

Ophiolite and Trench Deposits

Martin (1915) was the first worker to recognize the relationship of chert and pillowed greenstones (called ellipsoidal lavas by Martin) exposed on the tip of the Kenai Peninsula southeast of the schist belt. He noted the conspicous lack of fossil remains in these rocks but mentioned that there are poorly preserved radiolaria in the cherts which could not be dated. The cherts in this area bear a strong lithologic resemblance to the Upper Triassic Kamishak cherts on the west coast of Cook Inlet, which led Martin (1915) to assign an Upper Triassic age to the chert and pillowed greenstone sequence. Recently, Norian radiolaria have been recognized in the cherts of this area (Wm. Connelly, personal communication). This age represents sedimentation on a proto-Pacific plate, however, prior to its accretion to the continent.

The participants in a recent conference on ophiolites, sponsored by the Geological Society of America, agreed upon a general definition for ophiolite as follows:

> "Ophiolite, used by those present at the G. S. A. Penrose conference on ophio-lites, refers to a distinctive assemblage of mafic to ultramafic rocks. It should not be used as a rock name or as a litho-logic unit in mapping. In a completely developed ophiolite the rock types occur in the following sequence, starting from the bottom and working up:
>
> -Ultramafic complex, consisting of variable proportions of hartzburgite, lherzolite, and

> dunite, usually with a metamorphic tectonic fabric (more or less serpentinized).
>
> -Gabbroic complex, ordinarily with cumulus textures commonly containing cumulusperidotites and pyroxenites and usually less deformed than the ultramafic complex.
>
> -Mafic sheeted dike complex.
>
> -Mafic volcanic complex, commonly pillowed.
>
> -Associated rock types include (1) an overlying sedimentary section typically including ribbon cherts, thin shale interbeds, and minor limestones; (2) podiform bodies of chromite generally associated with dunite; (3) sodic felsic intrusive and extrusive rocks.
>
> Faulted contacts between mappable units are common. Whole sections may be missing. An ophiolite may be incomplete, dismembered, or metamorphosed in which case it should be called a partial, dismembered, or metamorphosed ophiolite. Although ophiolite is generally interpreted to be oceanic crust and upper mantle, the use of the term should be independent of its supposed origin." (Anonymous, 1972).

Forbes and Lanphere (1973) observed that the rocks of the Seldovia area bear a close resemblance to some of the lithologic types which are typical of ophiolite sequences. Since all members are not present, the sequence is a dismembered ophiolite. This sequence has also been metamorphosed under conditions of the prehnite-pumpellyite facies, and represents a vestige of the now consumed Kula plate of

Grow and Atwater (1970). The age of the emplacement of this plate is probably post Late Triassic, although the cherts themselves were probably deposited on a Late Permian to Late Triassic seafloor.

The pillow lavas and chert forming the dismembered meta-ophiolite crop out as a steeply-dipping, northeast trending mass exposed on the southeast side of Kachemak Bay. The pillow lava and chert occur in close association in several of the inlets, with the best exposures in Seldovia Bay. Based on an average dip of 55 degrees, the entire ophiolite exposed in Seldovia Bay is approximately 1800 meters thick, including some repetition of the sequence due to tectonic imbrication. Lithologies include ferruginous radiolarian ribbon chert intercalated with shale, pillowed greenstone, diabasic greenstone, and pods and stringers of serpentinite.

The chert sequence is approximately 850 meters thick from the top of the section just south of Watch Point to the base, where it is in depositional contact with underlying pillowed greenstone (Fig. 9). The chert is thinly bedded with varying amounts of intercalated greenish-gray shale in some outcrops. As previously mentioned, the chert is commonly red although gray and rare green varities are also present. The chert is commonly veined with secondary quartz

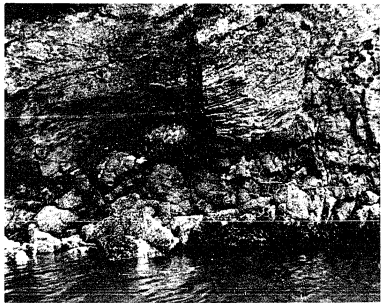

Figure 9. Contact between pillow basalt and overlying ferruginous chert in the dismembered ophiolite at Seldovia Bay.

Figure 10. Trace of the Port Graham fault zone on the north shore of Port Graham; Upper Triassic rocks are intensely broken due to movement on this fault which was caused by the emplacement of the adjacent metamorphic wedge.

and calcite, especially along shear zones. In some inlets northeast of Seldovia Bay, the chert may be sparse or absent even though there is an abundance of pillowed basalts.

The whole-rock compositions of two relatively unaltered pillowed greenstones are given in Table 1 along with CIPW norms. The norms indicate that these basalts are low-K tholeiites which are generally associated with spreading center magmatism. A method for discriminating between basalts with oceanic affinities and those with continental affinities was proposed by Pearce and others (1975) based on fields in the $TiO_2$-$K_2O$-$P_2O_5$ ternary diagram. Figure 11 illustrates that the greenstones plot well within the oceanic field. Weathering and metamorphic alteration would tend to move oceanic basalts toward the non-oceanic field (and not the other way) implying that the greenstones are unlikely to have a non-oceanic origin. Furthermore, the shaded area in Figure 12 represents the field of 100 low-K oceanic basalts taken from the literature. Both greenstones plot well within the boundary.

The individual pillows in the pillowed greenstone sequence are well developed but vary in both size and shape. The conspicuous lack of macrovessicles indicates that the basalt was emplaced at abyssal depths (Moore, 1965; Jones, 1969). Several of the studied outcrops contain interpillow breccia and limestone. The outer rim of the pillows is chiefly composed of devitrified glass. Some pillows contain

Table 1. Chemical analyses of pillowed greenstones from Seldovia Bay (Kl.4Z) and Port Graham (74AF-80.1).

| Sample Number | Kl.4Z | 74AF-80.1 |
|---|---|---|
| $SiO_2$ | 46.22 | 48.2 |
| $TiO_2$ | 2.08 | 2.0 |
| $Al_2O_3$ | 14.24 | 14.4 |
| $Fe_2O_3$ | 1.10 | 2.4 |
| FeO | 11.35 | 6.2 |
| MnO | 0.18 | 0.08 |
| MgO | 8.73 | 4.2 |
| CaO | 8.57 | 12.1 |
| $Na_2O$ | 1.25 | 3.2 |
| $K_2O$ | 0.20 | 0.04 |
| $P_2O_5$ | 0.25 | 0.17 |
| $H_2O^+$ | 4.86* | 2.25 |
| $H_2O^-$ | | 0.15 |
| $CO_2$ | | 0.75 |
| | C.I.P.W. NORMS | |
| Q | 1.98 | 3.18 |
| Or | 1.11 | 0.00 |
| Ab | 11.00 | 28.80 |
| An | 34.75 | 26.96 |
| Di | 6.83 | 30.28 |
| Hy | 37.65 | 2.59 |
| Ol | 0.00 | 0.00 |
| Mt | 1.62 | 3.71 |
| Il | 4.26 | 3.95 |
| Ap | 0.68 | 0.31 |
| Ne | 0.00 | 0.00 |

*Loss on ignition

Analyst: Kl.4Z, M. Hill, University of California, Santa Cruz; 74AF-80.1, Skyline Labs, Wheatridge, Colorado.

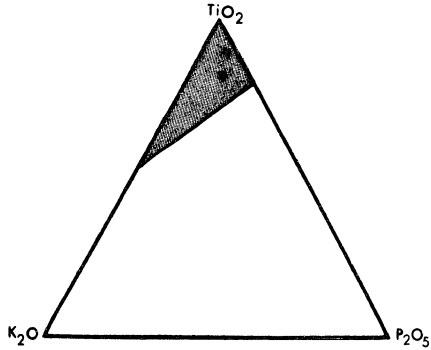


Figure 11. Diagram after Pearce and others (1975); shaded area is the field of oceanic basalts and non-shaded portion is the field of basalts with continental affinities. Data from Table 1.

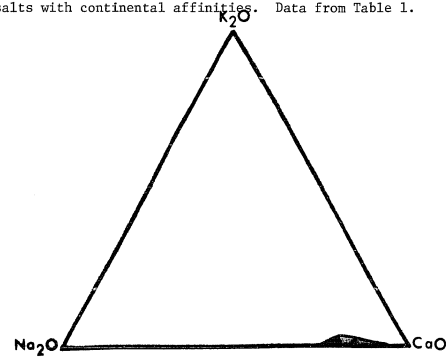


Figure 12. Shaded area is the field of 100 low-K tholeiites of oceanic affinities. Data from Miyashiro and others (1969), Shido and others (1971), Engle and others (1965), Engle and Engle (1963, 1964a,b), Aumento (1968), Aumento and Loncarevic (1969), Muir and Tilley (1964), Engle, Engle, and Havens (1965). Data from Table 1.

plagioclase and pyroxene spherulites suspended in a glassy or fine-grained matrix. The larger pillows display doleritic cores with well developed pyroxene and plagioclase. Hydration cracks and rare occurences of microvesicles are often filled with serpentine, quartz, and prehnite. At some localities, the pillows have incorporated rolled balls of limestone suggesting that calcareous ooze deposited on the flanks of rises above the depth of carbonate compensation were subsequently incorporated as molten material was extruded over the abyssal surface off the flanks of the rise.

A thick sequence of metatuff, bounded on both sides by pillow lava occurs near Powder Island at Seldovia Bay. Thinner beds of tuffaceous material occur throughout the sequence.

In close association with the chert and pillowed lava sequence are a number of greenstone and serpentinite bodies which display crosscutting relationships.

The serpentinite masses are greenish-black to black and are either massive or highly sheared. Relict olivine was not observed in thin section, the rock being composed mainly of chrysotile and antigorite.

The greenstone has a doleritic to gabbroic texture. Most samples are holocrystalline aggregates of anhedral plagioclase and subhedral pyroxene phenocrysts. Olivine

is either lacking or occurs only in trace amounts. Some of the plagioclase has been altered to clay minerals while the pyroxene has been altered to chlorite. One sample contained secondary biotite.

The rocks of the ophiolite sequence are easily distinguished from the metamorphic rocks of the Seldovia schist terrane, which are highly recrystallized, pervasively sheared, and have a more complex structural style.

Southwest of the dismembered ophiolite are a series of trench turbidites considered to be correlative with rocks of the McHugh Complex (Clark, 1973) and the Uyak Complex (J. C. Moore, personal communication). These strata are dominantly composed of massive to thickly bedded wacke sandstone and argillite which strike northeast and dip northwest. Associated with these rocks are minor amounts of gray chert and tuffaceous material which are locally interbedded with the more massive sandstone. Greenstone dikes commonly cut the sequence. The turbidites and ophiolite, although metamorphosed to the prehnite-pumpellyite facies, are dominantly non-schistose due to the lack of penetrative deformation. A fault separates the ophiolites from the McHugh Complex turbidites and is believed to be an extension of the Border Ranges Fault. The fault is not, however, obvious in Seldovia Bay or at Port Graham.

## Metamorphic Rocks

### Field Relationships

The metamorphic rocks in the Seldovia-Port Graham area form a tectonic sliver approximately 2 km thick near Seldovia Point, pinching southeastward along strike and finally disappearing in a gouge zone 16 km away on the southwest shore of Port Graham. Lithologies in this metamorphic block include quartz-mica schist, marble, metachert, chlorite-epidote schist, actinolite-epidote schist, and crossite-epidote schist.

The contact between the wedge of metamorphic rocks and the dismembered meta-ophiolite to the southeast is not exposed at Seldovia Bay nor in Port Graham, but a fault is indicated based on the sudden change in the degree of metamorphism and structural style. Along the northwest shore of Port Graham, the contact between the schist and the Upper Triassic volcaniclastic turbidites to the northwest is the Port Graham fault (Carden and others, 1977b). The fault has a well developed mega-shear zone nearly 0.5 km wide. This zone is characterized by the loss of bedding continuity and an increase in shear foliation in the bedded rocks toward the contact (Fig. 10). Bedding is completely obliterated adjacent to the contact, with broken remnants of more resistant beds rotated into the plane of foliation. Associated with the neo-foliation are stringers and veins of

remobilized calcite and quartz oriented at high angles to relict bedding. Small asymmetric drag folds suggests that the adjacent metamorphic sliver was moved upward relative to the turbidites. The Port Graham fault is interpreted as being a segment of the early Mesozoic plate boundary along southwestern Alaska. Upon cursory examination, the contact of the metamorphic block with the Lower Jurassic tuffaceous agglomerate at Seldovia Bay does not appear to be tectonic, although closer microscopic inspection of these rocks reveals a highly mylonitized fabric suggesting that this contact also has a tectonic origin.

The schist between Seldovia Point and Port Graham contains a number of lithologies which vary in mineralogy, degree of recrystallization, and metamorphic facies. The rocks have a steeply southeast dipping, isoclinal overturned fold style (Fig. 13) with fold axes having a northeasterly trend. The layering in these schists is believed to be primary because original bedding in many of the units, especially the marbles and metacherts, is still discernible (Fig. 14). The individual rock units tend to pinch out along strike, with the exception of an iron-stained, pyritiferrous quartzite-metachert unit which is more or less continuous for approximately 13 km along strike. This unit is well exposed at Red Bluff which derives its name from the weathering of the pyrite. The Red Bluff metacherts have

developed sparse sericite. In some cases across Seldovia Bay where the chert has locally recrystallized into thinly bedded quartzite, the rock has developed muscovite. The metacherts are commonly interbedded with thin layers of slaty material (Fig. 14) exhibiting evidence of flowage during deformation.

At Gray Cliff the predominant rock type is a massive grayish to white marble which is little deformed. The marble has incorporated metabasite boudins which have been metamorphosed to at least the greenschist facies. Included in the metabasite are rolled balls of carbonate similar to the carbonate balls observed in the ophiolite suite. The contact between the marble and greenschist is marked by a thin zone of pyrite and apple-green fuchsite. This marble was closely inspected by optical and X-ray methods for aragonite but none was discovered. Marble interbedded with actinolite and chlorite schist was observed on the south side of Seldovia Point, and marble float was observed on the southwest shore of Seldovia Bay and the northeast shore of Port Graham. The marble pinches out both to the northeast and the southwest and may represent a mega-boudin.

Quartz-mica schist is rare in the section, mainly occurring in back of Gray Cliff and as an outcrop of graphitic quartz-mica schist containing incipient garnet on the northeast shore of Port Graham. Highly crenulated argillite,

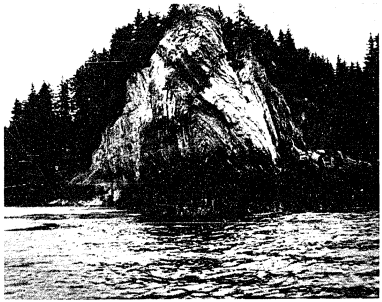

Figure 13. Camel rock at the entrance to Seldovia Bay, which illustrates the isoclinal overturned fold style of the Seldovia schists.

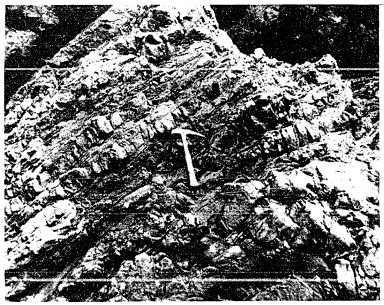

Figure 14. An outcrop of interbedded metachert and phyllite on the beach north of Seldovia bedding is still discernible.

less crystalline than the quartz-mica schist, is common near Seldovia Point, but absent elsewhere in the section.

A fairly large outcrop of metamorphosed and altered ultramafic rock is also located on the outer beach between Seldovia Point and Gray Cliff.

Greenschist facies rocks displaying differing degrees of recrystallization, mineralogy, and schistosity are the most common constituents of the Seldovia schists, although they are discontinuous along the strike. The most common among the greenschist facies rock is a chlorite-epidote-albite schist which crops out sporadically along the trend of the tectonic sliver. Some of these rocks are massive and exhibit little or no schistosity. In contrast, rare actinolite-albite-epidote schist, displays a well-defined schistosity due to a dominant nematoblastic alignment of amphibole prisms.

Chloritic greenschist commonly intercalated with blueschist (crossite-epidote-albite) on a scale ranging from centimeters to meters (Fig. 15). The contact between these two contrasting lithologies is usually straight and sharp in both outcrop and thin section. Boudinage structure has developed in scattered outcrops whereby the dense and more brittle blue amphibole layers have been pulled apart to form boudins whereas the adjacent chlorite schist, being more ductile, has deformed plastically around the blueschist boudins (Fig. 16).

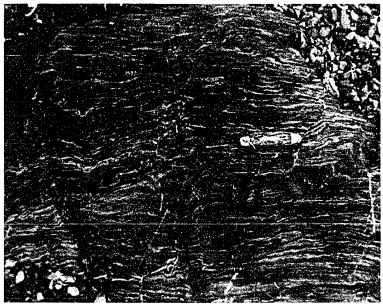

Figure 15. Intercalated blueschists and greenschists at Watch Point, near the entrance to Seldovia Bay.

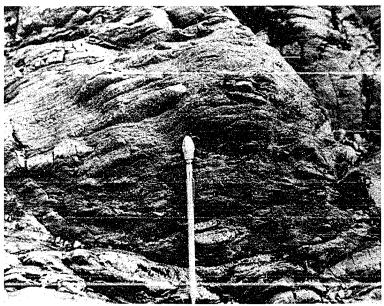

Figure 16. Outcrop of blueschist boudins surrounded by a more ductile greenschist matrix.

The origin of the layering is important in several respects. If blueschists and greenschists represent two different facies (P-T conditions) why do they occur together? As previously noted, this phenomena is not uncommon in other metamorphic terranes of the world which contain high temperature blueschists. Therefore, it is not necessary to invoke such bizarre mechanisms as micro-imbricate thrusting to juxtapose two seemingly unrelated facies together. Furthermore, it is highly unlikely that both schists formed under different physical conditions over such a small area. Other parameters such as bulk chemistry of these schists and the composition of the original protolith must be considered. Further discussion of this problem will be deferred to a later chapter. It is clear, though, that the differences cannot be due to thermal upgrading of former blueschist assemblages since there is neither microscopic nor geochronologic evidence for this hypothesis (see next section).

## Radiometric Ages

Analytical data for K-Ar mineral ages (determined by D.L. Turner) from Seldovia, Port Graham, and the Kodiak Islands are given in Table 2. The samples from which the dates were obtained are keyed into the locality map (Fig. 4). A striking feature of these data is the excellent agreement of the ages of the Seldovia schist terrane with the ages obtained from the extension of this belt on the Kodiak Islands (Carden and others, 1977b).

Five white mica ages from Seldovia and Port Graham agree within analytical uncertainty and have an average age of 190 m.y. Two actinolites yield an average age of 187 m.y. and two crossites give an average age of 158 m.y. (Table 2). The systematic difference between the apparent ages of crossite versus actinolite and white mica is greater than the analytical error of the individual measurements. Coleman and Lanphere (1971) first reported this phenomenon in blueschist facies rocks from the Franciscan Complex and ascribed it to inferior argon retentivity in blue amphiboles as compared to white micas during retrograde metamorphism (also see Suppe and Armstrong, 1972).

On Kodiak Island, crossite gives an average age of 166 m.y. although white mica yields an average age of 190 m.y. These ages are in agreement with those determined for the schists at Seldovia and Port Graham, including a similar

discordance between crossite and white mica ages. These data suggest that the two metamorphic terranes are segments of the same metamorphic belt (Carden and others, 1977b).

In addition to the mineral ages from the blueschist and greenschist facies rocks, three hornblende separates from directionless and gneissic hornblende diorite from the northwest coast of Raspberry Island and Afognak Island have been dated. These ages agree within analytical uncertainity and average 188 $\pm$ 6 m.y. (Table 2), an age which is essentially identical to those ages obtained from white micas and actinolites from the schist belt, as discussed above. Cowan and Boss (1977) obtained a K-Ar hornblende age of 187 $\pm$ 14 m.y. from quartz diorite on Ushagat Island in the Barren Islands (Fig. 3). This quartz diorite pluton is on the same structural trend as the Afognak pluton and is apparently contiguous with it.

Recent work by Turner (1978) has shown that three small diorite plutons near Pt. Bede, on the western tip of the Kenai Peninsula (Magoon and others, 1976) are coeval with the Afognak and Barren Islands plutons and may represent a northeastern extension of the same plutonic belt. All of these plutonic ages are about 10 m.y. older than the oldest episode of plutonic activity dated by Reed and Lanphere (1973) in the Alaska-Aleutian Range batholith.

Table 2. K-Ar analytical data for mineral ages from the Seldovia-Kodiak Islands area.

| Map No. | Sample No. | Rock Type | Mineral Dated | $K_2O$ (weight percent) | Sample Weight (grams) | $^{40}Ar_{rad}$ (moles/gm) x $10^{-11}$ | $\frac{^{40}Ar_{rad}}{^{40}Ar_{total}}$ | Age $\pm$ 1 $\sigma$ (m.y.) | References |
|---|---|---|---|---|---|---|---|---|---|
| | | | | | SELDOVIA | | | | |
| (1) | 74AF48.1 (76027) | Blueschist | crossite | 0.128<br>0.131<br>0.131 | 1.9651 | 3.270 | 0.580 | 162.9 $\pm$ 4.9 | 2 |
| (2) | 74AF23-9 (75107) | Qtz-mica schist | muscovite | 8.880<br>8.891 | 0.2641 | 263.05 | 0.947 | 190.4 $\pm$ 5.7 | 2 |
| (3) | 74AF23-10 (75128) | Amphibole-mica schist | amphibole | 0.503<br>0.513<br>0.511<br>0.512 | 1.294 | 14.594 | 0.729 | 184.4 $\pm$ 5.5 | 2 |
| (3) | 74AF23-10 (75125) replicate | Amphibole-mica schist | amphibole | 0.503<br>0.513<br>0.511<br>0.512 | 1.2561 | 14.571 | 0.830 | 184.1 $\pm$ 5.5<br>$\bar{x}$ =184.2 $\pm$ 5.5 | 2 |
| (3) | 74AF23-10 (75109) | Amphibole-mica schist | muscovite | 8.840<br>8.926 | 0.3032 | 265.68 | 0.863 | 192.2 $\pm$ 5.8 | 2 |
| (4) | SD3-3 | Greenschist | actinolite | | | | | 191.0 $\pm$ 11.0 | 1 |
| (4) | SD3-3 | Greenschist | white mica | | | | | 188.0 $\pm$ 10.0 | 1 |
| (4) | SD3-3 | Greenschist | chlorite | | | | | 181.0 $\pm$ 8.3 | 1 |
| (5) | SD9-3 | Blueschist | white mica | | | | | 189.0 $\pm$ 5.7 | 1 |
| (5) | SD9-3 | Blueschist | crossite | | | | | 154.0 $\pm$ 4.8 | 1 |
| | | | | | PORT GRAHAM | | | | |
| (6) | 74PG79 (75114) | Qtz-mica schist | muscovite | 8.890 | 0.3103 | 265.09 | 0.958 | 192.2 $\pm$ 5.8 | 2 |
| | | | | | KODIAK ISLANDS | | | | |
| (7) | UK-23 (75108) | Blueschist | crossite | 0.104<br>0.110<br>0.128<br>0.104 | 2.8118 | 2.777 | 0.636 | 161.4 $\pm$ 19.4 | 2 |

Table 2. Continued.

| | Sample No. | Rock Type | Mineral Dated | $K_2O$ (weight percent) | Sample Weight (grams) | $^{40}Ar_{rad}$ (moles/gm) x $10^{-11}$ | $\frac{^{40}Ar_{rad}}{^{40}Ar_{total}}$ | Age ± 1 σ (m.y.) | References |
|---|---|---|---|---|---|---|---|---|---|
| (8) | M1D (76051 | White mica-crossite schist | white mica | 6.580<br>6.640<br>6.665<br>6.655 | 0.1058 | 193.72 | 0.958 | 187.6 ± 5.6 | 2 |
| (8) | M1D (76105) | White mica-crossite schist | crossite | 0.161 | 0.8246 | 4.203 | 0.565 | 170.6 ± 5.1 | 2 |
| (9) | R2Y (75127) | Dioritic migmatite | hornblende | 0.178<br>0.181 | 0.8534 | 5.154 | 0.606 | 184.9 ± 5.5 | 2 |
| (9) | R2Y (75130) replicate | Dioritic | hornblende | 0.178<br>0.181 | 0.6558 | 5.087 | 0.413 | 182.6 ± 5.5<br>$\bar{x}$ = 183.7 ± 5.5 | 2 |
| (10) | R4A (75093) | Hornblende diorite | hornblende | 0.224<br>0.222 | 1.2344 | 6.531 | 0.377 | 188.4 ± 5.7 | 2 |
| (11) | B10-9Z (76112) | Hornblende diorite | | 0.292<br>0.295<br>0.290<br>0.290<br>$\bar{x}$ = 0.292 | 1.0667 | 8.749 | 0.818 | 192.7 ± 5.8 | 2 |
| (12) | V5C (76166) | Qtz-mica schist | muscovite | 9.480<br>9.500<br>$\bar{x}$ = 9.490 | 0.0836 | 283.553 | 0.934 | 192.1 ± 5.8 | 2 |

Note: 1. Forbes and Lanphere, 1973.
2. New Analysis.

Note: Potassium analyzed using an IL 343 digital flame photometer using $LiBO_2$ flux fusion technique and mineral calibration standards (Suhr and Ingamells, 1966; Ingamells, 1970; Engles and Ingamells, 1970). Argon determined by isotope dilution using $^{38}Ar$ tracers and 6-in. radius Nuclide mass spectrometer equipped with automated peak stepping and digital data acquisition systems. Argon extractions and potassium analyses by Diane Duvall. K-Ar dating was done at the Geophysical Institute, University of Alaska. Constants used in age calculations:

$$\lambda_c = 0.585 \times 10^{-10}/yr,\ \lambda_\beta = 4.72 \times 10^{-10}/yr,\ ^{40}K/K_{tot} = 1.19 \times 10^{-4}\ mol/mol.$$

The mineral ages of the Kodiak Island schist belt are coeval with those determined for the adjacent Afognak pluton. The concordant ages are subject to two interpretations: (1) The schist is actually older than 190 m.y., but its K-Ar ages have been reset by thermal overprinting of the Afognak pluton; or (2) The mineral ages from the schists are cooling ages initiated by passage through the argon blocking isotherms following metamorphic recrystallization. In this case, the Afognak and related plutons are part of a late synkinematic plutonic event.

The second hypothesis is preferred for the following reasons:

(1) No plutons occur adjacent to the schist belt at Seldovia-Port Graham, yet K-Ar ages there are essentially identical to those from the extension of this belt on the Kodiak Islands, including a similar discordance in crossite-white mica ages.

(2) Although Early Jurassic plutons do occur at the western tip of the Kenai Peninsula (Turner, 1977), they are more than 11 km from the nearest schist belt outcrop. The thick, intervening section of Triassic sediments shows no effects of thermal metamorphism, other than local contact effects adjacent to the small plutons.

(3) Petrologic relationships between the quartz diorite and migmatitic diorite gneiss of the Afognak pluton and the blueschists appear to indicate that these units have experienced a similar crystallization and cooling history and, therefore, support the proposed late synkinematic history of the migmatitic phase of this pluton.

(4) There is no evidence for arc-related plutonism or forearc sedimentation on the Alaska Peninsula compatable with a subduction event earlier than Late Triassic time.

Knik River Schist Terrane, South-Central Alaska

In a reconnaissance study of the bedrock geology of the Chugach Mountains near Anchorage, Alaska, Clark (1972a) distinquished a group of undifferentiated metamorphic rocks extending from the Eagle River vicinity to the Knik River. A recent map by Magoon and others (1976) extends this terrane northeast along strike to the area of Coal Creek (Fig. 17). This terrane is informally called the Knik River schist terrane (Carden and Decker, 1977).

Near Eklutna, the Knik River schist terrane is composed of marble, siliceous argillite, metachert, metasandstone, and metavolcanic rocks (Clark, 1972a). The marble forms discontinuous pod-like layers and lenses that can be seen from the highway. The dominant metavolcanic unit is an actinolite schist which forms massive, steep-sided outcrops near the Knik River. Rocks from the schist terrane have been metamorphosed to greenschist and possibly low-grade amphibolite facies. Most outcrops are highly sheared and display melange-like characteristics.

Carden and Decker (1977) believe that the Knik River schist terrane represents a segment of the Early Jurassic subduction complex that extends discontinuously from the Kodiak Islands to the Canadian Border and possibly into southeastern Alaska (Forbes and others, 1976, 1977).

Carden and Decker (1977) have suggested that the Knik River schist terrane represents an extension of the Seldovia-Kodiak Islands schist belt because both occupy the same tectonic position relative to major geologic features on the southern Alaska margin. They are located in the upper plate above the Border Ranges Fault, which is a suture zone that represents a major Mesozoic plate boundary separating older schists of the upper plate from volcanigenic sedimentary rocks of the Mchugh-Uyak and Valdez Complexes of the lower plate (MacKevett and Plafker, 1974). These rocks are believed to have been accreted to North America during a later pulse of subduction in Cretaceous time (Moore and Connelly, 1976). In the Kodiak and Seldovia area, slivers of a dismembered ophiolite occur between the schist and the Border Ranges Fault. Similar ultramafic rocks are represented in the Anchorage area by the mafic-ultramafic rocks of the Wolverine Complex (Clark, 1972b) which occur between the Knik River schist terrane and the McHugh Complex. The Kodiak-Seldovia and Knik River schist belts are both bordered on the northwest by Mesozoic shelf rocks that are interpreted by Moore (1974) as a forearc sequence. Rocks of both belts are structurally similar and are characterized by melange-like deformation and an isoclinal overturned fold style.

An age-dating study has been initiated to evaluate the proposed correlation between the Seldovia-Kodiak Islands and Knik River schists. A single K-Ar age of 173 $\pm$ 7 m.y. obtained on an actinolite separate from a greenschist collected at the mouth of the Knik River in the Anchorage B-6 quadrangle (Fig. 17, Table 2a) is the first radiometric age reported from the complex (Carden and Decker, 1977). Although the apparent age is Lower Jurassic, it is significantly younger than the average of nine K-Ar ages determined for actinolite and white mica (189 $\pm$ 3 m.y.) from the schist of the Seldovia-Kodiak Islands terrane. This difference may be due to thermal overprinting by a pluton, dated at 161 $\pm$ 5 m.y. (Clark, 1972a), emplaced 2 km from the sampled schist outcrop. Agreement at the 67 percent confidence level between the pluton and schist dates suggests that the actinolite schist age may have been either totally or partially reset from an older value.

An alternate hypothesis is that the Knik River schist may have experienced a different emergence history than the Seldovia-Kodiak schists located 500 km to the southwest. Following cessation of underflow of the Kula plate, an accelerated tectonic emergence would be necessary to preserve blueschist facies mineral assemblages formed at depth (Ernst, 1971a). If uplift is not sufficiently rapid, the isotherms will gradually establish a normal mantle profile

Table 2a. K-Ar analytical data for mineral ages from the Knik River schist terrane.

| Sample | Rock type | Mineral dated | $K_2O$ (wt.%) | Sample weight (g) | $^{40}Ar_{rad}$ (moles/g) x $10^{-11}$ | $\frac{^{40}Ar_{rad}}{^{40}K_{total}}$ x $10^{-3}$ | $\frac{^{40}Ar_{rad}}{^{40}Ar_{total}}$ | Age $\pm 1\theta$ (m.y.) |
|---|---|---|---|---|---|---|---|---|
| JD-1 (76181) | Greenschist | Actinolite | 0.165<br>0.165<br>0.175<br>0.164<br>$\bar{x}$=0.167 | 1.3690 | 4.489 | 10.63 | 0.644 | $173^{+}7$ |

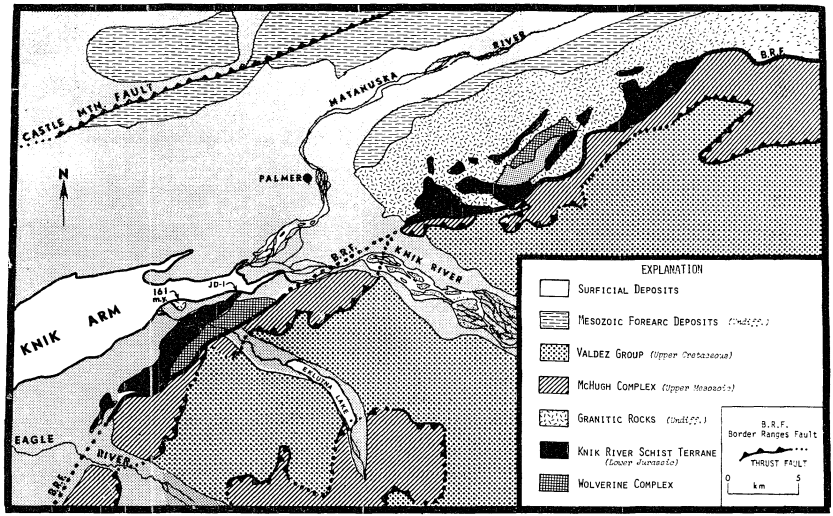


Figure 17. Generalized geologic map after Magoon and others (1976) showing the location of the Knik River schist terrane. Sample locality is near the eastern end of Knik Arm. Age of JD-1 is 173 m.y.

(i.e. higher temperature) obliterating the characteristic blueschist mineral assemblage and thermally upgrading the former blueschist to at least the greenschist facies. Furthermore, the slower rate of tectonic emergence would produce younger apparent ages, as the minerals pass through their characteristic argon-blocking isotherms at a later time.

Regional Significance

The Seldovia-Kodiak Islands and Knik River schists are remnants of as deeply subducted accretionary complex which was emplaced by Early Jurassic time. The combined evidence from volcaniclastic and plutonic rocks suggests a period of magmatism extending from Late Triassic through Middle Jurassic time (Detterman and Hartsock, 1966; Reed and Lanphere, 1973) which is consistent with ages determined from the schists. The sense of polarity, as suggested by the relative position of the Kodiak Islands, Seldovia-Port Graham, and Knik River schist in relation to the 180-160 m.y. magmatic arc of Reed and Lanphere (1973), is supported by chemical variation within the magmatic arc itself. Figure 18 is a diagram of the $K_2O$-$SiO_2$ ratio of plutonic rocks versus distance across the arc. The higher $K_2O/SiO_2$ pattern observed over the deeper parts of the inclined seismic zone are similar to those in modern magmatic arcs, as proposed by Miyashiro (1974) and Kuno (1960, 1966). This evidence indicates that during Late Triassic through Middle Jurassic time an arc was generated by underthrusting of a lithospheric plate from the southeast. Similar graphs may be plotted for Late Cretaceous-Early Tertiary plutonic arcs on the Alaska Peninsula (Fig. 19).

The relationship of other blueschist terranes along the southern Alaska margin to the Seldovia-Kodiak Islands schist terrane is uncertain. These localities include:

(1) The Valdez C-2 locality: P. Metz (1975, 1976) reported blueschist facies assemblages just north of Chitna, Alaska in a terrane dominated by meta-wacke, slates, volcaniclastics, and meta-igneous rocks of probable Permo-Triassic age. These rocks are characterized by the assemblage crossite-epidote-chlorite-albite as is the Seldovia-Kodiak terrane and are closely associated with rocks of the greenschist facies.

(2) The Hubbard Glacier locality: Blueschist facies assemblages were described in reports of the Harriman expedition and additional samples were collected as float blocks near the terminus of the Hubbard Glacier in the Russell fjord by G. Plafker of the U. S. Geologial Survey (G. Plafker, personal communication). The relationship of these rocks to other rocks in the area is not clear because the only samples collected to date are float.

(3) The Chichagof Island localities: The blueschist facies assemblages which were originally described by Reed and Coats (1941), occur in Pinta Bay and near Sister Lake. Additional samples were collected by Carden and Connelly during a reconnaissance trip in the fall of 1976 from a previously undescribed locality in Slocum Arm. The terrane consists dominantly of greenschists and meta-argillites.

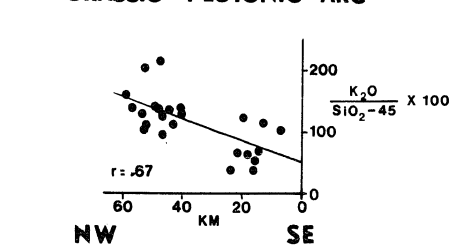


Figure 18. $K_2O/SiO_2-45$ x 100 vs. distance diagram across the Jurassic plutonic belt on the Alaska Peninsula. Data from Reed and Lanphere (1973,1974), diagram after Moore (1977).

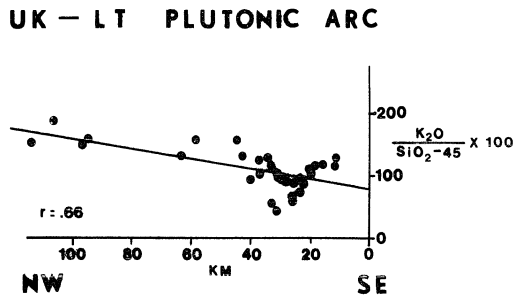


Figure 19. $K_2O/SiO_2-45$ x 100 vs. distance diagram across the Upper Cretaceous-Lower Tertiary plutonic belt on the Alaska Peninsula. Data from Reed and Lanphere (1973,1974), diagram after Moore (1977).

The blueschists are of the high temperature sub-facies containing crossite-chlorite-epidote and albite and are intimately intercalated with greenschists.

The scattered occurrences just described do not form a cohesive terrane. However, there are several factors common to each segment that suggest that these occurrences may represent a formerly contiguous subduction complex. These factors include: (1) metamorphic grade increases toward the continental block, (2) each is associated with ophiolites and/or melange-type rocks, (3) each is positioned just continentward of the Border Ranges Fault and younger volcanigenic turbidite sequences, and (4) all lack characteristic "high pressure" phases such as jadeite, lawsonite, and aragonite.

If these segments have the same Early Jurassic ages as the Seldovia-Kodiak Islands schists, they all may have participated in a common early Mesozoic evolution for much of the southern Alaska margin.

In addition, Dobretsov (1975) has described 180 m.y. old glaucophane schists from the Koryak Mountains of the Kamchatka Peninsula which are flanked on the oceanward side by Cretaceous turbidites. This blueschist belt may be the westward projection of the Seldovia-Kodiak Islands belt around the Bering Shelf edge (Scholl and others, 1975).

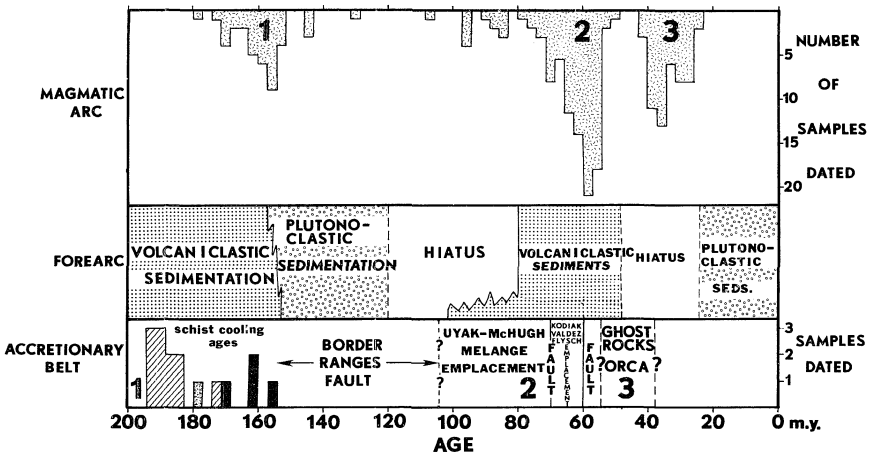


Figure 20. Diagram illustrating successive accretionary episodes on the Kenai Peninsula-Kodiak Islands and their relationship to magmatism on the Alaska Peninsula and associated forearc sedimentation in the Cook Inlet area. Diagonal pattern represents actinolite and white mica ages; solid pattern represents crossite dates; stippled pattern represents an actinolitic hornblende from the Knik River schist terrane. Data from Reed and Lanphere, 1973,1974; Detterman and Hartsock, 1966; Carden and others, 1977; Connelly, 1976; Moore, 1977 and personal communication; Clardy, 1974; Barnes and Payne, 1956; and Calderwood and Fackler, 1972.

Tectonic History

The rocks exposed on the Shumagin-Kodiak Islands-Kenai Peninsula accretionary belt represent at least three episodes of subduction which correlate with three separate but distinct pulses of plutonism and volcanism on the Alaska Peninsula (Fig. 20).

Figure 20 is a diagramatic representation illustrating the three successive accretionary episodes and the associated events taking place in the area of the magmatic arc (Alaska Peninsula) and forearc (southeast Alaska Peninsula and Cook Inlet) regions.

The Seldovia-Kodiak Islands and Knik River schist terranes represent the oldest and most highly metamorphosed of these accretionary belts. These rocks are represented by the histogram of cooling ages (labeled 1) in the accretionary belt of Figure 20. The cooling ages correlate well with plutonic ages of intrusives in the magmatic arc (also labeled 1) determined by Reed and Lanphere (1973, 1974).

The second accretionary event is designated by rocks of the Uyak-McHugh melange (labeled 2). This accretionary pulse is separated from the first by the Border Ranges Fault and correlates with a pulse of plutonism (labeled 2) in the magmatic arc. The youngest pulse of accretion is represented by rocks of the Ghost Rocks Formation and Orca Group.

This episode is also related to plutonism and volcanism in the rocks dated on the Alaskan Peninslua by Reed and Lanphere (1973, 1974).

Continentally derived flysch-type sediments, like those deposited in trench environments, are conspicuously absent as a protolith for the Seldovia-Kodiak Islands schists. This phenomenon may either be explained by a process of selective subduction or by the absence of a nearby continental mass.

Selective subduction, as described by Moore (1975), is a process whereby oozes of biogenitic origin are transported from a realm of pelagic deposition to a region of hemi-pelagic terrigenous sedimentation near a subduction zone. During this trip, the biogenitic oozes increase in strength due to diagenitic evolution. As subduction proceeds, newly deposited clastic sediments of low density and strength are scraped off and the pelagics are metamorphosed in the subduction zone along with basaltic oceanic crust in the absence of any appreciable amounts of hemi-pelagic material. It is also possible that there was no continental terrigenous material available to fill the trench associated with the Late Triassic pulse of subduction.

There are no rocks on the Alaska Peninsula which are suggestive of a major continental mass or appreciable magma-

tic arc developing prior to Triassic time. Either selective subduction or the lack of a nearby continent would result in highly metamorphosed biogenitic and basaltic material in the absence of hemi-pelagic sediments.

# BROOKS RANGE METAMORPHIC BELT

## Introduction: Location and Setting

The Brooks Range schist belt as defined by Fritts (1972) is an area confined to the south flank of the Baird-Schwatka Mountains, extending continuously from Chandalar Lake to an area just north of Kiana, a distance of approximately 550 km. The geologic history of the Brooks Range schist belt has been the subject of much discussion and debate over the past several years. Recently, the discovery of stratiform copper deposits in the belt has resulted in intensive mapping programs by federal and state agencies and private concerns. Geologists working within the area have estimated over two billion dollars worth of ore are present within the schist belt (Hawley, 1976).

It must be emphasized that many aspects of the origin and history of the schist belt are conjectural and not agreed upon by everyone working in the area. Several factors contribute to this uncertainty. First, the terrane is polymetamorphic with two and possibly three superimposed metamorphic events. Not only has this complicated the petrology of these rocks, but it has in part obscured the geochronologic record as well. Deformation and recrystallization have modified the original stratigraphy, creating discontinuous and lenticular units along strike.

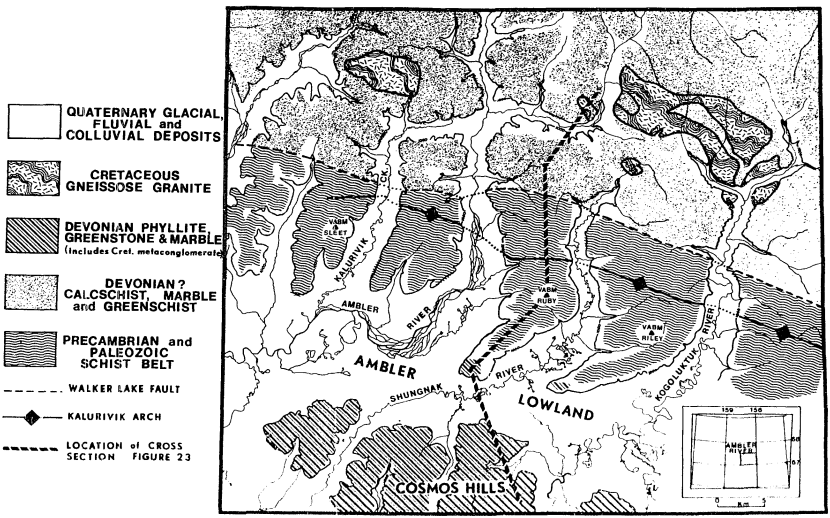


Figure 21. Generalized geologic map of Ruby Ridge and adjacent areas.

Secondly, complicated tectonic styles, including nappe-like structures and large scale thrust faults, have made geologic mapping difficult. Lastly, the varied backgrounds and bias of many geologists working within the same area have resulted in differing interpretations.

Areas selected for a study of the Brooks Range blueschist facies rocks included the VABM Ruby area in the southern part of the Ambler B-2 quadrangle, approximately 9 km north of Bornite (Fig. 21), and several localities in the Baird Mountains quadrangle of the western Brooks Range, 5 km north of Kiana (Fig. 22).

The study area in the vicinity of Ruby Ridge (Ridge containing VABM Ruby, Fig. 23) can be divided into three separate physiographic provinces: (1) the Baird-Schwatka Mountains, (2) the Cosmos Hills-Angayucham Mountains, and the (3) Ambler Lowland-Kobuk Trough.

## Brooks Range Schist Belt

### Introduction

The main part of the Brooks Range schist belt that contains the glaucophane-bearing assemblages extends from the low ridges on the south flank of the schist belt northward to the trace of the Walker Lake Fault (Fig. 21). This 15 km wide section, which broadens toward the Baird Mountains in the west, is dominated by buff-colored quartz-mica schist

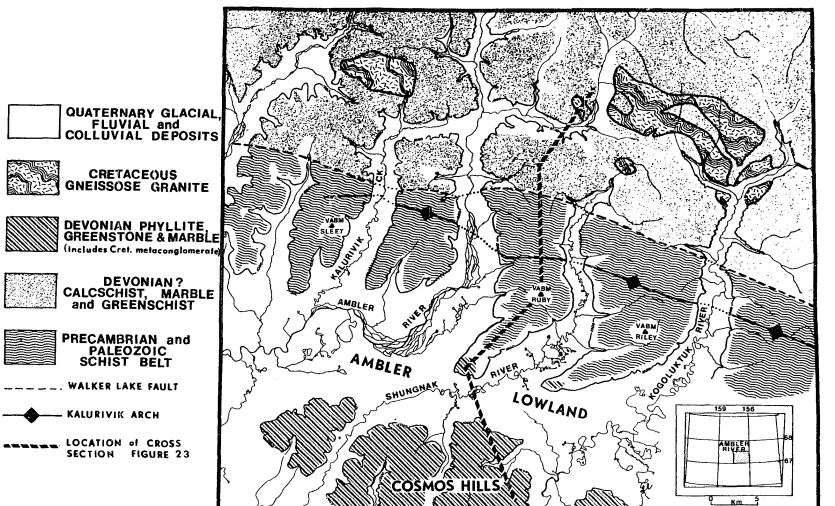


Figure 21. Generalized geologic map of Ruby Ridge and adjacent areas.

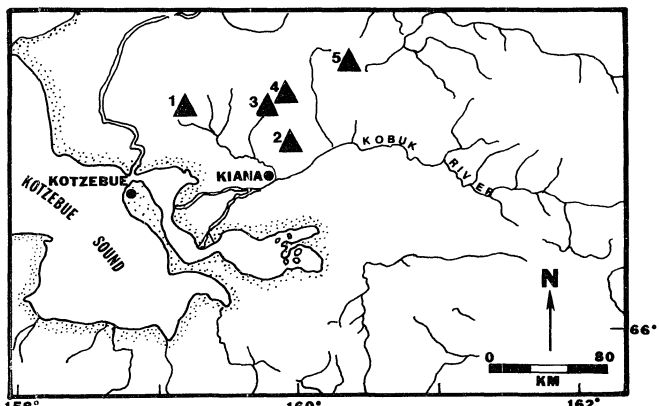


Figure 22. Location map of blueschist localities (triangles) in the Baird Mountains quadrangle, western Brooks Range.

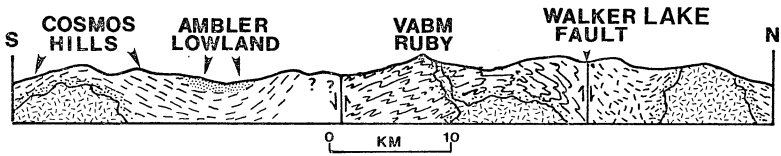


Figure 23. Generalized North-South cross section from the Cosmos Hills to the Walker Lake Fault.

which contain discontinuous layers and lens-shaped bodies of marble, metapsammite, and metavolcanic rocks ranging in thickness from 10 to 500 meters.

The polymetamorphic nature of the Brooks Range schist belt is clearly reflected in the rocks of Ruby Ridge. These rocks have experienced at least two periods of metamorphism. The first event metamorphosed the rocks to the blueschist facies, and the second dynamo-thermal event partially recrystallized these rocks under greenschist facies conditions (Gilbert and others, 1977).

The most pronounced and easily recognized structure in the schist belt is an antiform called the Kalurivik Arch (Pessel and others, 1973a). The axis of this structure is 5 km north of VABM Ruby. According to Gilbert and others (1977), the arch is defined by the arching of $S_1$ surfaces; however, it does not affect $S_2$ surfaces which may be synchronous with the development of the arching. The arching may have been caused by the emplacement of a Cretaceous granite pluton similar to the Shishsakshinovik or Redstone pluton (I. Tailleur, personal communication). Skarns observed near the crest of the arch by Wiltse (1975) tend to corroborate this hypothesis.

The Walker Lake Fault was originally described and mapped for 100 km along the strike of the schist belt by Fritts (1972). According to Fritts, it is the most important structural break in this region of the Brooks Range

and separates two differing terranes. The terrane to the north of the Walker Lake Fault is dominated by low-rank metasedimentary rocks containing the assemblage quartz-albite-muscovite-chlorite $\pm$ calcite and biotite. At several localities biotite appears to be incipient, forming from the reaction of chlorite and white mica. Several outcrops contain chloritoid in addition to the above phases (W. Gilbert, personal communication). Several small greenstone and marble bodies are intercalated with the pelitic schists along a narrow outcrop belt (Gilbert and others, 1977). The metabasite (chlorite-epidote-albite-actinolite) is generally of lower grade and finer-grained than the metabasite located south of the fault. Rocks north of the Walker Lake Fault may be stratigraphically correlative with the rocks of the Cosmos Hills terrane. If this inference is correct then it would imply that the glaucophane-bearing metabasites occur in a basement core which was mantled by now eroded Devonian rocks. The rocks north of the Walker Lake Fault, the low-lying spurs on the southwest tip of Ruby and adjacent ridges, and in the Cosmos Hills are all that presently remain of the Devonian section (Fig. 21), with the rare exception of infolded Devonian rock in the schist belt (which is described later).

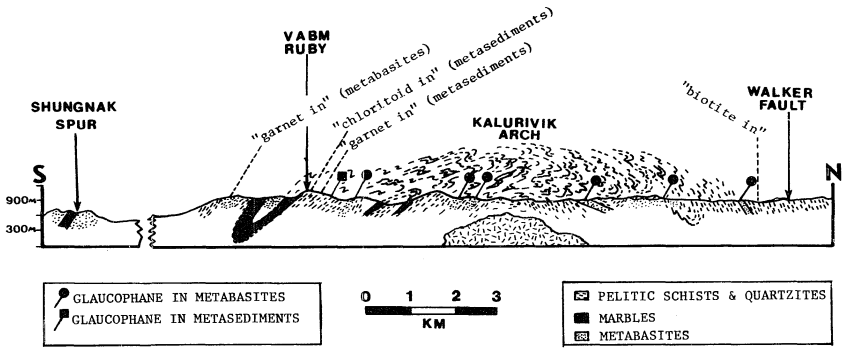


Figure 24. Generalized structure section through Ruby Ridge showing blueschist localities and relationship of major mineral phases. (Modified from Forbes and others, 1973).

Figure 25. Original bedding in weakly metamorphosed carbonate on Shugnak Spur, south of Ruby Ridge.

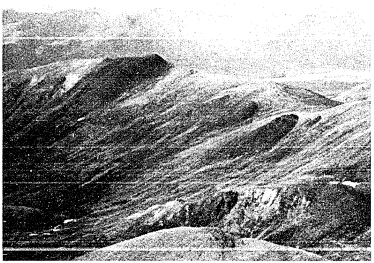

Figure 26. Dark, lens-shaped masses of metabasite containing coarse-grained glaucophane rocks on Ruby Ridge.

## Petrology and Metamorphism

### Pelitic Schist

Pelitic schist which is the dominant unit in the schist belt is mainly composed of quartz, mica, albite, and chlorite, although graphitic varieties are abundant north of the Kalurivik Arch.

Chloritoid is present in trace amounts north of the Walker Lake Fault, but the dominant occurrence is in a narrow zone across several ridges in the area of Ruby Ridge (Fig. 24). At Ruby Ridge, this zone crops out just north of VABM Ruby. According to Halferdahl (1961), chloritoid occurs in highly aluminous, low-temperature metapelites and indicates that the parent rocks had a high $Fe^{+2}/Mg$ ratio.

Biotite is conspicuously absent in most of the section with the exception of the contact zone around intercalated feldspathic schists. The absence of biotite in the metapelites, particulary those containing both muscovite and chlorite, suggests that these rocks recrystallized under temperatures below the biotite isograd. Toward the Walker Lake Fault, however, incipient biotite is present indicating that the metamorphic gradient of the second event increases toward the north (Gilbert and others, 1977).

Garnet is rare in metapelites, but when present, it occurs as incipient skeletal grains. Garnet appears to be

late, probably formed during the second period of metamorphism.

Marble and Fossil Aragonite

Marble occurs as gray weathered lens-like bodies which pinch out along strike. Because the marbles are intimately associated with blueschist facies rocks, they were inspected closely for aragonite.

Biaxial carbonate was found in the metamorphic rocks in the western Baird Mountains quadrangle 29 km west of the north fork of the Squirrel River and 20 km south of the Agashashok River (Fig. 22, Locality 1). Although the carbonate is associated with glaucophane, other high pressure phases such as jadeite and lawsonite are conspicuously absent. The glaucophane lenses are boudin-like masses in fossiliferous Devonian carbonates and appear to have been rolled up in thrust masses.

Carbonate crystals occur as elongate prisms up to 1.3 cm long with the c-axis preferentially oriented in the rock (Fig. 29). Optical studies of the carbonate on a four axis universal stage reveal biaxial optic angles which average 20 degrees suggesting the presence of aragonite. However, subsequent x-ray studies revealed that the carbonate is now calcite.

All aragonite which is formed during high pressure metamorphism is not preserved in the geologic record. Aragonite easily undergoes back reaction to calcite, especially at high temperatures or in the presence of fluids (Davis and others, 1965). Consequently, aragonite is unknown in retrograde metamorphic terranes. It may, however, be possible to determine whether pressures suitable for the formation of aragonite were attained by observing the interference figures of calcite. Boettcher and Wyllie (1967a) have found that aragonite grains which have inverted to calcite have anomalous optic angles ranging up to 20 degrees and suggest that such figures are indicators of inverted aragonite (fossil aragonite).

Because biaxial calcite can be formed in other ways, it is not unique evidence for the prior existence of aragonite. El-Hinnawi (1973) acknowledges that calcite inverted from aragonite can exhibit biaxial interference figures, but he also notes that biaxiality may be produced by several other means. During preparation of a thin section, if a basal face should parallel the surface of the glass slide, microstrain may cause translation in the crystal lattice producing large biaxial optic angles. Furthermore, the presence of twin lamellae in calcite develops abnormal biaxial optic angles due to dislocations in the crystal lattice. However, both of these conditions would produce strained uniaxial

figures with optic angles which are no greater than 10 degrees.

The Squirrel Creek carbonate has sufficiently larger optic angles (15-20 degrees) than strained calcite and agrees well with the 20 degree figure that Boettcher and Wyllie observed in back-reacted aragonite. Because aragonite is difficult to preserve in the geologic record, its former existence may be inferred from the presence of biaxial carbonate which has optic angles greater than 15 degrees, especially if it occurs with other high pressure phases such as lawsonite, jadeite, or glaucophane.

The presence of aragonite by itself does not necessarily imply high pressure of crystallization because Vance (1968) described metastable aragonite in recrystallized limestones and vein fillings associated with low-grade metamorphic rocks in the prehnite-pumpellyite facies. Vance notes that the high pressure recrystallization of laumontite to lawsonite that takes place well below the calcite-aragonite transition curve (Fig. 27) is conspicuously lacking in the rocks of the San Juan Islands of Washington state. The coexistence of laumontite and aragonite is an apparent petrologic paradox because laumontite should react to form lawsonite before the stability field of aragonite is reached. In addition, Vance presents structural and stratigraphic

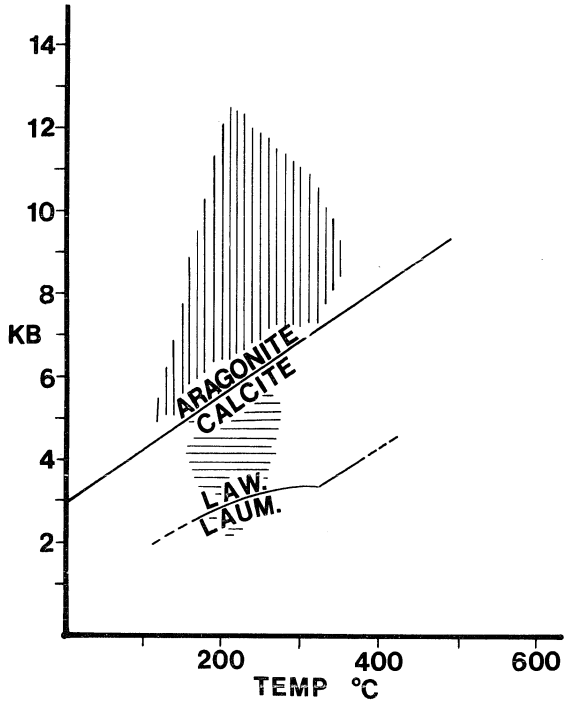


Figure 27. Phase diagram of the calcite-aragonite (Boettcher and Wyllie, 1967) and laumontite-lawsonite (Liou, 1971) univariant boundaries. Also illustrated are the fields of blueschist and prehnite-pumpellyite facies metamorphism (Turner, 1968).

evidence precluding burial to a depth which would develop those pressures required for the recrystallization of metamorphic aragonite. Based on the above observations, Vance questioned the validity of aragonite as a reliable indicator of high pressure metamorphism.

Newton and others (1969) have described two conditions which explain the crystallization of aragonite at lowered pressures. The first cause is the result of deformational strain energy stored in the calcite. It was found that significant amounts of aragonite are produced at pressures considerably below the usual stability field (Fig. 27) from a starting mixture of calcite previously strained by mechanical grinding. The lowering of the univariant curve for the calcite-aragonite transition is approximately equal to $\varepsilon/\Delta V$, where $\varepsilon$ is the plastic strain energy in calories per mole and $\Delta V$ is the change in volume. Newton states that the pressure necessary to produce aragonite at the expense of strained calcite is reduced by 14.8 kb per kcal of strain energy per mole. Thus, an accumulated strain energy of only 170 cal/mole would effectively lower the stability field by 2.5 kb, placing the calcite-aragonite univariant curve below the laumontite → lawsonite reaction curve but still within the prehnite-pumpellyite facies (Fig. 28). The second source of recrystallization below the usual experimentally derived transition curve is due to the metastable oversatura-

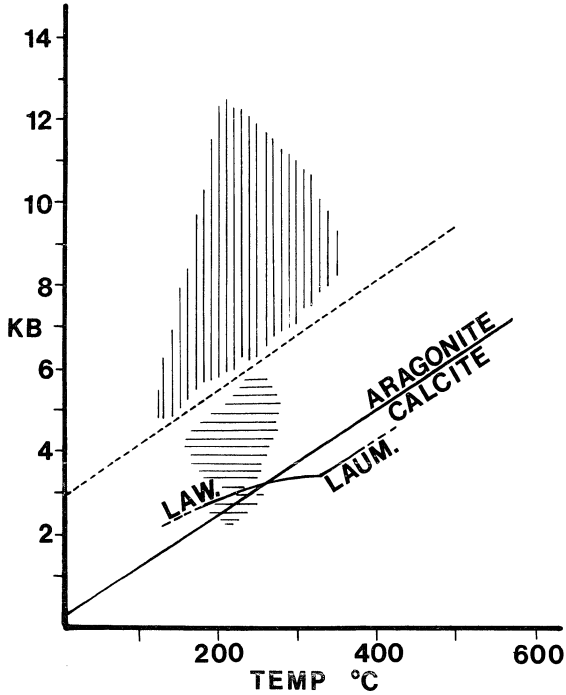


Figure 28. P-T diagram illustrating the reduction of the aragonite-calcite univariant curve by an applied strain of 170 cal/mole. Dotted line is the former position of the univariant curve.

Figure 29. Calcite pseudomorphs after aragonite prisms. Dark trains are graphite and represent original layering.

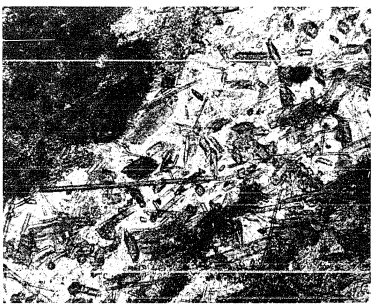

Figure 30. Glaucophane-bearing rock from the Squirrel Creek area (Figure 22, Locality 1) showing random orientation of glaucophane (needle-like crystals) in a carbonate matrix. Dark area at upper left and lower right is chlorite.

tion of $MgCO_3$ in calcite (Folk, 1974), which effectively lowers the pressure constraints for the transition to aragonite. Both factors could conceivably lower the stability field of aragonite under metamorphic conditions. Accordingly, the structural history of a metamorphic terrane and the chemical composition of the carbonate must be taken into account if the calcite-aragonite geobarometer is to be of any value, particulary in those terranes which lack other high pressure minerals such as lawsonite and jadeite.

The lack of schistosity and preferred orientation of the Squirrel Creek schist is indicated by the random orientation of the coexisting glaucophane needles (Fig. 30), the absence of twinning in the calcite of the marbles, and to the presence of undeformed crinoid columnals in the surrounding limestone. These criteria strongly suggest that the schist was not subjected to a pervasive penetrative deformation either during or subsequent to metamorphism. Rather, the strain appears to be homogeneous suggesting that uniform confining pressure (hydrostatic type) was the dominant element of stress.

Therefore, strained calcite is not an important criterion in depressing the stability field for the formation of aragonite in these rocks. Furthermore, the calcium carbonate was x-rayed for the presence of Mg by looking at the d-spacing of critical calcite peaks. Based on x-ray

data, the calcium carbonate is pure end-member calcite with very little or no Mg. Thus, the calcite represents the retrogradation of aragonite which was once present in the rock. Assuming a minimum temperature of 200° C necessary for the formation of coexisting glaucophane, a pressure of at least 5 kb is necessary if aragonite is stable under conditions like those determined under experimental laboratory conditions.

Metavolcanic Rocks

Both felsic and mafic metavolcanic rocks occur on Ruby Ridge. The most obvious difference between the two types, besides chemistry, is that the metabasite is completely composed of metamorphic minerals with no relict igneous phases present. Conversely, the metafelsite has a blastoporphyritic texture with many relict igneous phases present. As discussed in the next chapter, microstructural analysis of the metabasite indicates that it has experienced a polymetamorphic history as evidenced by mineral zonation, retrograde textures, overgrowths and cross-cutting mineral foliations; whereas the metafelsites do not show evidence of polymetamorphism.

This evidence suggests that the metabasite is older than the metafelsites and that the formation of the metafelsite was subsequent to the glaucophane forming metamorphic

event. Although inconclusive, the dates obtained by Turner and others (1977) support this line of reasoning because glaucophane-bearing metabasites yield K-Ar ages older than Cambrian, whereas the oldest metafelsite dated is of Cretaceous age. However, only mica has been dated out of the metafelsite unit and it is probable that if the micas were older than Cretaceous, they would have been among the first minerals reset by the Cretaceous episode of metamorphism.

According to Wiltse (1975), the felsic metavolcanic rocks have a schistose microstructure containing quartz, microcline, muscovite, biotite, and albite. Blastoporphyritic quartz and microcline crystals are often euhedral with deep embayments within the megacrysts suggesting that the protolith is of either hypabyssal or volcanic origin. The most easily recognized of the metafelsite units is the "button schist" which derives its name from the large megacrysts or "buttons" of relict microcline. The origin of the biotite that occurs within and adjacent to the button schist and related K-spar variants is of importance in determining the pressures and temperatures of metamorphism of the second event.

Biotite does not occur as a coeval phase in metapelitic or metabasic assemblages within the blueschist zone. However, incipient biotite does occur to the north of the Kalurivik Arch (Fig. 24) and may be related to an increase

in metamorphic grade in the second (greenschist facies) metamorphic event (Gilbert and others, 1977). It is probable that the formation of biotite is not related to the earlier blueschist event because it is not retrograded or cut by a later foliation; furthermore, biotite is characteristically absent in blueschist facies events (Taylor and Coleman, 1968).

It is generally agreed that the brown biotite that occurs within the felsic schists is of igneous origin (Wiltse, 1975). However, the incipient biotite, which occurs a few feet from the metafelsite-pelitic schist contact, is of disputed origin. Wiltse (1975) believes that the incipient biotite is related to tuffaceous volcanic debris shed from subaqueous marine felsic lava domes which gave the surrounding pelitic sediments a high potassium content. Accordingly, a subsequent period of metamorphism to the quartz-albite-epidote-biotite subfacies of Barrovian greenschist metamorphism formed the incipient biotite which is found in the adjacent schists.

I do not agree with Wiltse's hypothesis. If the second period of metamorphism was of high enough grade to form biotite adjacent to the intrusives, then it should also be found elsewhere in the section where coexisting chlorite and muscovite occur in the absence of biotite. Furthermore, at least some of the biotite in schists on Ruby Ridge adjacent

to metavolcanic rocks is discordant to the dominant foliation defined by the white micas suggesting that the biotite is post-kinematic and due to contact metamorphism. Finally, it is unlikely that a felsic lava which was emplaced subaqueously would have relict phenocrysts at all but, rather more probably, the texture would be holohyaline. Therefore, the phases we see should be derived from the recrystallization of glass rather than coarse-grained igneous fabrics.

An alternative hypothesis which more reasonably explains the observed relations is that the metafelsite is synkinematically emplaced hypabyssal material related to the Cretaceous plutonism seen throughout the area. If this hypothesis is correct, then shallow level dikes or sills carried their own thermal pertubation with them hornfelsing the adjacent rocks and forming the incipient biotite. Furthermore, hypabyssal intrusions would better explain the relict igneous phenocrysts in the metafelsites. This hypothesis is in agreement with the radiometric ages obtained from the micas dated from the metafelsite (Turner and others, 1977) which are Cretaceous in age.

The most conspicuous and easily identified rocks in the vicinity of Ruby Ridge and in the western Brooks Range are metabasite which form blocky weathered, prominent, dark colored ridges and pod-like outcrops (Fig. 26). These rocks are generally massive with little or no schistosity developed

in metamorphic grade in the second (greenschist facies) metamorphic event (Gilbert and others, 1977). It is probable that the formation of biotite is not related to the earlier blueschist event because it is not retrograded or cut by a later foliation; furthermore, biotite is characteristically absent in blueschist facies events (Taylor and Coleman, 1968).

It is generally agreed that the brown biotite that occurs within the felsic schists is of igneous origin (Wiltse, 1975). However, the incipient biotite, which occurs a few feet from the metafelsite-pelitic schist contact, is of disputed origin. Wiltse (1975) believes that the incipient biotite is related to tuffaceous volcanic debris shed from subaqueous marine felsic lava domes which gave the surrounding pelitic sediments a high potassium content. Accordingly, a subsequent period of metamorphism to the quartz-albite-epidote-biotite subfacies of Barrovian greenschist metamorphism formed the incipient biotite which is found in the adjacent schists.

I do not agree with Wiltse's hypothesis. If the second period of metamorphism was of high enough grade to form biotite adjacent to the intrusives, then it should also be found elsewhere in the section where coexisting chlorite and muscovite occur in the absence of biotite. Furthermore, at least some of the biotite in schists on Ruby Ridge adjacent

to metavolcanic rocks is discordant to the dominant foliation defined by the white micas suggesting that the biotite is post-kinematic and due to contact metamorphism. Finally, it is unlikely that a felsic lava which was emplaced subaqueously would have relict phenocrysts at all but, rather more probably, the texture would be holohyaline. Therefore, the phases we see should be derived from the recrystallization of glass rather than coarse-grained igneous fabrics.

An alternative hypothesis which more reasonably explains the observed relations is that the metafelsite is synkinematically emplaced hypabyssal material related to the Cretaceous plutonism seen thr[illegible]rea. If this hypothesis is correct, th[illegible] or sills carried their own thermal [illegible]felsing the adj[illegible]more, hypabyssal in[illegible]ite. Furthermor[illegible]igneous phenocrysts [illegible]lain the relict ign[illegible]in agreement with the r[illegible]nis hypothesis is in agreement with the r[illegible]btained from the micas dated from the metafelsite (Turner and others, 1977) which are Cretaceous in age.

The most conspicuous and easily identified rocks in the vicinity of Ruby Ridge and in the western Brooks Range are metabasite which form blocky weathered, prominent, dark colored ridges and pod-like outcrops (Fig. 26). These rocks are generally massive with little or no schistosity developed

within the core zones. However, the margins are frequently schistose and display a higher degree of retrograde metamorphism on the outer margin than within the core. Pillow structures are present in metabasites of Horse Creek north of VABM Ruby and near Picnic Creek in the Survey Pass quadrangle (Wiltse, 1975).

At the outset of this study, it was believed that the blue and green amphibole-bearing metabasites occurred together in time as well as space and that the blue amphibole basites were the high temperature type as discussed by Taylor and Coleman (1968). This view stemmed from the absence of aragonite and lawsonite, a situation which is analogous to the relationship between the blueschists and greenschists at Seldovia. This study will show that there is a continuous gradation between the two end members (greenschist-blueschist) due to a strong thermal event that upgraded the blue amphibole-bearing metabasites to the greenschist facies.

Futhermore, it is now evident that the original blueschist event was not the high temperature type as previously interpreted from the presence of calcite rather than aragonite, epidote rather than lawsonite, and the scarcity of jadeite. Instead, most of the low-temperature blueschist facies mineral assemblages have been retrograded to high temperature assemblages due to a strong subsequent thermal event.

As previously noted, there is strong evidence for the prior existence of aragonite in these rocks and although lawsonite has not been found in situ, it nevertheless has been found as a detrital phase in the sediments which have been shed from the Brooks Range (Luepke, 1975). Jadeite in association with quartz and glaucophane was discovered by R. Forbes (Forbes and others, 1973) just northwest of VABM Ruby in a relict fabric cut by a later foliation defined by sericite, chlorite, paragonite, and sodic actinolite. Furthermore, a previously undescribed jadeite locality was discovered during this study in an outcrop which forms the southwestern tip of the divide between the Kogoluktuk River and an unnamed tributary to the east (Fig. 21). These lines of evidence indicate that the metamorphic event responsible for the formation of glaucophane in these rocks is the low-temperature type of Taylor and Coleman (1968).

The newly discovered jadeite locality also has regional significance. This rock was previously thought to have incipient blue amphibole rimming relict augite phenocrysts and to be equivalent to Devonian metabasite found in the Cosmos Hills (I. Tailleur, personal communication). This occurrence called for a hypothesis postulating two blue-schist facies metamorphic events: (1) a Precambrian event explaining the retrograded glaucophane-bearing metabasites in the main part of the Brooks Range schist belt and (2) a

post-Devonian episode which formed the incipient blueschist facies metamorphism in the volcanic rocks located along the south margin of the Precambrian (age discussed in next section) Brooks Range schist belt (Forbes and Turner, 1974). The pyroxene thought to be relict augite has an abnormally low $z\wedge c$ ($29^{\circ}$) and an optic angle of 60 degrees, both which are low for augite or diopside. Upon x-ray examination of a whole rock sample, three of the most intense peaks for jadeite were discovered (Table 3). In thin section, the

Table 3. Table of observed d-spacings versus the three most intense reflections from A.S.T.M. jadeite standards.

| 75-JC-01 split one | 75-JC-01 split two | A.S.T.M. 9-463 | A.S.T.M. 2-0723 | hkl |
|---|---|---|---|---|
| 2.45 | 2.44 | 2.42 | 2.42 | 221 |
| 2.83 | 2.84 | 2.83 | 2.84 | 310 |
| 2.95 | 2.94 | 2.92 | 2.94 | $\bar{2}21$ |

glaucophane associated with the pyroxene is not incipient on pyroxene as was previously thought, but is seen to be replacing it on a wholesale basis. This relationship indicates that the glaucophane is a retrograde product. Furthermore, the high degree of crystallinity of associated rocks collected from the same locality indicates that these rocks are not part of the feebly metamorphosed Devonian(?) section cropping out on the south flank of the main part of the schist belt, as typified by the rocks on the south end of Ruby

Ridge and in the Cosmos Hills. Rather, they most likely belong to the higher grade retrograded metabasites from the Brooks Range schist belt which are characterized by a higher degree of crystallinity. The jadeite is relict, as it is in the Ruby Ridge outcrop which Forbes and others (1973) described and has probably retrograded to glaucophane during the waning stages of the blueschist facies metamorphic event. Similar retrograde relations have been described in the glaucophane schists of the Alps (Cortesogno and others, 1977).

As discussed under interpretations of the Cosmos Hills, the Devonian rocks of the Cosmos Hills probably have been downwarped under the Ambler Lowlands and re-appear as low-grade metavolcanics, marbles, and phyllites on the south spurs of the main part of the Brooks Range schist belt. Evidence indicates that the increase in metamorphic grade is enough to warrant a fault between the south spurs and the schist belt (Fig. 23). Previously, the jadeite locality was thought to be on the south side of this fault in the low-rank Devonian(?) rocks but the evidence indicates that the locality must be on the north side of the presumed extension of the fault. Therfore, there is no evidence for a Post-Precambrian blueschist event in the Brooks Range.

## AGE

Details of the age relationships on the timing of the metamorphic events in the Brooks Range schist belt have been discussed by Turner and Forbes (1978) and Turner and others (1978). The relationships are summarized in a histogram (Fig. 31) which shows the distribution of 62 individual mineral ages from the metamorphic rocks of the schist belt by mineral type.

There are two main groups on the histogram. One group is composed mainly of micas around 115 m.y., and the other group is composed mainly of glaucophanes but includes actinolite and white mica ages grouping at about 625 m.y. There is a more or less continuous distribution of actinolite ages between the two groups with a minor secondary grouping(?) around 210 m.y., defined by 4 paragonites and several actinolites, although it may be part of a continuous distribution trailing off the 115 m.y. peak.

The micas and actinolites which make up the 90-130 m.y. group come from many locations along the length of the schist belt from the Baird Mountains quadrangle on the west to the Survey Pass quadrangle on the east. According to Turner and others (1978), the event defined by these micas represents cooling ages from the waning stages of an upper Mesozoic orogeny which was probably accompanied by a syn-kinematic belt of east-west trending gneissose granitic

plutons yielding similar Late Cretaceous ages. These ages are compatible with the stratigraphy of immature flysch-type sediments which were shed off the proto-Brooks Range due to an orogenic event in mid- to late Mesozoic time and were deposited in a basin north of the present Brooks Range (Payne, 1955).

The distribution of the data that constitute the Cretaceous group on the histogram (Fig. 31) is of interest. The biotites are notably younger than the muscovites which trail off toward older ages. These biotites were probably crystallized during the Cretaceous event, whereas some of the muscovite composing the Cretaceous group probably formed during the earlier Precambrian event. The reasoning behind this statement is that all of the biotite seen is late, cross-cutting the dominant foliation, or associated with feldspathic schists which appear to be of hypabyssal origin and related to synkinematic plutonism. There is good evidence that at least one sample of muscovite (74AF 145-1), collected north of Kiana in the western Brooks Range, has not been reset by the subsequent Cretaceous event. Also, a rock collected on the south side of Ruby Ridge (RR7g) has coexisting glaucophane and muscovite. The muscovite yields a K-Ar age of 124 $\pm$ 4 m.y. while the glaucophane gives a K-Ar age of 587 $\pm$ 59 m.y. suggesting that the mica was reset by the pervasive Cretaceous event. The histogram (Fig. 31)

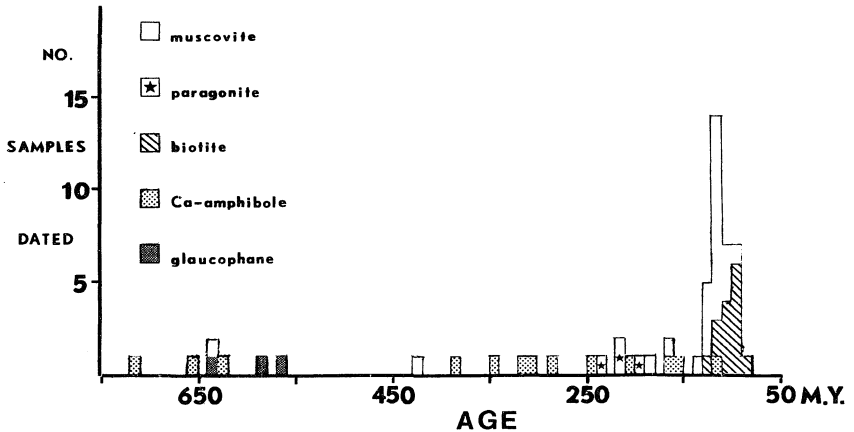


Figure 31. Histogram illustrating the distribution of K-Ar ages of the Brooks Range schist belt by mineral type. Data from Turner and others (1977).

is interpreted by Turner and others (1978) as evidence of incomplete argon degassing by the Cretaceous event.

The late Precambrian ages (Turner and others, 1978) have been challanged by some geologists working in the area who believe that the Brooks Range schist belt is of Devonian age and that the older age may be due to inherited argon (argon not formed from the decay of $^{40}K$ in the mineral dated since the recrystallization event). In order to distinguish between ages which are geologically meaningful and those which are anomalously old, Turner and others (1978) have plotted the Late Precambrian K-Ar age data on a $^{40}K$/apparent $^{40}Ar_{rad}$ isochron diagram similar to the one represented in Figure 32.

On this type of diagram the moles/gram of $^{40}K$ define the abscissa and the moles/gram of apparent $^{40}Ar_{rad}$ define the ordinate on a cartesian coordinate system. Ideally, for a suite of coeval samples, the data points will define a straight line or isochron. The slope of this line is a function of the age of the group of rocks which were plotted, and the y-intercept is the apparent initial $^{40}Ar_{rad}$ content of the system when the potassium-argon clock was set. It is important to determine if inherited argon was present in a system prior to the time at which the potassium-argon clock is set because one of the basic assumptions of the method is that the mineral has been a closed system

since $t_0$ and there has been no loss or gain of $^{40}Ar$ except for that which results from the radioactive decay of $^{40}K$ (Dalrymple and Lanphere, 1969). The inherited argon problem becomes particulary important for low-potassium minerals such as glaucophane because as little as $4x10^{-11}$ moles/gram of argon may increase the age of a 560 m.y. glaucophane to 1166 m.y. when the $K_2O$ content is 0.028.

Some low potassium glaucophanes, collected from the vicinity of Ruby Ridge, plot off the histogram (Fig. 31) and yield ages of 1.3 to 2.6 billion years. Turner and others (1978) believe that these low potassium minerals have occluded argon during their crystallization because they plot above the 634 m.y. isochron which is composed of three glaucophanes, two actinolites, one hornblende, and one muscovite. It is doubtful that the isochron age has been affected by the inherited argon problem because it would take an improbably large amount of inherited argon to significantly change the age of the muscovite that contains 11.0 percent $K_2O$ and controls the age of the isochron. Also, such a problem would cause the points to be scattered off the isochron due to incorporation of different amounts of argon.

The scatter of the thirteen actinolite ages, which are fairly equally distributed between the two main pulses of metamorphism, may be explained by one of two hypotheses: (1) the actinolite formed during the waning stages of the Pre-

cambrian blueschist event; during the Cretaceous greenschist event a dynamo-thermal episode caused incomplete degassing of the argon in the actinolite which yields an age pattern that trails away from the Precambrian peak, or (2) the green amphibole formed during the Cretaceous event and the older ages are due to the incorporation of various amounts of inherited argon. When the actinolites are plotted on a $^{40}K$/apparent $^{40}Ar_{rad}$ diagram, they show considerable scatter and almost no correlation. This is not surprising since it is unlikely they have gained or lost argon in a systematic manner according to their K content. Turner and others (1977) favor the first hypothesis because one would expect to see an inverse correlation between the ages and the potassium content of the minerals if the second hypothesis were operative. They see no such correlation in their data.

As previously noted, there is a suggestion of a peak around 210 m.y. on the histogram (Fig. 31). When the data are plotted on a $^{40}Ar_{rad}$ diagram, the points lie close to a 217 m.y. "isochron" which intercepts the y-axis through the origin (Fig. 32). Upon close inspection of data, however, five of the eight points are seen to plot off the "isochron"; therefore, the isochron is not real. Turner and others (1978) stated that the minerals represented by these ages are incompletely overprinted by the Cretaceous event. At present, there are no other geologic data of which I am aware of that indicates another metamorphic event.

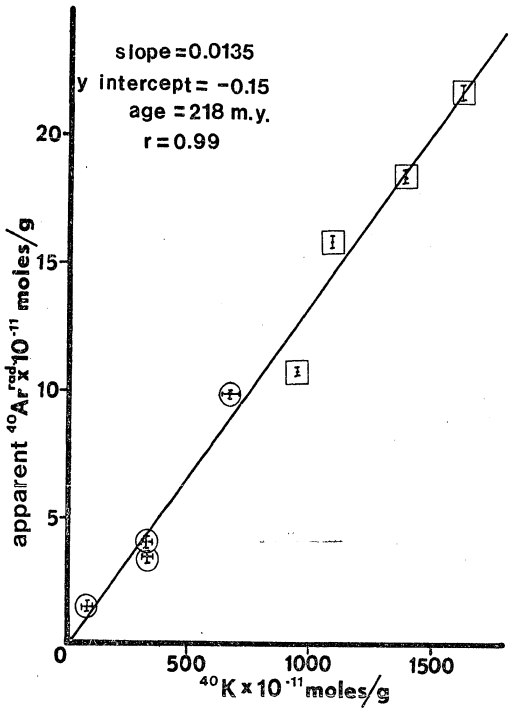


Figure 32. $^{40}K$-apparent $^{40}Ar_{rad}$ "isochron" diagram of the suspected 218 m.y. event. Circles are actinolite; squares are paragonite. Error bars are indicated for each analysis. Data from Turner and others (1978). Five of the eight points plot off the "isochron" indicating that the "isochron" age is not valid.

Cosmos Hills

Geologic Relations

Most of the early work in the Cosmos Hills was done by Fritts (1969, 1970a, 1970b, 1972). The Cosmos Hills are primarily composed of phyllites with lesser amounts of metacarbonates intercalated with metavolcanic rocks. This sequence is Devonian in age based on fossil collections from the metacarbonate layers which are intercalated with metavolcanic rocks near Stout Mountain and Fergeuson Peak (Fritts, 1969, 1970b). Cretaceous metaconglomerates with subordinate amounts of phyllite and metabasalt overlie the Devonian section and are thought to be in thrust contact (Fritts, 1970b). A gneissic granitic pluton nearly 3 km in diameter intrudes the Paleozoic strata near the Kogoluktuk River. An abundance of garnets occurring near the contact suggests that the intrusion locally hornfelsed the surrounding schists in the area. The intrusion may also be responsible for the doming observed in the Cosmos Hills (Fritts, 1970b). Similar Cretaceous intrusions may be responsible for doming and arching seen elsewhere in the Brooks Range (I. Tailleur, personal communication).

The Ambler Lowland-Kobuk Trough separates the Cosmos Hills-Angayucham Mountains from the Baird-Schawtka Mountains. The trough is a lowland area devoid of outcrop and heavily

mantled with Quaternary surficial deposits. Its origin is regarded as a locus of thrust faulting (Fritts, 1972) or as a tectonic trough (Pessel, 1973b) in which Devonian rocks of the Cosmos Hills have undergone a synformal downwarp, (Fig. 23) reappearing as low rank marble, phyllite, and greenstone on the low-lying outcrops at the tip of Ruby (ridge containing VABM Ruby) and adjacent ridges (Fig. 21).

## Interpretations

Some workers believe that much of the schist belt is correlative with rocks of the Cosmos Hills. This theory is based on three lines of evidence. First, fossils collected from the schist belt are Paleozoic. Second, glaucophane occurs in the Cosmos Hills. Third, structural evidence suggests that the two terranes may be equivalent.

Fossil-like forms from the Brooks Range schist belt have only been recovered from the Arctic Camp area, and locality 17 in the western Survey Pass quadrangle (Brosge and Pessel, 1977). The Arctic Camp occurrence has been discredited because the fossil-like forms have been interpreted as inorganic phenomena by M. Churkin of the U. S. Geological Survey (M. Churkin, personal communication). However, fossil locality 17 in the Survey Pass quadrangle (Brosge and Pessel 1977) contains inferred Middle Devonian to Early Mississippian crinoid columnals which have been

identified by G.D. Webster of Washington State University. However, Bill Oliver of the U. S. Geological Survey has assigned them as Paleozoic undifferentiated (I. Tailleur, personal communication). This locality is the only occurrence of fossils ever documented in the Brooks Range schist belt; all other marble outcrops investigated were barren. The Devonian age is particularly troublesome because the fossils are intercalated with schists that are thought to be Precambrian in age (Turner, 1978). Furthermore, in the western Brooks Range, Brosge and Pessel (1977) have mapped strata containing Ordovician graptolites which appear to depositionally overlie the schist belt. If this relationship is correct, the Paleozoic Devonian age for the schist belt is inconsistent with the stratigraphic relations in some areas and with geochronologic constraints in others. The apparent differences may be explained if the marble layer containing the fossil assemblage is infolded or infaulted near the top of the Precambrian section. This relationship is possible because Gilbert and others (1977) have described the schists as having undergone isoclinal recumbent folds and nappe-like features coupled with thrusting in the schist.

During the summer of 1972, I. Tailleur (1973, personal communication) found what he believed to be a glaucophane occurrence at an elevation of 2000 feet near Stout Mountain

in the Cosmos Hills. This occurrence was checked by the author during a reconnaissance visit in the summer of 1975; however, no glaucophane schists were found. However, numerous samples of glaucophane schist derived from the schist belt across the Ambler Lowland were found as float in the morainal debris near the mining community of Bornite. Since Fritts (1969) reported glacial debris as high as 2200 feet in elevation plastering the slopes in the Cosmos Hills, it is possible that the blueschist sample reported by Tailleur could be float. Furthermore, the rock picked up by Tailleur is more coarse-grained than any sample reported in the Cosmos Hills and is similar to typical Brooks Range glaucophane schists which contain the largest porphyroblasts of glaucophane yet found in worldwide blueschist belts.

Finally, it is probable that the rocks of the Cosmos Hills have been downwarped under the Ambler Lowland, to reemerge as low-grade metavolcanics and marbles on the southernmost outcrops of the schist belt (Fig. 23). However, the hypothesis that these rocks increase in metamorphic grade to the north and are equivalent to the rocks of the main part of the Brooks Range schist belt is unsubstantiated. Rocks exposed on the southernmost flank of the schist belt are dominantly low-rank greenstone with intercalated marble, metachert, metasiltstone, and meta-argillite. Original bedding and layering is still clearly discernible (Fig. 25).

In thin section the rocks show only incipient recrystallization with a blastoporphyritic texture of plagioclase and augite in a chlorite-serpentine mesostasis which appears to have replaced the original glassy matrix. Forbes and others (1973) originally stated that metamorphic grade increases in these low-rank metamorphics to the north. This increase in metamorphic grade is true for the main part of the schist belt (Fig. 21), but prograde relations are obscure, if present, in the three kilometers of intervening section between the south ends of the ridges and the southernmost portion of the belt. The main part of the schist belt is dramatically different in lithology, structure, and degree of metamorphism. It is unlikely that these rocks have experienced an increase in metamorphic grade in such a short distance because other isograds in the main part of the schist belt are not telescoped. A fault, as shown in Fig. 23, or an unconformity between the two sequences would more satisfactorily explain the relationships observed in the field. Unfortunately, the intervening section is covered and no fault can actually be seen.

This evidence indicates that the proposed correlation between the schist belt and the rocks of the Cosmos Hills is improbable; such a correlation must be regarded as tenuous and suspect on the basis of present knowledge.

## PETROGRAPHY

### ANALYTICAL METHODS

The following discussion is based on the study of over 250 thin sections from the Brooks Range and 75 from the Seldovia-Port Graham-Kodiak Islands area. Micrometric analyses using standard petrographic techniques were employed to determine the modes and describe the mineralogy. Extinction and optic angles were determined on a four-axis universal stage according to the methods described by Wahlstrom (1969, p. 401-422). Modes are based on 1000 points per thin section and analytical error is calculated to be less than 2 percent (van der Plas and Tobi, 1965).

X-ray analyses were performed using a Norelco x-ray diffractometer to determine the presence or absence of critical phases. For routine work, the samples were scanned from 5 to 60 degrees $2\theta$ at a speed of one degree $2\theta$/minute and recorded on a chart at a drive speed of 1 inch per minute. The work involving the shift of the glaucophane $d_{310}$ reflection as related to Na-amphibole chemistry was done at a scan speed of 1/8 degree $2\theta$/minute and recorded using the same chart speed noted above. The location of sodic amphibole $d_{310}$ reflections was refined by calibrating amphibole peaks with those of an admixed quartz standard whose parameters were precisely known. Glaucophane and

quartz peaks ($d_{310}$ and $d_{110}$ respectively) were scanned 16 times (8 reversals) and the absolute positioning of the glaucophane peak was corrected according to the known peak position of the admixed standard. This method is believed to have a maximum error of less than 0.0025 Å.

## SELDOVIA-KODIAK TERRANE

### Blueschist and Greenschist Mineralogy

All of the sodic amphibole in the blueschist from Seldovia and the Kodiak Islands was determined by petrographic and x-ray analyses to be crossite ($Rb_{40}$-$Rb_{68}$). The crossite, which constitutes between 20 to 80 percent of the blue-amphibole-bearing schists of this area, generally occurs as small (<2.0 mm) acicular idioblastic to subidioblastic grains (x=clear to pale yellow; y=lavender; z=medium blue) which define the foliation in these schists. An exception is specimen UK-23c from Uyak Inlet on Kodiak Island. Crossite in this sample has a flamboyant texture, composed of radiating bundles of fine-grained blue amphibole which imparts an almost directionless fabric to the rock. Crossite may also occur as minute (0.025 mm) poikiloblastic inclusions in coexisting quartz or calcite.

A possible explanation for the close, interleaved association of blueschist facies assemblages (crossite-albite-epidote) with greenschist facies assemblages (chlor-

ite-albite-epidote) is retrogression of crossite to chlorite + albite according to the following equation:

2 albite + chlorite → crossite (Miyashiro and Banno, 1958)

However, the crossite is always fresh and unaltered, and there are no textures suggesting that it has retrograded or prograded to the chlorite-albite assemblage.

Actinolite is the other amphibole found in these rocks, always occurring with greenschist facies assemblages and never coexisting with crossite. The actinolite is found as well developed idioblastic to subidioblastic prisms up to several millimeters in length. The prisms are parallel to subparallel and define the foliation in the rock. Actinolite is characteristically pleochroic (x=yellow; y=medium to dark green; z=emerald to blue-green) which suggests that it may be sodic actinolite or barrowsitic hornblende. Most of the actinolite observed was homogeneous; in one sample (AF23-4) however, it exhibited patchy pleochroism. Furthermore, several of the grains in the same outcrop are incipiently rimmed by biotite, suggesting a more complex history.

Pistacitic epidote is the dominant calcium aluminum silicate associated with the blueschist and greenschist facies rocks. It typically occurs as strongly pleochroic subidioblastic laths (x=clear; y=greenish yellow; z=yellow) up to 2 mm in length, which tend to be elongated along the b axis the plane of schistosity. In many instances, espe-

cially in the chlorite schist, cracks are present in the larger epidote porphyroblasts perpendicular to the direction of elongation. The cracks are usually dilated and filled with secondary quartz or calcite. The epidote possibly formed during the major metamorphic event and subsequently, during the tectonic emplacement of the metamorphic wedge, some of the stress was relieved by fracture. Silica and carbonate later migrated into the low pressure fracture. Epidote also occurs as a fine-grained xenoblastic granular matrix in these rocks, as well as in minute poikilolitic inclusions in albite.

Lawsonite was found in one blue amphiobole-bearing outcrop, as confirmed by optical and x-ray data (Table 4). Blueschist facies rocks collected from other outcrops near Uyak Bay, however, contained pistacitic epidote. This occurrence is the only in situ lawsonite yet reported from the state of Alaska. In thin section the mineral occurs as equant subidioblastic porphyroblasts approximately 0.2 x 0.2 mm in diameter, in a fine-grained crossite-chlorite-sphene matrix. The mineral is very distinct from epidote due to the lack of pleochroism and parallel extinction.

Chlorite, the dominant mafic mineral in the greenschist, also occurs in blue amphibole-bearing rocks. It is characteristically pleochroic from yellow to green and has a tabular habit which tends to parallel the dominant foliation in the rock. It is commonly intimately intergrown with white

Table 4. X-ray data for measured reflections from sample UK-19-20 collected near Bear Island (Fig. 5) vs. reflections from synthetic (13-567) and naturally occurring lawsonite (13-533) from the Tiburon Peninsula, California. Data are from A.S.T.M. files. Sample analyzed was a concentrate which contained some glaucophane and chlorite as impurities.

| UK-19-20 | ASTM 13-533 | ASTM 13-567 | hkl |
|---|---|---|---|
| 6.60 | 6.58 | 6.56 | 020 |
| 4.88 | 4.84 | 4.86 | 101 |
| 4.57 | 4.57 | 4.57 | 111 |
| 4.18 | 4.18 | 4.17 | 210 |
| -- | 3.91 | -- | 121 |
| 3.67 | 3.66 | 3.65 | 220 |
| 3.25 | 3.26 | -- | 040 |
| 2.94 (diffuse) | 2.93 | 2.92 | 002 |
| 2.73 | 2.73 | 2.72 | 141 |
| 2.68 | 2.68 | 2.67 | 022 |
| 2.63 | 2.62 | 2.63 | 240 |
| -- | 2.57 | -- | 311 |
| 2.43 | 2.43 | 2.43 | 202 |
| 2.39 | 2.39 | 2.39 | 212 |
| -- | 2.31 | 2.31 | 151 |
| 2.29 | 2.28 | 2.28 | 222 |
| 2.24 | 2.25 | 2.25 | 250 |
| -- | 2.19 | 2.19 | 400 |
| 2.13 | 2.13 | 2.13 | 232 |

mica (Fig. 33). The absence of biotite in rocks which have chlorite-white mica intergrowths constrains the maximum temperature at which these rocks recrystallized.

The white mica associated with both blueschist and greenschist assemblages is paragonite. Muscovite is found only in quartz-mica $\pm$ garnet schists. Quartz is only rarely present in these rocks and, when present, occurs as xenoblastic interstitial grains.

Common accessories include sphene, apatite, opaques, and, less commonly, tourmaline and stilpnomelane.

Carbonate occurs only as vein filling and secondary void filling material in both blueschists and greenschists at Seldovia. It appears to be one of the primary constituents associated with the greenschist studied on Kodiak Island, indicating that at least some of the Kodiak greenschist may have had a sedimentary protolith.

Blueschist Mineral Assemblages and Textures

The blueschist facies rocks at Seldovia fall into three major catagories based on the coexisting minerals present:

A. Chlorite-crossite-albite schist (AF 25-3a)

B. Chlorite-white mica-epidote-crossite schist (AF 4B.1)

C. Epidote-chlorite-albite-crossite schist (AF 4.7)

Two textural variations are evident within these major groups. The first group (A) is characterized by the lack of

epidote and white mica and is dominated by albite porphyroblasts. In outcrop the rock occurs as massive boudins interleaved and surrounded by chloritic greenschists (Fig. 16). Microscopically, the rock has a granoblastic texture (Fig. 34) dominated by equant xenoblasts of albite (0.25 mm in diameter) surrounded by crossite and scattered chlorite. The chlorite and crossite define an incipient schistosity which is microscopically visible. Idioblastic prisms of crossite averaging 0.05 mm long show subparallel orientation and are typically imbedded in albite porphyroblasts.

The second textural type is represented by the mineral assemblages, group B and C. Group B is characterized by abundant epidote and white mica; however, group C lacks white mica but contains epidote. In outcrop, these rocks display a strong schistosity. Microscopically, the rocks have a nematoblastic texture due to the alignment of chlorite and idioblastic to subidioblastic crossite grains, 0.1 to 1 mm long. Epidote is typically elongate in the plane of schistosity; however, it also appears as equant subidioblastic grains 0.1 to 0.3 mm in diameter. When white mica is present, it displays a strong optic orientation parallel to the foliation. Albite generally occurs as slightly elongated xenoblastic interstitial matris material. Trains of sphene often parallel the foliation. Calcite, if present, occurs as fracture fillings and veins discordant to the synkinematic fabric, and is thought to be secondary.

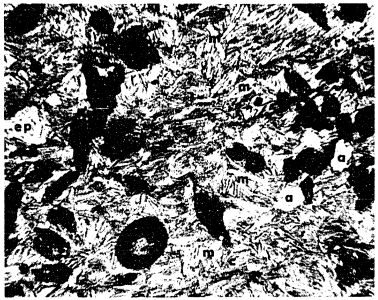


Figure 33. Intergrown white mica (m) and chlorite (c) in a chlorite schist intercalated with crossite schist layers. Dark grains are sphene; ep=epidote; a=albite.

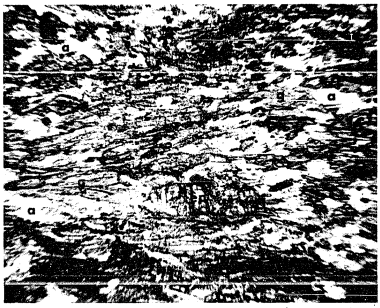


Figure 34. Typical nematoblastic texture of a type C crossite schist from Seldovia. Dark grains near bottom of photo are chlorite; ep=epidote; a=albire; g=crossite.

The crossite schists from Seven Mile Beach (Kodiak Island) and Afognak Island are intimately intercalated with chlorite schists on a scale ranging from centimeters to meters as is the case at Seldovia. There is no evidence that the greenschists were derived from thermal upgrading of former blueschist assemblages. The crossite-bearing schist has been divided into four groups based on mineral assemblages. Each group represents a major textural variation.

Group 1 is characterized by crossite-epidote-stilpnomelane assemblages. In outcrop, the rocks have a blue hue, and display a coarse schistosity. In thin section, the fabric is dominated by (80%) fine-grained radiating bundles of flamboyant crossite. Pistacitic epidote occurs as subhedral laths up to 1.0 mm and stilpnomelane is present as an accessory phase.

Group 2 includes rocks with well preserved relict igneous textures and superimposed blueschist facies mineral assemblages. These rocks have a blastoporphyritic texure and an incipient schistosity. Relict clinopyroxene occurs as subhedral to anhedral grains up to 0.3 mm in diameter along with randomly oriented, relict plagioclase laths. Relict minerals and textures indicate that the parent rock for these schists was fine-grained basalt. The matrix is composed of fine-grained crossite, chlorite, epidote, albite, and sphene.

Group 3 is characterized by the assemblage lawsonite-crossite-chlorite-sphene, with well developed nematoblastic texture. Crossite occurs as subhedral prisms up to 1.0 mm long which tend to define the schistosity. Lawsonite occurs as subhedral and euhedral porphyroblasts approximately 0.2 mm in diameter in a crossite-chlorite-sphene matrix.

The schist of group 4 is believed to be derived from a pelitic sedimentary protolith because of an abundance of quartz and muscovite, which are conspicuously absent in schist derived from a basaltic protolith. This group is characterized by the assemblage quartz-epidote-crossite-muscovite. The rock is coarse-grained with a well developed nematoblastic texture.

Intercalated Blueschist-Greenschist

The character of the layering of the intercalated crossite and chlorite schist is important in determining their origin. As previously stated, the contact between the layers is razor sharp on both the macro- and microscopic scale, and intercalations range in thickness from meters to millimeters with no apparent cyclic pattern. Some of the blueschist layers have necked out to form boudins. Actinolite-bearing greenschist is never intercalated with crossite-bearing schist.

The layering observed within the Seldovia schist terrane is primary and not the product of metamorphic differentiation. Evidence for primary layering is suggested by the following: (1) contacts between major lithologic units are sharp and have not been transposed or tectonically mixed; (2) superposition and general stratigraphy has been preserved, as indicated by a marker chert unit which was mapped for 16 km along the srike; (3) relict bedding within many of the lithologic units is preserved as ascertained by preservation of delicate interlayering of metachert and slate (Fig. 14); and (4) graphitic layers in the marble, interpreted to be $S_0$, are preserved undisturbed and easily recognized.

Ramberg (1973, p. 213) states that when two chemically incompatable rocks are in contact during recrystallization, chemically active components will migrate in either direction across the contact and a "reaction zone" of stable minerals will form at the boundary. At Seldovia the chemistry of the two mineralogically dissimilar layers are significantly different (see chapter 5); however, reaction zones have not been observed either in outcrop or in thin section. Furthermore, as will be discussed later, there is no evidence that differring lithologies were homogenized by a pervasive metamorphic fluid. Therefore, it may be concluded that there has not been much, if any, chemical exchange between the blueschist and greenschist units.

## BROOKS RANGE TERRANE

### Metabasite

Metabasite of the Brooks Range schist belt is characterized by polymetamorphic textures and is easily recognized in the field by its dark massive appearance and coarse-grained, almost gabbroic texture. The metabasite occurs as dike or sill-like layers in a terrane dominated by quartz-mica schist. There is a continuous variation from massive, coarse-grained glaucophane garnet rocks lacking schistosity to foliated, fine to medium-grained rocks that contain greenschist facies mineral assemblages. The greenschist assemblage contains actinolite to sodic actinolite or barrowsite which has partially or totally replaced glaucophane concommitant with the chloritization of garnet and the growth of clinozoisite-zoisite which rims cores of pistacitic epidote. The parental gabbroic rocks have undergone two and perhaps three episodes of prograde metamorphism and at least one period of retrograde metamorphism between late Precambrian to Cretaceous time, as discussed below.

#### Eclogite Event

In several outcrops a few relict mineral assemblages exist, which suggest former eclogites. Amphibolized eclogite occurs within the thicker metabasite lenses where it has escaped obliteration by later retrograde effects.

Relict green omphacitic pyroxene has been almost completely altered to barrowsitic hornblende or glaucophane, and associated garnets have been heavily chloritized obscuring micro-textures. Because of their rare occurrence, little is known about the genesis and age of these rocks. It is evident, however, that this eclogite facies event did precede the blueschist event because some of the omphacite occurs as cores surrounded by late (retrograde?) glaucophane. Metastable eclogites have been found in several blueschist terranes around the world. Typically, sodium amphibole forms at the expense of omphacite during a pressure drop or temperature rise.

Although certain conditions would tend to make eclogite rather than blueschist under transitional conditions, I interpret at least some of the eclogite to represent the highest pressure facies attained during the late Precambrian episode of metamorphism. Subsequent blueschistic and greenschistic events may represent waning stages of the early high-pressure stage.

## Blueschist Event

The oldest clearly discernible metamorphic event is characterized by the following mineral assemblages:

(1) Glaucophane-garnet-sphene $\pm$ rutile

(2) Glaucophane-garnet-epidote-sphene $\pm$ white mica

(3) Glaucophane-garnet-chlorite-sphene

(4) Glaucophane-garnet-white mica-sphene

In outcrop these rocks are massive, having no apparent schistosity, with the exception of those at station 73RR52 which exhibit a well defined schistosity. Fresh samples are blue to blue-green highlighted by reddish-brown garnets which stand out in relief against the preferentially weathered glaucophane fabric. The protoliths for the glaucophane-bearing rocks described above were probably gabbros and diabases.

Microscopically, these rocks display evidence of retrograde metamorphism to varying degrees. In some samples glaucophane occurs only as a relict phase. Fresh specimens of these rocks display a directionless fabric characterized by porphyroblasts of garnet set in a matrix of decussate subidioblastic glaucophane (Fig. 35). The absence of schistosity, which is rather unusual for glaucophane schist, is due to the competence of igneous parent bodies in contrast to the surrounding metasediments. A crude foliation is present in a few of the retrograded samples, especially near the margin of metabasite lenses. The foliated fabric is defined by chlorite, actinolite, and white mica which appear to have crystallized during a later greenschist facies event. A notable exception is a sample collected near the axis of the Kalurivik Arch, which has developed a well-

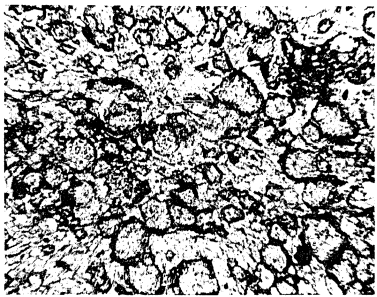

Figure 35. A typical coarse-grained directionless fabric in a glaucophane-bearing metabasites from Ruby Ridge. The high relief mineral is garnet (ga) and the remainder of the rock is glaucophane (g).

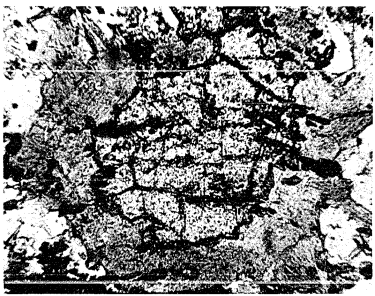

Figure 36. Garnet (ga) which has undergone retrograde metamorphism and has been pseudomorphed by chlorite (c).

defined schistosity by the parallel alignment of subidioblastic glaucophane prisms.

The main assemblage of metamorphic minerals characterizing the metabasite includes garnet, glaucophane, epidote, sphene, rutile, chlorite, and white mica.

The sodic amphiboles were determined by x-ray diffraction analysis to be glaucophane (Table 6). They occur typically as large pleochroic porphyroblasts (x=clear; y=pale lavender; z=pale blue) up to 3 cm in diameter. The glaucophane grains commonly form a directionless mosaic of subidioblastic prismatic crystals (decussate) which surround the garnet. In some cases, the glaucophane is almost perfectly pseudomorphous after original gabbroic augite.

Retrograde reactions are suggested by mottled zones in the blue pleochroic orientations grading to wholesale replacement by actinolite (Fig. 37). In some specimens, retrograde aggregates of chlorite and actinolite have formed on the margins of glaucophane grains. Actinolite is not in equilibrium with the blue amphibole, but rather is replacing it.

Garnet, comprising between 10 to 60 percent of these rocks, occurs as pinkish-brown porphyroblasts ranging from 0.4 mm to 1.5 mm in diameter. Garnet commonly exhibits irregular chlorite filled fractures. The garnet exhibits all degrees of retrogradation from thin chlorite jackets to

small islands of garnet that have been completely engulfed by chlorite (Fig. 37).

Epidote is the common calcium-aluminum silicate mineral in the glaucophane-bearing rocks, often displaying zonal structure that varies from iron-rich cores to iron-poor (clinozoisite?) rims (Fig. 38). Sample 73RR87-2 contains both epidote and clinozoisite; however, the latter is probably in equilibrium with the later greenschist facies episode which has pervasively overprinted these rocks. The sequential decrease in iron content of epidote is probably due to an increase in metamorphic grade (Miyashiro and Seki, 1958; Ernst, 1972; Hormann and Raith, 1973). The depletion of $Fe^{+3}$ in epidote, coupled with other evidence such as actinolite replacing glaucophane, aragonite inverting to calcite and the destruction of the jadeite, indicates that the event causing the retrograding took place at higher temperatures than the episode which formed the blue amphibole.

Sphene is present as a ubiquitous accessory phase and occurs as small euhedral grains averaging less than 0.1 mm and in aggregates up to 2.0 mm.

Rutile commonly occurs as cores armored and replaced by sphene, probably during the subsequent greenschist thermal event.

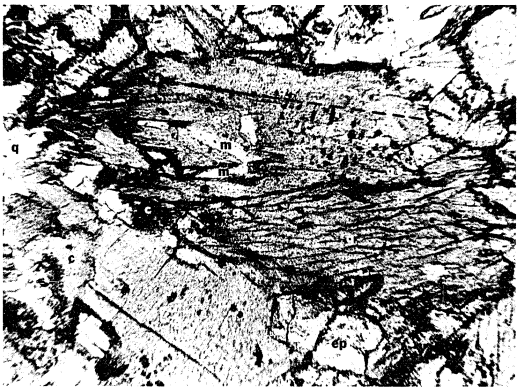


Figure 37. Crystal of glaucophane (g) which has been replaced by actinolite (ac) and chlorite (c). Ep=epidote; m=white mica; q=quartz; ga=garnet.

White mica has optic angles of about 20 degrees (-). This mica was determined to be paragonite based on its low potassium content (Turner and others, 1978).

Most of the chlorite found in these rocks has been produced by retrograde metamorphism; however, a small portion may have been in equilibrium with the intial blueschist assemblages.

## Greenschist Event

In many cases the greenschist rocks in this terrane were previously blueschists; however, it is difficult to distinguish between greenschist which has completely retrograded from blueschist and greenschist which was derived from gabbroic parent rocks that have not experienced a blueschist event. In many specimens, however, there is excellent evidence for a complete mineralogic gradation from blueschist facies rocks to greenschist facies rocks.

The first minerals to be attacked by the retrograde metamorphism are glaucophane and garnet. Glaucophane is usually replaced on a constant volume basis by a pale green amphibole which mimics the original glaucophane grain (Fig. 37). Garnet alters to chlorite which forms pseudomorphous aggregates after the original porphyroblasts. The epidote in some of the blueschist assemblages has undergone a more subtle transition. South of V.A.B.M. Ruby, epidote grains are commonly zoned from iron-rich cores to iron-poor rims

(clinozoisite, in many instances). North of the Cliff Claims on Ruby Ridge clinozoisite is the stable epidote mineral and is usually found as larger porphyroblasts. If epidote is found, it is usually as inclusions in garnet or albite.

Possible reactions with idealized, iron-free components for the above relations include:

(1) $25Na_2Mg_3Al_2Si_8O_{22}(OH)_2$ + $6HCa_2Al_3Si_3O_{12}(OH)$ + $7SiO_2$ + $14H_2O \rightleftharpoons 50NaAlSi_3O_8 + 9Mg_5Al_2Si_3O_{14}(OH)_4 + 6Ca_2Mg_5Si_8O_{22}(OH)_2$

glaucophane, epidote, quartz, water, albite, chlorite, actinolite

(2) garnet + epidote + water $\rightleftharpoons$ chlorite + clinozoisite + white mica

Mineral assemblages observed in these greenschists are listed below:

(1) Actinolite-epidote-albite-garnet-sphene ($\pm$ quartz)

(2) Actinolite-albite-epidote-chlorite-calcite-sphene

(3) Actinolite-clinozoisite-albite-sphene ($\pm$ white mica

(4) Actinolite-epidote-albite-stilpnomelane-chlorite ($\pm$ calcite)

(5) Albite-chlorite-white mica-actinolite-sphene

Actinolite typically occurs as pleochroic (x=clear; y=pale green; z=light green) porphyroblasts or as felted aggregates which account for 20 to 60 modal percent of the rock.

Two generations of garnet have been recognized in these rocks: (1) the earliest generation is related to the Precambrian blueschist or eclogite event, is retrograded, and occurs as small xenoblasts surrounded by chlorite and (2) a later generation of garnet related to the subsequent greenschist facies event. Similar garnets also occur as porphyroblasts, but are typically idioblastic and have not altered to chlorite.

Chlorite also occurs as interstitial laths and aggregates located between larger amphibole, clinozoisite and garnet grains. The chlorite is faintly pleochroic from clear to pale green. Extinction angles are nearly parallel. The chlorite and amphibole fabrics are primarily responsible for the faint schistosity observed in these rocks. Several samples of chlorite, which appear to be replacing actinolite, contained incipient biotite along grain margins.

Epidote or clinozoisite typically occurs as idioblastic to subidioblastic prisms (0.25-1.0 mm long) which are elongated along the b axis and parallel to the plane of the schistosity. Generally the epidote is zoned (iron-rich cores to iron-poor rims). The zoning may be due to the increase in crystallization temperature associated with the late Precambrian event or may have formed during the later Cretaceous pulse of synkinematic metamorphism.

Albite is present as helicitic untwinned xenoblasts up to 1.5 mm in diameter.

Stilpnomelane, when present, characteristically occurs as radiating aggregates (0.5-1.0 mm) associated with calcite. Grains are generally idioblastic and are pleochroic from amber to dark reddish-brown (Fig. 39).

Quartz occurs as clear, equant and/or lenticular grains. Sphene is the most common non-opaque accessory mineral, occurring in euhedral grains, in trains, or on aggregates.

Metasedimentary Rocks

The rock types which constitute the largest volume of the Brooks Range metamorphic belt can be sub-divided into three groups: (1) metapelites, (2) carbonate-rich metapelites, and (3) metacarbonates. The following is a list of recorded metamorphic mineral assemblages in metasedimentary rocks:

(1) Calcite

(2) Quartz-white mica-albite-chlorite ($\pm$ chloritoid, rutile)

(3) Quartz-white mica-albite-chlorite-garnet ($\pm$ opaques)

(4) Quartz-white mica-albite-chlorite-graphite

(5) Quartz-white mica-chlorite-chloritoid

(6) Quartz-white mica-chlorite-glaucophane-chloritoid

(7) Quartz-white mica-albite-chlorite-carbonate

(8) Quartz-white mica-albite-graphite-opaques

The quartz-mica schist and the carbonate-rich metapelite are characterized by a well developed schistosity. In

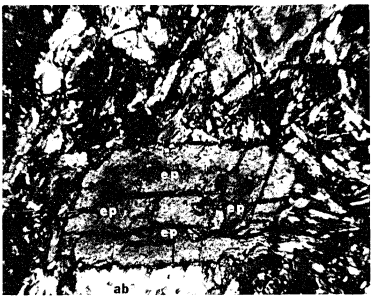


Figure 38. Zoned Ca-aluminimum silicate from a blueschist from Ruby Ridge. The pisticitic core (ps) is surrounded by an epidote rim (ep) which is in turn rimmed by clinozoisite (cz). ab=albite. (Crossed nicols.)


Figure 39. Typical stilpnomelane-bearing greenschist from the south Ruby Ridge. s=stilpnomelane; ab=albite; ac=actinolite; c=chlorite.

some samples, at least two elements surfaces are discernable, the $S_1$ foliation being defined by parallel to sub-parallel flakes of white mica. Glaucophane and chloritoid, when present, are also aligned parallel to $S_1$. A superimposed axial surface, $S_2$, is present in rocks which have undergone a strong crinkling of the $S_1$ folia.

As is the case with the metabasite, some of the metasedimentary rocks display effects from a secondary dynamothermal pulse of metamorphism. The most striking evidence is the biotization of chlorite which is especially noticeable in samples collected north of the Cliff Claims (on Ruby Ridge north of VABM Ruby). This usually takes place in rocks which also contain abundant white mica since chlorite does not contain enough potassium alone for the reaction. One possible reaction may be:

muscovite + chlorite:antigorite $\rightleftarrows$ biotite + chlorite:amesite + quartz + water

Biotite of another origin also occurs in a quartz-mica schist (73RR18f) which crops out west of V.A.B.M. Ruby. The biotite is not associated with chlorite and occurs as randomly oriented xenoblastic crystals. The biotite may have formed due to a thermal overprinting from an adjacent synkinematically emplaced K-spar-bearing granitoid body.

In the pelitic schists glaucophane and chloritoid-bearing assemblages are confined to a narrow zone centered around V.A.B.M. Ruby. This relationship was also observed

in a similar position on other N-S ridges at least 50 km east and west of V.A.B.M. Ruby. To the north along Ruby Ridge, glaucophane and chloritoid disappear with an apparent increase in metamorphic grade.

Generally, the marble forms relatively thin units that pinch out along the strike. Most of the marble units are confined to the southern part of the Ruby Ridge.

Discussion

There is evidence that the minerals aragonite, jadeite, and lawsonite were probably originally stable during the crystallization of glaucophane. Subsequently, a post or late-kinematic thermal event which was probably accompanied by a drop in lithostatic pressure, almost obliterated this assemblage, leaving glaucophane and relict jadeite to attest to the prior high pressure-low temperature metamorphism.

The association of epidote-clinozoisite, albite, calcite, and garnet with the sodic amphibole glaucophane suggests recrystallization under conditions similar to the Type IV blueschists of the Cazadero area of California (Coleman and Lee, 1963). It must be realized, however, that the calcite, epidote, and albite are obvious retrograde phases. The two blueschist metamorphic sub-facies are related by the reaction:

$3CaAl_2Si_2O_7(OH)_2O{\cdot}H_2O + CaTiSiO_5 \rightarrow 2Ca_2Al_3Si_3O_{12}(OH) + TiO_2 + SiO_2 + 5H_2O$

lawsonite sphene epidote rutile quartz

Taylor and Coleman (1968) estimated temperatures for recrystallization of Type IV rocks from Cazadero at 400-500 degrees C while those of Type III containing no epidote are believed to recrystallize at 200-325 degrees C.

From the relict mineralogy it may be concluded that the original blueschist event in the Brooks Range was similar to the Type III conditions described above, although P-T conditions of the schist belt probably passed through the higher temperature Type IV subdivision on its way to the low-grade greenschist facies. The low-grade greenschist facies event caused the actinolitization of the glaucophane, the chloritization of the garnet, the inversion of aragonite to calcite, and the lawsonite → epidote → clinozoisite paragenesis. There is some inconclusive evidence, based on actinolite dates as previously mentioned, that this initial retrograde episode occurred during the waning of the blueschist event in late Precambrian or Early Cambrian time.

## PHYSICAL CONDITIONS OF METAMORPHISM

### GLAUCOPHANE AS A GEOBAROMETER

De Roever and Beunk (1976) have obtained tentative stability parameters for naturally occurring sodic amphiboles in the glaucophane-riebeckite solid solution series (Fig. 40). They found that if the glaucophane content of a sodic amphibole is known, then it may be used as an indicator of pressure conditions present during recrystallization, and when used in conjunction with experimentally derived phase equilibria of minerals coexisting with the sodic amphiboles, parameters concerning the physical conditions of metamorphism may be inferred.

#### Variation of $d_{310}$ as Indicator of Sodic Amphibole Composition

Substitution in the general amphibole formula $AX_2Y_5Z_8O_{22}(OH)_2$ is the basis of a nomenclature proposed by Miyashiro (1957). Basically, he classified sodic amphiboles based on $Fe^{+2}$ substitutions for $Mg^{+2}$ in the $M_1$ and $M_3$ cation site (R'') and $Fe^{+3}$ substitution for $Al^{+3}$ in the $M_2$ cation site (R'''). Accordingly, end member glaucophane ($Na_2Mg_3Al_2Si_8O_{22}(OH)_2$) could theoretically have a solid solution relationship with magnesioriebeckite ($Na_2Mg_3Fe_2^{+3}Si_8O_{22}(OH)_2$) if substitution takes place only in the $M_2$ site; or ferroglaucophane ($Na_2Fe_3^{+2}Al_2Si_8O_{22}(OH)_2$) if substitution only takes place in the $M_1$ and $M_3$ sites. When

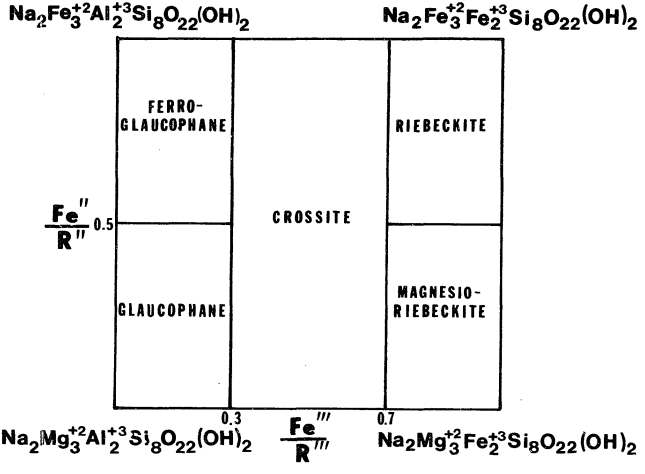


Figure 40. Compositional variation of sodic amphiboles using Miyashiros' (1957) classification. R''=$Fe^{+2}$ + Mg + Mn; R'''=$Fe^{+3}$ + Al + Ti.

substitution takes place in all three sites, as generally is the case, then riebeckite ($Na_2Fe_3^{+2}Fe_2^{+3}Si_8O_{22}(OH)_2$) is the end member.

To date, amphiboles with the composition of ferroglaucophane have not been found in nature, and amphiboles with the composition of magnesioriebeckite are rare and occur only in rocks which are rich in Na and $Fe^{+3}$ with the sodium in excess of aluminum. Most amphiboles from high pressure-low temperature metamorphic terranes fall in the glaucophane-riebeckite solid solution series with amphiboles of intermediate composition called crossite (Palache, 1894). There is a very close correspondence to a concomitant 1:1 substitution of divalent with trivalent iron in the R'' and R''' sites respectively (Borg, 1967, Fig. 1; Coleman and Papike, 1968, Fig. 1). Assuming a perfect 1:1 correspondence, the glaucophane-riebeckite system may be thought of as a binary series with one end-member perfectly miscible in the other.

Because divalent iron has a larger ionic radius than $Mg^{+2}$, and trivalent iron is larger than the $Al^{+3}$ it replaces, riebeckite has a larger cell volume (918 $\mathring{A}^3$) than glaucophane (864 $\mathring{A}^3$). Figure 41 illustrates the variation between cell volume and mole percent of the riebeckite molecule dissolved in the sodic amphibole and shows that it approaches a linear function for 20 naturally occurring amphiboles. Table 5 shows that greater than 80% of the increase in the cell volume is accounted for by expansion in the direction of the a

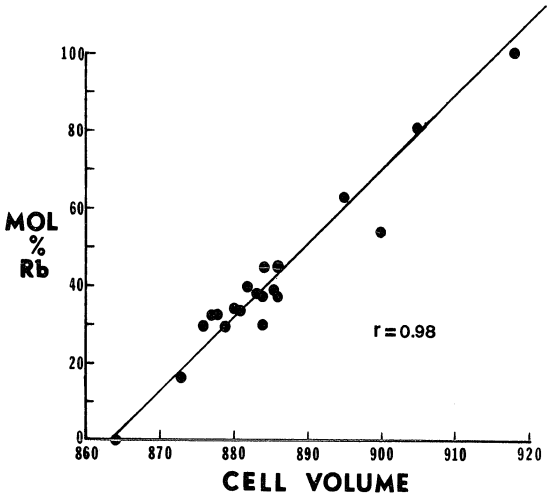


Figure 41. Diagram illustrating the variation in sodic amphibole composition vs. change in cell volume. Data from ASTM files; Coleman and Papike (1968); Ernst (1964); Borg (1967); and Himmelberg and Papike (1969).

Table 5. Relationship between the change in the axial lengths of the a, b, and c crystallographic axes versus end-member amphibole composition.

| Parameter | Glaucophane | Riebeckite | % change | Total change accounted for* |
|---|---|---|---|---|
| A | 9.50 A | 9.78 A | 2.9% | 49% |
| B | 17.67 A | 18.01 A | 1.9% | 32% |
| C | 5.29 A | 5.34 A | 0.9% | 15% |
| Volume | 864 A | 918 A | 5.9% | 100% |

* The total change in a, b, and c do not total to 100% because ß, which accounts for approximately 4% of the change, is not considered.

and b crystallographic axis. Therefore, hk0 reflections should vary significantly with change in the cell volume. The $d_{310}$ reflection occurs at a relatively high $2\theta$ angle and because it is one of the most intense amphibole reflections, it can be located precisely and is clearly resolvable from its neighbor reflections; therefore, it was chosen for use in this study. Figure 42 illustrates this dependant relationship in five naturally occurring amphiboles from the Franciscan of California. The best-fit curve through these points approximates a straight line.

It has previously been shown that the cell volume varies with the mole percent riebeckite dissolved in a sodic amphibole; accordingly, Figure 43 illustrates that the mole percent riebeckite in an amphibole of the glaucophane-riebeckite series varies as a linear function with the spacing of the $d_{310}$ crystallographic plane. Thus, it is possible to precisely determine the end-member components in the amphibole by measuring the spacing of the $d_{310}$ and applying it to the following formula:

$$\text{Mole\% Rb} = 938.3\ (d_{310}) - 2829.5$$

This formula is the equation of the straight line through the points in Figure 43.

Seven sodic amphibole separates from the Brooks Range and five sodic amphibole separates from the Seldovia-Kodiak Islands were analyzed by x-ray diffraction using methods

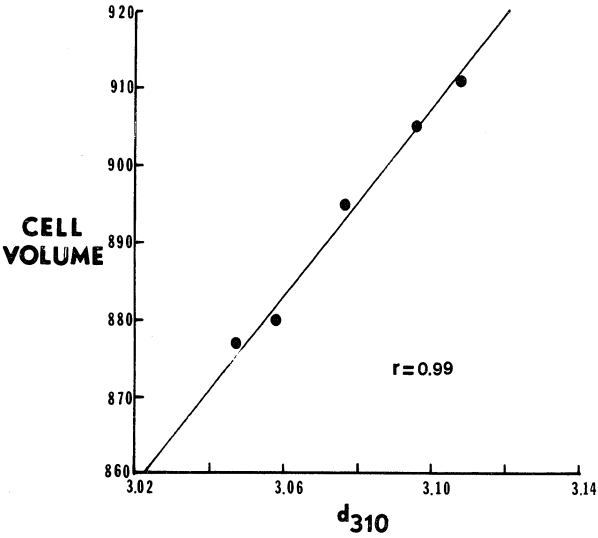


Figure 42. Diagram illustrating the variation in cell volume of five naturally occurring alkali amphiboles vs. spacing of the $d_{310}$ reflection. Data from ASTM files (15-516,15-592) and Coleman and Papike (1968).

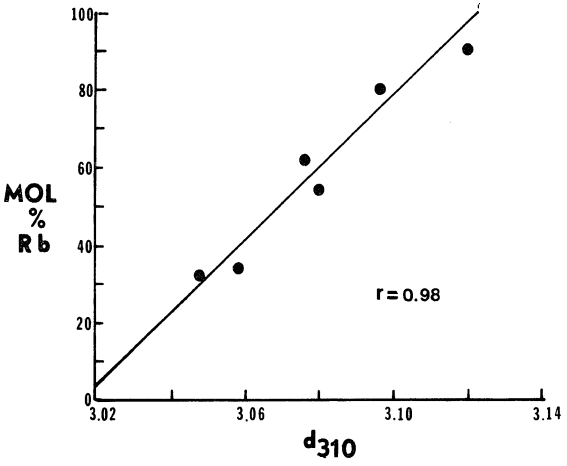


Figure 43. Diagram illustrating the variation in mole percent riebeckite vs. spacing of $d_{310}$ of sodic amphibole. Data from ASTM files (15-516,19-1061,20-376) and Coleman and Papike (1968).

described at the beginning of this chapter. Spacing of the $d_{310}$ reflections and calculated amphibole composition are summarized in Table 6. From these measurements it is evident that the sodic amphibole from the Brooks Range is true glaucophane averaging $Gl_{72}Rb_{28}$ while the sodic amphiboles from the Seldovia-Kodiak Islands area are more iron-rich crossites which have an average composition of $Gl_{50}Rb_{50}$.

Pressure Constraints

The average sodic-amphibole composition given above may be applied to a petrogenetic grid (Fig. 44) which contains the lower stablility limit for sodic amphiboles between the composition $Gl_{30}Rb_{70}$ and $Gl_{90}Rb_{10}$ (curve 5; from de Roever and Beunk, 1976). These data indicate that the minimum pressures existing during the late Precambrian Brooks Range blueschist episode were 6.5 kb or nearly 1 kb higher than the 5.5 kb minimum pressure which accompanied the recrystallization of the Seldovia-Kodiak Islands schist terrane.

The maximum pressures of crystallization may be inferred from the stable calcium-aluminum silicate present. On Kodiak Island the blueschists containing lawsonite must have recrystallized at a temperature of about 300° C (Taylor and Coleman, 1968) in the absence of aragonite or jadeitic pyroxene. Therefore, curve 3 (Fig. 44) serves as a ceiling for the pressure attained (6.5 kb). The higher temperature

Table 6: Table of $d_{310}$ spacings from sodic amphiboles of the Seldovia-Kodiak Islands terrane and the Brooks Range metamorphic belt.

| Locality | Sample Number | $d_{310}$ | Amphibole Composition |
|---|---|---|---|
| Brooks Range | A-1 | 3.042 | $Gl_{75}Rb_{25}$ |
| Brooks Range | A-2 | 3.042 | $Gl_{75}Rb_{25}$ |
| Brooks Range | C-1 | 3.045 | $Gl_{72}Rb_{28}$ |
| Brooks Range | RR-7g | 3.049 | $Gl_{69}Rb_{31}$ |
| Brooks Range | 74AF-155-13 | 3.050 | $Gl_{68}Rb_{32}$ |
| Brooks Range | 73RR-52 | 3.046 | $Gl_{71}Rb_{29}$ |
| Brooks Range | 73RR-54 | 3.046 | $Gl_{71}Rb_{29}$ |
| Seldovia | 74AF-4B.1 | 3.066 | $Gl_{53}Rb_{47}$ |
| Seldovia | 74AF-25-3a | 3.065 | $Gl_{54}Rb_{46}$ |
| Kodiak Islands | M1D | 3.069 | $Gl_{50}Rb_{50}$ |
| Kodiak Islands | UK-23-C | 3.088 | $Gl_{32}Rb_{68}$ |
| Kodiak Islands | UK-19-20 | 3.058 | $Gl_{60}Rb_{40}$ |

Seldovia terrane, containing epidote as the stable calcium-aluminum silicate in equilibrium with crossite, crystallized at temperatures between 400°-475° C. Maximum pressure constraints may be inferred from curves 1 and 3 (Fig. 44) in which epidote undergoes a reaction to lawsonite at 9 kb, almost coincident with the calcite to aragonite transition.

The pressure that accompanied metamorphism on the Kodiak Islands were between 5.5 and 6.5 kb, and those at Seldovia-Port Graham were between 5.5 and 9 kb (Fig. 44).

P-T constraints for the Brooks Range blueschist event is more uncertain. From the glaucophane composition, a minimum pressure limit on the order of 6.5 kb may be inferred; however, because almost pure jadeite occurs with aragonite, the maximum pressure must have been above 10 kb if eclogite facies conditions were obtained.

## OXYGEN ISOTOPE GEOTHERMOMETRY: SELDOVIA-KODIAK ISLANDS

Oxygen isotope analyses have been made on separates of coexisting metamorphic minerals from rocks in the Seldovia-Kodiak Islands area and from the Brooks Range metamorphic belt. Mineral separates had a purity of greater than 99%. The mineral separates were analyzed by James O'Neil and Carlos Masi of the U.S. Geological Survey using methods discussed in a paper by O'Neil and Ghent (1975). The results of these analyses are summarized in Table 7, along

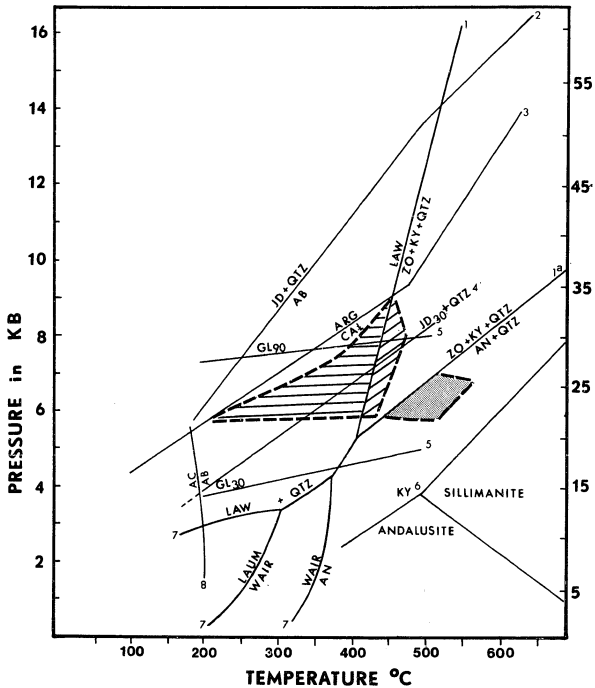


Figure 44. Petrogenetic grid for the Seldovia-Kodiak Islands and Knik River schist terrane showing approximate P-T conditions inferred from oxygen isotope data, and coexisting mineral assemblages. Horizontally ruled area represents P-T conditions for the Kodiak Islands; diagonally ruled area represents the Seldovia terrane; stippled area represents the Knik River schist terrane. Stability curves compiled from Figure 1, minimum stability limits of $Gl_{30}$ and $Gl_{90}$ after deRoever and Beunk (1976).

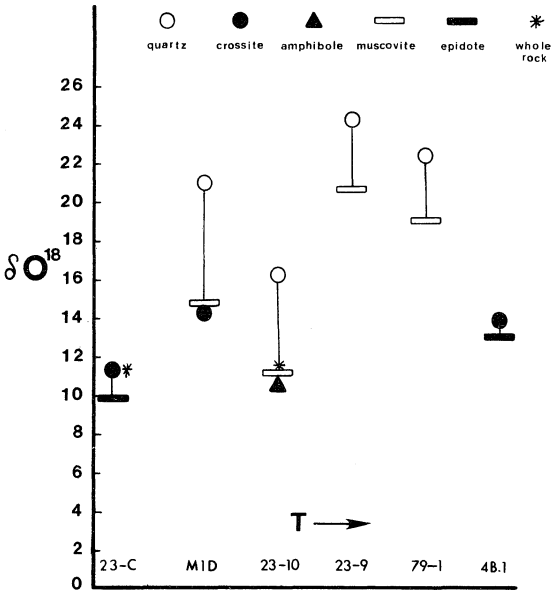


Figure 45. Values of $\delta O^{18}$ for coexisting minerals from six selected rocks from the Seldovia-Kodiak Islands metamorphic terrane arranged in order of temperature of crystallization. Numbers at bottom refer to samples in Table 7.

Table 7: Summary of oxygen isotope data for the Seldovia-Kodiak Islands area. Values determined by James O'Neil and Carlos Masi of the U. S. Geological Survey.

| Sample No. | Locality | Mineral | $\delta O^{18}$‰ | Temperature |
|---|---|---|---|---|
| UK-23c | Kodiak Is. | whole rk. | 11.31 | |
| | | epidote | 9.95 | |
| | | crossite | 11.35 | |
| M1D | Kodiak Is. | quartz | 21.05 | (298)[1] |
| | | crossite | 14.35 | (270)[2] |
| | | muscovite | 14.80 | |
| AF-23-10 | Seldovia | whole rk. | 11.66 | |
| | | quartz | 16.32 | (353)[1] |
| | | muscovite | 11.24 | (340)[2] |
| | | amphibole | 10.59 | |
| AF-23-9 | Seldovia | quartz-1 | 24.32 | (461)[1] |
| | | quartz-2 | 23.98 | |
| | | muscovite | 20.76 | |
| 74PG-79-1 | Port Graham | quartz | 22.56 | (472)[1] |
| | | muscovite | 19.13 | |
| AF-B.1 | Seldovia | epidote | 13.12 | |
| | | crossite | 13.88 | |

[1]Denotes temperature derived from Δq-mu using calibration expression of Bottinga and Javoy (1973).

[2]Denotes temperature derived from Δq-gl or Δq-am using curves given in Taylor and Coleman (1968).

with temperatures derived from the fractionation of $\delta O^{18}$ between coexisting silicate phases using equations of Bottinga and Javoy (1973) for quartz-mica pairs and Taylor and Coleman (1968, Fig. 11) for other mineral pairs. The isotopic compositions of the minerals are given in notation where $\delta O^{18}$ is the relative difference in parts per thousand of $O^{18}/O^{16}$ between the sample and SMOW (standard mean ocean water) (for an example, see Epstein, 1959). Analytical uncertainties in $\delta O^{18}$ values are $\pm$ 0.1 per mil.

These data suggest that the rocks of the Kodiak Islands may have undergone lower temperatures of recrystallization ($\bar{x}$=289° C) than the metamorphic rocks of the Seldovia-Port Graham area ($\bar{x}$=406° C). The temperatures given by this study are corroborated by the work of Taylor and Coleman (1968) who have found that terranes containing lawsonite as the stable Ca-aluminum silicate (i.e. Kodiak Islands) experienced recrystallization temperatures between 270° C and 325° C, while those with epidote (i.e. Seldovia terrane) have recrystallized between 400° C and 550° C. Furthermore, the grade of metamorphism may have increased toward the northeast in the Knik River schist terrane where some actinolitic hornblendes are found in the absence of epidote and in the presence of coexisting oligoclase-andesine. This evidence suggests that the temperatures were above the zoisite + kyanite + quartz $\rightarrow$ anorthite + quartz curve in

Figure 44. Assuming a pressure of 6 kb, the minimum temperature at which this transition may occur is 450° C. Therefore, I have concluded that there may have been a temperature gradient along strike in the metamorphic terranes which were formed during Late Triassic time along the southern Alaska margin. The gradient may have been caused by different rates of lithospheric underflow or emergence along this 600 km long segment of the Kula plate.

In several metamorphic terranes studied by other workers there is evidence that metamorphic mineral assemblages have equilibrated with a mobile, pervasive, oxygen-bearing fluid phase, as demonstrated by Taylor and others (1963) in Vermont, Devereux (1968) in New Zealand, and O'Neil and Ghent (1973) in British Columbia. The interaction results in a smoothing out of isotopic gradients such that the same minerals from differing protoliths show a limited range in $\delta O^{18}$ values (Taylor and Coleman, 1968; O'Neil and Ghent, 1973). No such relationship seems to exist for the schist of the Seldovia-Kodiak Islands, even though it is likely that an intergranular $H_2O$-bearing fluid phase was present as a medium of oxygen exchange, as suggested by the occurrence of abundant hydrous minerals including muscovite, epidote, glaucophane, chlorite, lawsonite, and actinolite. As shown in Table 7, it is clear that these rocks were not involved in a homogenization event as evidenced by $\delta O^{18}$ values which

range 8 per mil for quartz (samples 23-9 and 23-10 were collected 6 meters apart), 9.5 per mil for muscovite, and 3.0 per mil for glaucophane. Strictly speaking, an increase in $\delta O^{18}$ may be expected in quartz at lower temperatures but an increase on the order which is reported here is anomalous.

These data suggest that there was poor oxygen isotope communication between lithologic units and the coexisting pore fluid that accompanied metamorphism. This further argues against metasomatism as an explanation for the interlayered greenschist and blueschist assemblages. It is probable that fluids diffused or circulated only on a local scale during metamorphism and that their $O^{18}/O^{16}$ ratios would be determined by average $O^{18}/O^{16}$ ratios of the rocks and not the inverse relationship.

## TEMPERATURE CONSTRAINTS: BROOKS RANGE

For several reasons, temperature conditions which accompanied the blueschist event in the Brooks Range are difficult to ascertain by oxygen isotope geothermometry. First, in the glaucophane schist, either quartz is lacking or, if it is present, it is so scarce that it is difficult to obtain a suitable concentrate. Secondly, the quartz which could be separated and analyzed apparently did not equilibrate with the glaucophane during the blueschist event but rather reequilibrated with the mica that recrystallized

during the later Cretaceous event. Samples 73RR7g and 75RR155-13 contain the phases quartz, glaucophane, and muscovite. The glaucophane-quartz pair give anomalously high temperatures of over 1100° C while the quartz-muscovite pairs from the same rock gave temperatures between 500° C and 600° C. This temperature is a reasonable one to expect from the Cretaceous greenschist event.

Temperature conditions for the earlier episode of blueschist facies metamorphism must, therfore, be inferred from the presence of low temperature blueschist assemblages of lawsonite-aragonite-jadeite, which are believed to have been stable during the early stages of the blueschist event. Taylor and Coleman (1968) have estimated temperatures accompanying the recrystallization of such assemblages between 200° C and 325° C. Subsequently, the temperatures increased to the high temperature subdivision of the blueschist facies as attested by the reaction of jadeite → glaucophane ($\pm$ albite + quartz) lawsonite → epidote and aragonite → calcite, concomitant with the crystallization of some garnet. This subgroup is believed to be representative of temperatures between 400° C and 550° C (Taylor and Coleman, 1968).

Temperatures increased until blue amphibole became unstable, but apparently did not rise high enough for the epidote to break down and reconstitute as the anorthite molecule (Fig. 46, curve 1a). Inferred P-T paths are illustrated in Fig. 46.

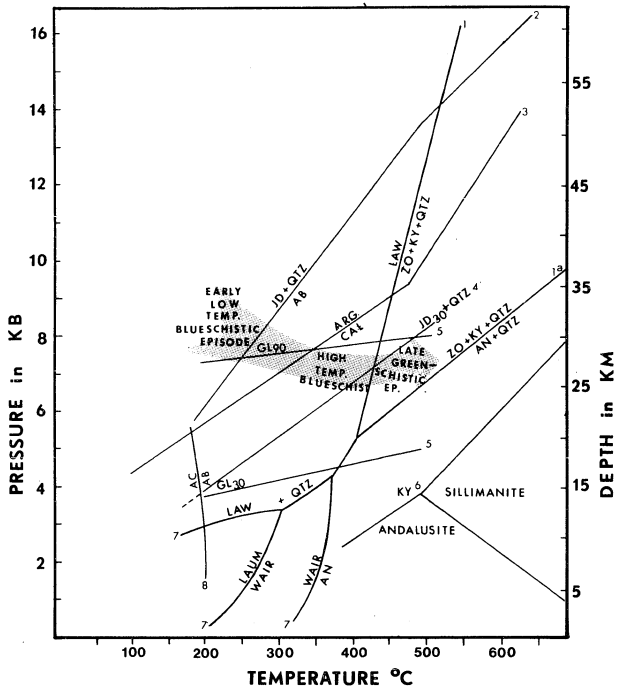


Figure 46. Petrogenetic grid for the Brooks Range metamorphic belt showing approximate P-T conditions inferred from mineral assemblages. Stability curves compiled from Figure 1, minimum stability limits of $Gl_{30}$ and $Gl_{90}$ after deRoever and Beunk, 1976.

## BULK CHEMISTRY

### INTRODUCTION

The samples chosen for whole rock chemical analysis were selected on the basis of representative mineralogy and minimal alteration. All samples were sawed to remove weathering rinds and crushed in an agate mortar to less than 250 mesh. Major and minor elements for rocks collected in the Brooks Range were analyzed at the United States Geological Survey in Reston, Virginia by L. Artis and H. Smith using methods similar to those described in U.S.G.S. Bulletin 1036-C. The results of these analyses are listed in Appendix 1.

Some of the samples collected from the Seldovia-Kodiak Islands terrane were analyzed at the U.S.G.S. by L. Artis (Appendix 2). The remaining samples were analyzed by Skyline Labs of Wheat Ridge, Colorado (Appendix 2; samples denoted by asterisk).

The high $CO_2$ values listed for some of the blueschists and greenschists in Appendix 2 require comment. As previously noted, the high carbonate in these rocks is due to calcite veins which transect the schistosity and are believed to be secondary. Analyses from such rocks result in a high calcium content (in addition to $CO_2$) while the weight percent of other element-oxides in the rock is depressed. In order to deduce the chemistry of the original protolith,

the oxide values of each rock have been adjusted by recalculating the analysis carbonate free (Appendix 2; designated by the letter "a" next to each analysis). To recast the values, the moles of $CO_2$ were combined proportionally with the proper amount of calcium to make calcite and were subtracted from the analysis. The remaining elemental oxides were increased proportionally to compensate for the subtracted calcite.

In addition to the chemical analyses listed in Appendix 1 and 2, standard C.I.P.W. normative mineral calculations were made on the University of Alaska Honeywell computer using a Fortran IV program written by L. Heiner. Niggli numbers (Niggli, 1954) are also given for each analysis and were calculated using the computer program NIGGLI.

Table 8 lists values obtained by the U.S.G.S. and Skyline Labs for the French standard basalt BR (Roubault and others, 1968). This table may be used as an indication of the accuracy of the results listed in Appendix 1 and 2.

## ROCK GROUPS

The averages and standard deviations for analyses of rocks in the blueschist and greenschist groups listed in Appendix 1 and 2 are presented in Table 9 (Groups 1-6). For comparison and use as training groups for discriminate analysis, averages and standard deviations of selected

Table 8. Chemical analyses of French standard basalt BR determined by the U.S.G.S. Lab in Reston, Virginia and by Skyline Lab in Wheat Ridge, Colorado.

| | Skyline Lab | USGS Lab | Basalt BR Standard* |
|---|---|---|---|
| $SiO_2$ | 41.0 | 38.7 | 38.40 |
| $TiO_2$ | 3.0 | 2.6 | 2.62 |
| $Al_2O_3$ | 10.0 | 10.6 | 10.20 |
| $Fe_2O_3$ | 3.7 | 5.5 | 5.58 |
| FeO | 6.3 | 6.6 | 6.61 |
| MnO | 0.12 | 0.17 | 0.21 |
| MgO | 13.1 | 13.1 | 13.28 |
| CaO | 13.9 | 13.5 | 13.74 |
| $Na_2O$ | 3.1 | 3.0 | 3.05 |
| $K_2O$ | 1.3 | 1.3 | 1.40 |
| $P_2O_5$ | 0.69 | 1.2 | 1.04 |
| $H_2O^+$ | 2.2 | 2.3 | 2.3 |
| $H_2O^-$ | 0.29 | 0.59 | 0.46 |
| $CO_2$ | 0.20 | 0.65 | 0.87 |
| Total | 99.00 | 99.81 | 99.76 |

*As reported in Roubault and others (1968).

Table 9: Means and standard deviations of rock groups used in this study.

| Group | 1 | SD | 2 | SD | 3 | SD | 4 | SD |
|---|---|---|---|---|---|---|---|---|
| | Chemical Analyses (Weight Percent) | | | | | | | |
| $SiO_2$ | 48.73 | 3.85 | 47.08 | 2.40 | 49.77 | 5.20 | 46.85 | 3.20 |
| $TiO_2$ | 1.63 | 0.54 | 1.88 | 0.80 | 1.97 | 0.74 | 2.38 | 0.68 |
| $Al_2O_3$ | 14.66 | 1.88 | 14.37 | 1.61 | 13.72 | 2.83 | 15.90 | 1.63 |
| $Fe_2O_3$ | 3.18 | 1.03 | 2.43 | 0.89 | 5.27 | 2.22 | 4.50 | 1.80 |
| FeO | 9.60 | 2.16 | 10.04 | 2.24 | 5.71 | 2.51 | 5.92 | 2.93 |
| MnO | 0.16 | 0.06 | 0.17 | 0.06 | 0.10 | 0.05 | 0.12 | 0.04 |
| MgO | 6.55 | 2.29 | 7.54 | 2.82 | 5.41 | 0.64 | 6.12 | 1.67 |
| CaO | 8.36 | 3.65 | 9.27 | 2.33 | 7.01 | 3.17 | 7.81 | 4.05 |
| $Na_2O$ | 2.96 | 1.18 | 2.38 | 1.03 | 4.61 | 0.92 | 2.96 | 1.04 |
| $K_2O$ | 0.46 | 0.55 | 0.25 | 1.96 | 0.80 | 0.75 | 1.21 | 0.97 |

Group 1: 25 glaucophane metabasites from the Brooks Range metamorphic belt. Data from Appendix 1.

Group 2: 30 glaucophane-free metabasites from the Brooks Range metamorphic belt. Data from Appendix 1.

Group 3: 15 crossite schists from the Seldovia-Kodiak Islands terrane. Data from Appendix 2.

Group 4: 11 greenschists (crossite-free) from the Seldovia-Kodiak Islands terrane. Data from Appendix 2.

Table 9 (continued)

| Group | 5 | SD | 6 | SD | 7 | SD |
|---|---|---|---|---|---|---|
| | Chemical Analyses (Weight Percent) | | | | | |
| $SiO_2$ | 51.95 | 3.89 | 49.18 | 2.69 | 49.57 | 0.78 |
| $TiO_2$ | 2.06 | 0.74 | 2.47 | 0.67 | 1.46 | 0.39 |
| $Al_2O_3$ | 14.39 | 3.13 | 16.67 | 1.61 | 16.30 | 1.62 |
| $Fe_2O_3$ | 5.51 | 2.17 | 4.71 | 1.79 | 2.12 | 1.12 |
| FeO | 5.94 | 2.46 | 6.17 | 3.01 | 7.29 | 1.54 |
| MnO | 0.11 | 0.06 | 0.12 | 0.05 | 0.17 | 0.03 |
| MgO | 5.67 | 0.71 | 6.40 | 1.60 | 7.55 | 1.26 |
| CaO | 4.62 | 1.53 | 5.21 | 1.90 | 11.34 | 0.71 |
| $Na_2O$ | 4.83 | 0.89 | 3.11 | 1.10 | 2.78 | 0.26 |
| $K_2O$ | 0.84 | 0.82 | 1.25 | 1.00 | 0.20 | 0.10 |

Group 5: 15 crossite schists (corrected for subtraction of calcite) from the Seldovia-Kodiak Islands terrane. Data from Appendix 2.

Group 6: 11 greenschists (corrected for subtraction of calcite) from the Seldovia-Kodiak Islands terrane. Data from Appendix 2.

Group 7: 101 ocean floor tholeiites. Data from Engle and Engle, 1963, 1964a, 1964b; Engle and others, 1965; Miyashiro and others, 1969; Shido and others, 1971; Aumento, 1968; Aumento and Loncarevic, 1969; Muir and Tilley, 1964.

Table 9 (continued)

| Group | 8 | SD | 9 | SD | 10 | SD |
|---|---|---|---|---|---|---|
| | Chemical Analyses (Weight Percent) | | | | | |
| $SiO_2$ | 48.93 | 1.74 | 49.40 | 4.93 | 46.81 | 2.66 |
| $TiO_2$ | 2.36 | 0.42 | 1.76 | 0.86 | 2.70 | 0.66 |
| $Al_2O_3$ | 14.46 | 1.00 | 15.61 | 1.87 | 16.23 | 2.42 |
| $Fe_2O_3$ | 3.42 | 1.29 | 3.48 | 2.54 | 4.05 | 1.69 |
| FeO | 8.11 | 1.24 | 6.98 | 2.43 | 7.44 | 2.12 |
| MnO | 0.17 | 0.02 | 0.19 | 0.10 | 0.18 | 0.05 |
| MgO | 8.23 | 1.88 | 5.16 | 1.95 | 6.18 | 3.15 |
| CaO | 10.38 | 0.65 | 6.97 | 2.00 | 8.90 | 1.85 |
| $Na_2O$ | 2.05 | 0.22 | 4.65 | 0.94 | 3.83 | 1.08 |
| $K_2O$ | 0.33 | 0.14 | 0.82 | 0.62 | 1.56 | 0.71 |

Group 8: 110 oceanic island tholeiites. Data from Yoder and Tilley, 1962; MacDonald and Katsura, 1964.

Group 9: 90 spillites. Data from Aumento and Loncarevic, 1969; Cann, 1969; Joplin, 1963; Hess and others, 1966; Vallance, 1960, 1969, 1974; Turner and Verhoogen, 1960.

Group 10: 99 alkali basalts. Data from Turner and Verhoogen, 1960; Yoder and Tilley, 1962; Engle and Engle, 1963, 1966; Joplin, 1963; MacDonald and Katsura, 1964; Engle and others, 1965; Forbes and Hoskins, 1969; Forbes and others, 1969; Carmichael and others, 1974; Laughlin and others, 1974; Wilkinson, 1974; Brotzv and others, 1974.

Table 9 (continued)

| Group | 11 | SD | 12 | SD | 13 | SD | 14 | SD |
|---|---|---|---|---|---|---|---|---|
| | Chemical Analyses (Weight Percent) | | | | | | | |
| $SiO_2$ | 54.49 | 2.03 | 58.61 | 3.99 | 67.78 | 3.89 | 50.02 | 4.71 |
| $TiO_2$ | 1.08 | 0.52 | 0.93 | 0.62 | 0.57 | 0.19 | 1.44 | 1.32 |
| $Al_2O_3$ | 17.13 | 1.98 | 16.41 | 1.53 | 13.54 | 1.79 | 14.11 | 3.25 |
| $Fe_2O_3$ | 3.38 | 1.38 | 2.73 | 0.93 | 1.04 | 0.66 | 2.12 | 1.57 |
| FeO | 5.93 | 1.97 | 5.06 | 1.67 | 3.83 | 1.54 | 10.81 | 4.88 |
| MnO | 0.16 | 0.09 | 0.14 | 0.06 | 0.16 | 0.21 | 0.21 | 0.13 |
| MgO | 4.57 | 1.67 | 3.24 | 1.51 | 2.20 | 0.91 | 7.86 | 6.86 |
| CaO | 8.25 | 0.81 | 6.51 | 1.72 | 2.34 | 1.36 | 9.08 | 2.33 |
| $Na_2O$ | 3.10 | 0.61 | 3.56 | 0.89 | 3.12 | 0.75 | 2.36 | 0.89 |
| $K_2O$ | 1.03 | 0.42 | 1.36 | 0.58 | 1.84 | 0.42 | 0.67 | 0.48 |

Group 11: 14 basaltic andesites. Data from Hess and Poldervaart, 1967.

Group 12: 76 andesites. Data from Joplin, 1963; McBirney, 1969; Ray, 1967; Turner and Verhoogen, 1960; Carmichael, 1964; Carmichael and others, 1974; Kuno, 1950; MacDonald, 1944, 1949, 1960; Bandy, 1937; Williams, 1935.

Group 13: 15 graywacke. Data from Rivalenti and Sighinolfi, 1969.

Group 14: 112 continental tholeiites. Data from Wager and Brown, 1967; Walker and Poldervaart, 1949.

groups of igneous and sedimentary rocks were included (see also graphical representation Fig. 47). The training groups were chosen for their intermediate to basic composition and are representaive of major tectonic regimes. Eight groups were defined in this manner.

Ocean floor tholeiites (Group 7), representative of divergent plate margins, are erupted at mid-oceanic ridges and rises. Although differentiated magmas in the series andesite-rhyolite do occur (Aumento, 1969; Thompson and others, 1972), they are extremely rare. This group of rocks as a whole is homogeneous with a narrow range of $SiO_2$, CaO, $Na_2O$, and $K_2O$ values. They differ from other groups of oceanic basalts by virtue of having the lowest $K_2O$ values.

Oceanic island tholeiites (Group 8) are more rare on intraoceanic islands than alkali basalts. Still, they comprise large volumes on islands such as Hawaii, Iceland, and the Galapagos, differing from ocean floor tholeiites in major element chemistry. These rocks appear to have a different mechanism of generation than the ocean floor tholeiites as indicated by the lower sodium and slightly higher potassium contents. The lower $Al_2O_3$ and higher MgO contents indicate that these rocks may be less fractionated.

Spilites (Group 9) represent rocks which are included in the Steinmann trinity (Steinmann, 1927) or ophiolite association. These rocks, however, are subordinate in

abundance to normal ocean floor tholeiites (Melson and van Andel, 1966; Cann, 1969). They are equivalent in $SiO_2$ and $Al_2O_3$ to normal oceanic tholeiites but are characterized by their higher $Na_2O$ and lower MgO and CaO contents. The sodium content of spillites is higher than other basaltic training groups used in this study. Several authors attribute this sodium enrichment phenomenon to a redistribution of elements with adjustments to lower temperature hydrous-conditions (Vallance, 1965; Cann and Vine, 1966; Melson and van Andel, 1966; Cann, 1969). The sodium in seawater is exchanged for calcium and magnesium in the pillows. The calcium and magnesium is subsequently precipitated as dolomitic limestone (Vallance, 1960, 1965; Cann and Vine, 1966; Melson and van Andel, 1966).

Oceanic alkaline basalt (Group 10) is characteristic of the majority of intraoceanic archipelagos. These rocks are characterized by their high alkali content and relatively low silica content. Several workers believe this type of basalt is generated by hotspots or mantle plumes (Morgan, 1971; Schilling, 1973).

Island-arc volcanic rocks, represented by basaltic andesite (Group 11) and andesite (Group 12) are characteristic of convergent plate-margins. Although the products of volcanic arcs are considerably more complex, andesite and basaltic andesite comprise the greatest amount of material

by volume. These rocks are distinquished by their higher $SiO_2$ content which is higher than any of the igneous rocks described above.

Graywackes (Group 13), indicative of trench sedimentation, are postulated to be frequently subducted and incorporated onto continental margin accretionary belts. In the case of the Franciscan complex, jadeitized graywacke represents the bulk of the exposed material (Ernst and Seki, 1967). Graywackes are distinquished from other intermediate rocks by their higher contents of $SiO_2$ and $K_2O$. CaO and MgO are lower than any other group of rocks in this study.

Continental dolerites and gabbros (Group 14) represent continental mafic intrusive activity. They may be distinquished from oceanic basalts by lower $Al_2O_3$ and $Na_2O$ content (albite molecule) and extremely low $Fe_2O_3/FeO$ ratio which also serves as a guide for distinquishing intrusive from extrusive igneous rocks.

## DISCUSSION

### Brooks Range

Normative mineral compositions for metabasite containing glaucophane and metabasite devoid of glaucophane are presented in Appendix 1. The results show that none of the samples are undersaturated with respect to silica. All

samples contain normative hypersthene, and fifty percent contain normative quartz, suggesting that the rocks originally had the composition of olivine tholeiite to oversaturated quartz tholeiite (Yoder and Tilley, 1962). Figure 48 is a conventional AMF diagram with the classic Skaergaard tholeiitic (Wager and Deer, 1939) and calc-alkaline (Daly, 1933) differentiation trends. From this plot it is evident that both blueschist and greenschist facies analyses lie very close to the classic Skaergaard tholeiitic trend. Furthermore, there is no evidence that blueschists (circles) are more enriched with respect to the alkalis than the greenschists (triangles).

Figure 50 is a plot of $Na_2O$ versus $SiO_2$ for both blueschists and greenschists from the Brooks Range showing that the blueschist facies metabasite are not particularly enriched in sodium with respect to greenschist facies metabasite of similar $SiO_2$ content. In this case it is not necessary to invoke sodium metasomatism as a mechanism for the formation of sodic amphibole.

In Figure 47 it may be seen that there is little difference in the means and standard deviations of glaucophane-bearing and glaucophane-free metabasites. Microscopic evidence shows that many of the greenschist facies assemblages have been derived from the retrogression of blueschist facies assemblages. Although it is impossible in

some cases to know whether rocks containing greenschist assemblages had a prior blueschistic history, the fact that at least some of the greenschist assemblages were derived from retrograded blueschists is evident from microscopic examination and may also be deduced from chemical relations.

Analyses 17, 34, and 35 (Table 10) are rocks collected at 10 meter intervals from the center to the margin of a metabasic pod-shaped body approximately 5 km north of V.A.B.M. Ruby.

Table 10. Chemical analyses of metabasite samples from a zoned boudin (glaucophane-bearing core to glaucophane-free margin). Analyses are from Appendix 1.

| | 17 (blueschist) core | 35 (greenschist) → | 34 (greenschist) margin |
|---|---|---|---|
| $SiO_2$ | 47.6 | 47.8 | 47.4 |
| $TiO_2$ | 1.4 | 1.5 | 1.7 |
| $Al_2O_3$ | 15.8 | 15.7 | 16.0 |
| $Fe_2O_3$ | 1.7 | 1.7 | 1.9 |
| FeO | 9.9 | 9.8 | 9.4 |
| MnO | 0.15 | 0.12 | 0.14 |
| MgO | 8.3 | 7.6 | 7.1 |
| CaO | 6.9 | 6.8 | 8.1 |
| $Na_2O$ | 2.5 | 3.4 | 3.3 |
| $K_2O$ | 0.24 | 0.20 | 0.12 |
| $P_2O_5$ | 0.21 | 0.23 | 0.23 |
| $H_2O^+$ | 3.3 | 3.1 | 3.2 |
| $H_2O^-$ | 0.10 | 0.19 | 0.18 |
| $CO_2$ | 1.00 | 0.67 | 1.00 |

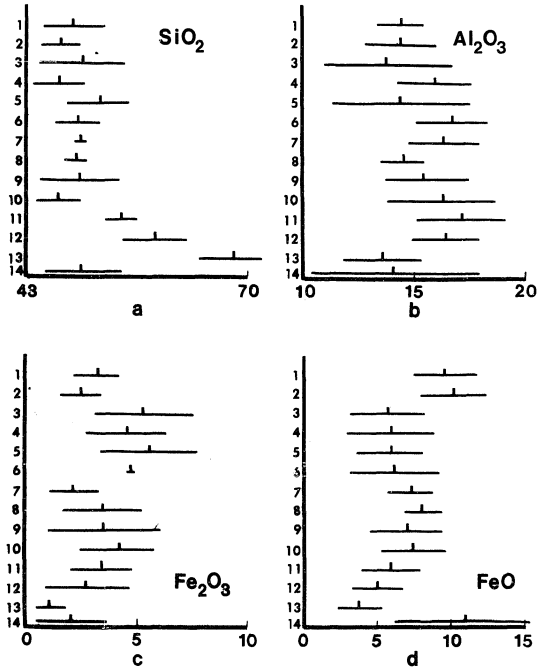


Figure 47. Bar diagram representation of means and standard deviations listed in Table 11.

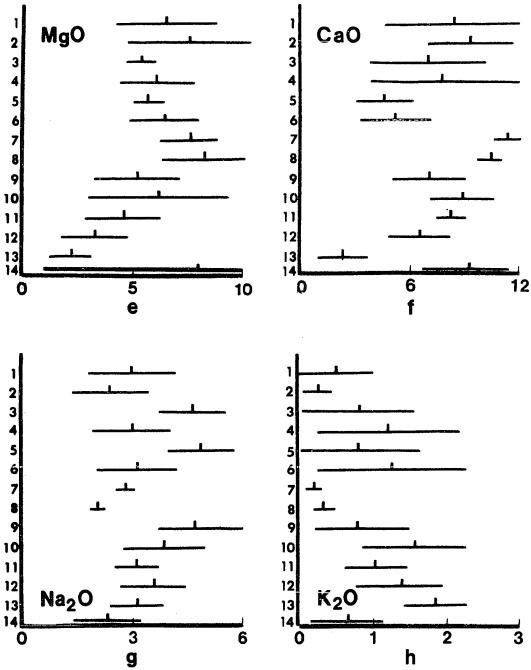


Figure 47. Continued.

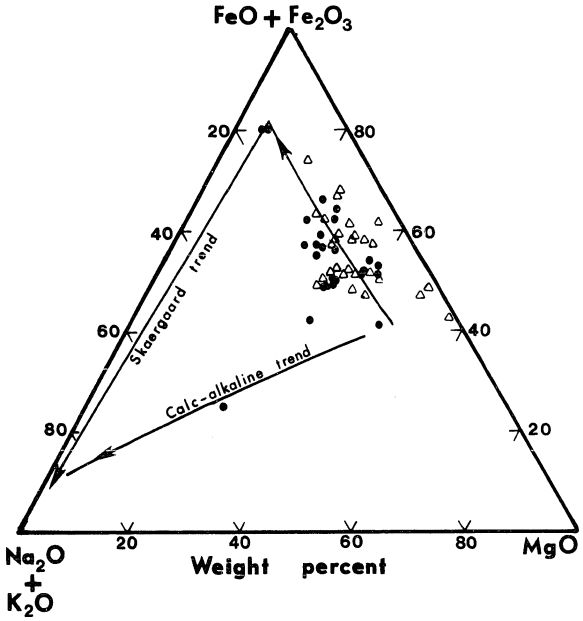


Figure 48. Conventional AMF diagram for bulk rock analyses of metabasites from the Brooks Range metamorphic belt. Solid circles refer to glaucophane-bearing metabasite (Table 8, analyses 1-25) and open triangles refer to metabasite devoid of glaucophane (Table 8, analyses 26-55). Tholeiitic and calc-alkaline fractionation trends are also shown after Wager and Deer (1939) and Daly (1933) respectively.

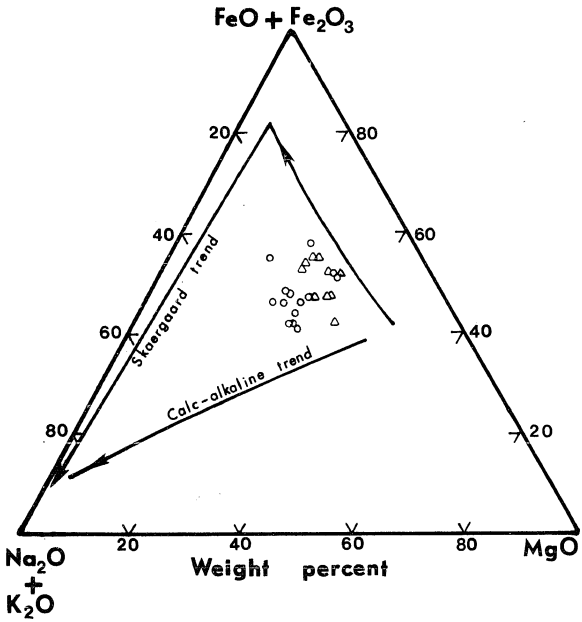


Figure 49. Conventional AMF diagram for bulk rock analyses of the Seldovia-Kodiak Islands terrane. Open circles refer to blueschist facies metabasites corrected for calcite and open triangles refer to greenschist facies metabasites corrected for calcite. Tholeiitic and calc-alkaline fractionation trends are also shown after Wager and Deer (1939) and Daly (1933) respectively.

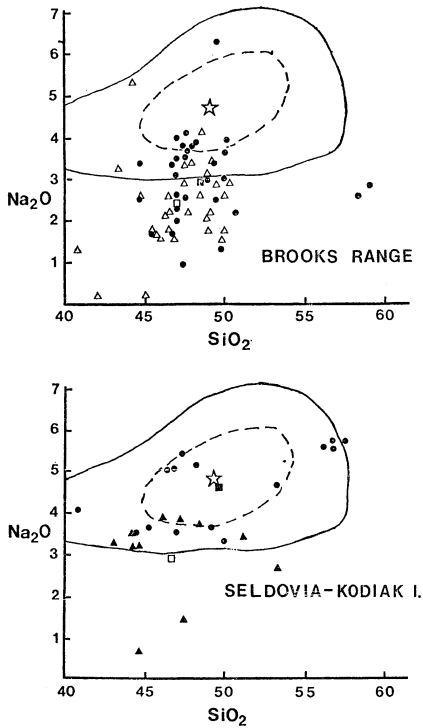


Figure 50. $Na_2O$ vs. $SiO_2$ diagram of data from the Brooks Range (top) and Seldovia-Kodiak Islands terrane (bottom). Symbols for Brooks Range conform to usage in Fig. 48. Solid circles in Seldovia plot refer to blueschist and solid triagnles refer to greenschist assemblages. Solid square=mean composition of all blueschist; open square= mean composition of all greenschist; solid line outlines field of spillites at the 2σ level; dotted line outlines the field of spillites at the 1σ level; star=the mean composition of spillite.

Analysis 17 is a sample from the core of the body which is composed of glaucophane, garnet, epidote, and chlorite. Analyses 35 and 34 are of actinolitic greenschists from the main body which are devoid of glaucophane. These analyses are virtually identical within analytical uncertainty with respect to the major elements. These data lend support to the view that some greenschist assemblages have been derived from retrograded blueschist assemblages and that the retrograde process was essentially isochemical.

Seldovia-Kodiak Islands

The normative mineral composition of the rocks from the Seldovia-Kodiak Islands terrane indicates that all of the analyzed rocks except two were derived from a tholeiitic parent. However, Figure 49 shows that the schists from this terrane do not follow the normal tholeiitic trend as they do in the Brooks Range, but rather are significantly shifted toward the alkali portion of the ternary diagram. This shift is particulary noticeable among the blueschists (circles). Figures 47(g) and 50 show that most of the blueschists are enriched in sodium compared to greenschists from the same terrane. Furthermore, Figure 50 shows that all blueschists fall within the field of spilites at the two sigma level and that the mean of the blueschists (solid square) falls very close to the average of 90 spilites (star).

## DISCRIMINANT ANALYSIS

In order to determine the parentage of metamorphic rocks, discriminant analysis may be used to fit the rocks in question to a preassigned group of rocks whose composition is known. For example, from the bar graphs in Figure 47 it appears that the blueschists from Seldovia closely parallel the major element distribution pattern for the spilite group (Group 9). The Brooks Range situation is not as clear. Other plots may also be utilized such as the Harker variation diagram or AMF plots. The drawback to these projections is that, at most, only two or three variables are considered at one time. This method results in considerable overlap between different fields of igneous or sedimentary rock.

Another approach is statistical assignment through multivariate discriminant analysis. In order to assign rocks of unknown origin to a known group, the application of stepwise discriminant analysis was carried out using the BioMed statistics package program BMD07M (Dixon, 1970).

This procedure depends on the ability of selecting a set of standard samples representative of two or more groups on an apriori basis. One or more linear functions of the variables measured are calculated, which achieves the greatest discrimination between groups in n dimensional space.

Discriminant analysis consists of finding a transform which gives the minimum ratio of the difference between a pair of group multivariate means to the multivariate variance within the two groups. Utilizing these functions, a sample of unknown origin can be assigned to the group with which it has the greatest statistical probability of belonging. BMD07M performs a multiple discriminant analysis in a stepwise manner such that the first step takes into account the variable with the greatest discriminating power and subsequent steps account for smaller degrees of discrimination.

The idea of classification of rocks into tectonic regimes has been carried out to a lesser extent by Chayes and Velde (1965) and Pearce and Cann (1971). This study involves the nomination of the six Alaska groups to one of eight theoretical categories (discussed earlier) as a possible protolith. Tables 11, 12, and 13 are the results of the sequential stepwise fitting.

Table 11 is an assignment table based on the consideration of only one variable, $SiO_2$ which the BMD program chose as the most powerful discriminator. From this table it may be determined that a fairly good discrimination is attained in the training groups of high silica content which do not overlap with each other. However, poor results are obtained in rock groups with $SiO_2$ concentrations that are

Table 11. Assignment table of stepwise discriminant analysis based on one variable, $SiO_2$ (step 1). Group labels given in Table 9.

| Group | 7 | 8 | 9 | 10 | 11 | 12 | 13 | 14 | % correctly assigned |
|---|---|---|---|---|---|---|---|---|---|
| 7 | 16 | 24 | 15 | 3 | 0 | 0 | 0 | 43 | 16 |
| 8 | 11 | 27 | 4 | 29 | 1 | 0 | 0 | 38 | 24 |
| 9 | 6 | 14 | 5 | 20 | 19 | 1 | 0 | 25 | 6 |
| 10 | 4 | 17 | 3 | 62 | 1 | 0 | 0 | 12 | 62 |
| 11 | 0 | 0 | 0 | 0 | 11 | 1 | 0 | 2 | 78 |
| 12 | 0 | 1 | 0 | 2 | 10 | 56 | 3 | 4 | 73 |
| 13 | 0 | 0 | 0 | 0 | 0 | 2 | 13 | 0 | 87 |
| 14 | 0 | 18 | 0 | 26 | 28 | 5 | 1 | 34 | 30 |
| 1 | 3 | 3 | 1 | 12 | 0 | 2 | 0 | 4 | |
| 2 | 0 | 4 | 4 | 18 | 0 | 0 | 0 | 4 | |
| 3 | 0 | 1 | 1 | 7 | 2 | 3 | 0 | 1 | |
| 4 | 0 | 1 | 0 | 8 | 1 | 0 | 0 | 1 | |
| 5 | 0 | 3 | 0 | 2 | 1 | 4 | 0 | 5 | |
| 6 | 1 | 2 | 2 | 3 | 2 | 0 | 0 | 1 | |

Table 12. Assignment table of stepwise discriminant analysis based on $SiO_2$ and $Na_2O$ (step 2). Group labels given in Table 9.

| Group | 7 | 8 | 9 | 10 | 11 | 12 | 13 | 14 | % correctly assigned |
|---|---|---|---|---|---|---|---|---|---|
| 7 | 90 | 5 | 0 | 1 | 0 | 0 | 0 | 5 | 89 |
| 8 | 2 | 74 | 0 | 0 | 1 | 0 | 0 | 33 | 67 |
| 9 | 5 | 0 | 59 | 23 | 2 | 1 | 0 | 0 | 66 |
| 10 | 20 | 7 | 33 | 59 | 0 | 0 | 0 | 0 | 60 |
| 11 | 1 | 0 | 0 | 0 | 10 | 0 | 0 | 2 | 71 |
| 12 | 1 | 3 | 4 | 1 | 11 | 51 | 3 | 2 | 67 |
| 13 | 0 | 0 | 0 | 0 | 0 | 2 | 13 | 0 | 87 |
| 14 | 19 | 35 | 2 | 9 | 14 | 5 | 0 | 28 | 25 |
| 1 | 4 | 6 | 1 | 10 | 0 | 2 | 0 | 2 | |
| 2 | 9 | 16 | 1 | 4 | 0 | 0 | 0 | 0 | |
| 3 | 1 | 0 | 9 | 5 | 0 | 0 | 0 | 0 | |
| 4 | 1 | 2 | 0 | 7 | 1 | 0 | 0 | 0 | |
| 5 | 2 | 0 | 10 | 3 | 0 | 0 | 0 | 0 | |
| 6 | 0 | 2 | 1 | 6 | 2 | 0 | 0 | 0 | |

Table 13. Assignment table of stepwise discriminant analysis based on $SiO_2$, $Na_2O$, $K_2O$, CaO, and $TiO_2$ (step 5). Group labels given in Table 9.

| Group | 7 | 8 | 9 | 10 | 11 | 12 | 13 | 14 | % correctly assigned |
|---|---|---|---|---|---|---|---|---|---|
| 7 | 98 | 3 | 0 | 0 | 0 | 0 | 0 | 0 | 97 |
| 8 | 0 | 104 | 0 | 0 | 0 | 0 | 0 | 6 | 94 |
| 9 | 4 | 1 | 70 | 12 | 2 | 1 | 0 | 0 | 77 |
| 10 | 5 | 10 | 5 | 78 | 0 | 0 | 0 | 1 | 79 |
| 11 | 0 | 1 | 0 | 0 | 9 | 1 | 0 | 3 | 64 |
| 12 | 0 | 1 | 1 | 4 | 11 | 51 | 3 | 5 | 68 |
| 13 | 0 | 0 | 0 | 0 | 0 | 0 | 15 | 0 | 100 |
| 14 | 18 | 12 | 5 | 1 | 15 | 7 | 0 | 54 | 48 |
| 1 | 4 | 1 | 11 | 0 | 0 | 3 | 0 | 6 | |
| 2 | 7 | 9 | 5 | 0 | 0 | 0 | 0 | 9 | |
| 3 | 1 | 0 | 11 | 3 | 0 | 0 | 0 | 0 | |
| 4 | 3 | 0 | 4 | 3 | 0 | 1 | 0 | 0 | |
| 5 | 0 | 0 | 13 | 2 | 0 | 0 | 0 | 0 | |
| 6 | 0 | 0 | 7 | 1 | 0 | 1 | 1 | 1 | |

approximately similar to ocean floor (Group 7) and oceanic island (Group 8) tholeiites.

Table 12 is the assignment table produced after step two in which the variables $SiO_2$ and $Na_2O$ are considered. When compared to the previous assignment table, more variables yield a better characterization of the groups with considerably better results in groups of lower silica content. Steps three and four have been eliminated in order to conserve space. They show a sequential increase in the percentage of groups correctly assigned.

Step five is the optimal table in the characterization of the study set (Table 13). This table is based on the variables $SiO_2$, $Na_2O$, $K_2O$, CaO, and $TiO_2$. Additional steps have no effect, or a negative effect, on correct group assignments of the study set. From this table it is seen that there is over a 90 percent probability of correctly assigning low-potassium tholeiites, ocean island tholeiites, and graywackes. There is over a 75 percent probability of correctly assigning spilites, alkali basalts, and andesites. Continental tholeiites give disappointingly low discrimination values with only a 48 percent probability of correct assignment.

Statistical assignment of the Brooks Range and Seldovia-Kodiak Islands terranes was carried out using the same discriminant analysis program, treating groups of rocks as unknowns.

Discussion

After assessing the extent of separation between groups, the program assigns the unknown analysis to the category with which it has the greatest probability of belonging. The results are shown in Table 13. In the case of the Seldovia-Kodiak Islands rocks, 13 out of 15 blueschist facies rocks and 7 out of 11 greenschist facies rocks most likely belong to the spillite group (after the correction for the subtraction of calcite).

The case of the Brooks Range metabasites is not as clear. In the Brooks Range, the group classified as blueschist metabasite clearly has a bimodal distribution with 11 classified as spillitic and 10 out of the 25 classified as either ocean floor or continental tholeiites. The results are also poor for the greenschists, with considerable scatter in the data to cover the rocks of the tholeiitic group. In order to resolve the problem, the mean blueschist and greenschist analyses from the Brooks Range (Table 9) were entered as unknowns. The program assigned both the average blueschist and the average greenschist as well as the average metabasite (average of all blueschists and greenschists from the Brooks Range metamorphic belt) to the continental tholeiite group.

Preto (1970) and Elliott and Cowan (1966) have calculated oxidation ratios (Mol $2Fe_2O_3$ x $100/2Fe_2O_3$ + FeO) of

metamorphic rocks and have compared the values with similar ratios calculated for various assemblages of associated intrusive and extrusive mafic rocks. The average oxidation ratio of several intrusive assemblages is 16.5 and for several extrusive assemblages is 26.8 (Elliot and Cowan, 1966). Chinner (1960) has stated that metamorphism (including high grade) does not appreciably affect the oxidation state of the rocks. Therefore, the oxidation state may be thought to be inherited from the protolith (Preto, 1970), and may further aid in characterizing the nature of the original parent material to intrusive or extrusive origin.

The average oxidation ratio of metabasite from the Seldovia-Kodiak Islands terrane is 43, suggesting that the rocks were strongly oxidized as expected from a spillitic parent. The average oxidation ratio for the Brooks Range metabasite is 20.4, implying that the parent continental tholeiites were intrusive in nature. These data are supported by microscopic evidence which indicate that some metabasites from the Brooks Range were derived from gabbros and diabases.

## GEOCHEMICAL TRENDS

The problem of distinguishing between para- and orthometamorphic rocks has been of concern to geologists over the past several decades. Either blueschist or greenschist

facies assemblages may be derived from the metamorphism of mafic extrusive or intrusive igneous rocks. However, the same product may also be derived from the metamorphism of a decarbonated calcareous or dolomitic shale. From a single analysis or group of analyses it is difficult to distinguish between the two.

Evans and Leake (1960) and Leake (1964) suggested that the protolith of metamorphic rocks may be traced to a sedimentary or igneous origin by comparing the chemical properties, in the form of Niggli values (Niggli, 1954), of a large suite of samples to define a variation trend. Similar studies have been performed on metamorphic rocks by Nelson (1969), van de Kamp (1969), Preto (1970), van Alstine (1971), Hertz and Banerjee (1973) and Armbrustmacher and Simmons (1977). In each case the discussion is based on the presumption that the metamorphism was isochemical and metasomatism did not occur to a significant degree.

For several reasons, I believe that metamorphism in the Brooks Range and the Seldovia-Kodiak Islands terranes was isochemical. First, several workers (e.g., Ramberg, 1952) have stated that large scale metasomatic changes are not important at low temperatures (probably metasomatism does not occur until the high temperature of the amphibole facies). Secondly, many workers believe that the blueschist-making mechanism is an isochemical process (Coleman

and Lee, 1963; Ernst, 1963b; Ghent, 1965; Hyndmann, 1972). Lastly, when plotted on an AMF diagram (Fig. 48), the rocks of the Brooks Range follow normal geochemical trends for igneous rocks. Although the Seldovia-Kodiak Islands group does not follow a normal tholeiitic trend (Fig. 49), it must be considered that they are not normal tholeiites, but rather have a spillitic origin. Furthermore, it appears that there was poor oxygen-isotope equilibration among lithologic units and the fluid accompanying metamorphism suggesting that metasomatic exchange was unimportant.

Figure 51 shows the plot of Niggli mg versus c values for metabasites from the Brooks Range metamorphic belt (Niggli values are discussed in Appendix 3). Also shown are the field of Karroo dolerites (Leake, 1964) and Skaergaard gabbros (this study) as well as the field of shale (Leake, 1964) and the field of graywacke (Rivalenti and Sighinolfi, 1969). On this plot, rocks which have an igneous parentage should develop a concave-downward horizontal trend (indicated by the arrow marked Karroo-Skaergaard trend). This is due to olivine crystallizing before clinopyroxene and calcic plagioclase during the early stages of crystallization. The early crystallization results in a sharp increase in the trend of Niggli c in the magma. Later, the plagioclase becomes more albitic and both Niggli c and mg decrease. Rocks which are composed of pelitic and Ca-Mg carbonate

mixtures should develop a roughly vertical trend which is oblique to the igneous trend. Plots for the blueschist and greenschist metabasite from the Brooks Range closely follow the variation trend for basic igneous rocks and suggest that these metamorphic rocks had igneous progenitors which were middle stage differentiates. Figure 52 is a slightly different projection for Niggli c versus al-alk for the same Brooks Range metabasites. On this plot, rocks which have an igneous parentage should display a roughly SW-NE trend on the diagram and lie within the igneous field; rocks of sedimentary parentage should display a NW-SE trend. The diagram shows that all metabasites from the Brooks Range are within the field of igneous rocks and that the trend is roughly oblique to that expected from dolomitic shale.

Figures 53 and 54 are the same plots for the Seldovia-Kodiak Islands data. The plots indicate possible sedimentary influence for several of the samples. Furthermore, the majority of the samples tend to cluster (Fig. 53) somewhat below the average trend line for a differentiated basic magma. When the analyses are corrected for calcite and replotted (Figs. 55 and 56) it can be seen that the samples no longer display a sedimentary trend, but trend roughly parallel to the Karroo-Skaergaard trend although still somewhat depleted with respect to Niggli c (lime). For reference, the field of 90 spilites as compiled for this

study is shown by the shaded area. The spillite trend roughly parallels the Karroo-Skaergaard trend although it is depleted in Niggli c. The Seldovia-Kodiak Islands metabasites all fall within and parallel the spilitic trend.

Figure 57 shows that the metabasites from the Brooks Range closely follow the combined Karroo-Skaergaard trend rather than the sedimentary composition trends. Furthermore, the bulk of the analyses indicate that the metabasites were middle stage differentiates which is in line with the observations deduced from Figure 51.

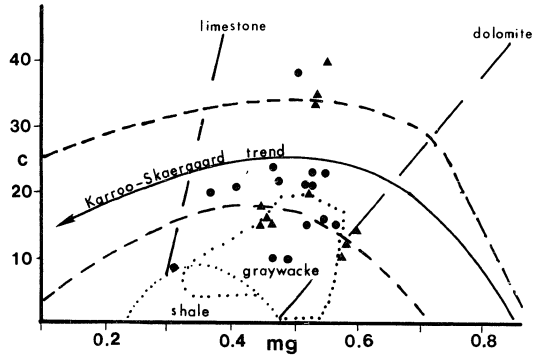


Figure 51. Niggli mg vs. c plot for Brooks Range metabasites. After Leake (1964). Area between dashed line indicates field of Karroo dolerites and Skaergaard gabbros.

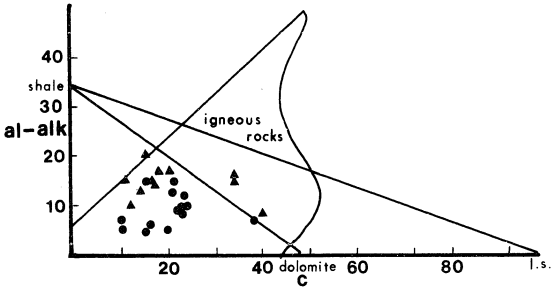


Figure 52. Niggli c vs. Al-Alk plot for Brooks Range metabasites. After van de Kamp (1969).

# ORIGIN OF THE INTERCALATED BLUESCHISTS AND GREENSCHISTS AT SELDOVIA

Although crossite-epidote and chlorite-albite assemblages are commonly accepted as diagnostic assemblages of the blueschist and greenschist facies, these assemblages occur as delicate intercalations on a scale of centimeters at Seldovia, and on the Kodiak Islands.

There are several models which could explain their apparent anomaly, including: 1) metamorphic differentiation, 2) tectonic imbrication, 3) retrograde or prograde P-T conditions, and 4) differences in parental chemical composition.

Although metamorphic differentiation might produce the observed relations, metasomatic transfer in these rocks is unlikely because of the poor exchange of pore fluids which accompanied metamorphism. Oxygen isotope compositions are significantly different in layers of contrasting mineralogy, indicating that pore fluids did not migrate beyond the boundary zones between layers. Furthermore, there are no reaction zones between layers, as predicted by Ramberg (1973); rather, the contacts are razor sharp.

The razor sharp contact between layers and excellent preservation of the relict stratigraphy, argues against metamorphic differentiation imbrication as viable mechanisms.

There is no textural or mineralogical microscopic evidence to suggest that the chlorite-albite schists were derived by the prograde or retrotrade recrystallization of crossite-bearing assemblages, even though this mechanism is in part responsible for the close association of blueschist and greenschist facies metabasites in the Brooks Range metamorphic belt.

The most probable explanation is that the different mineral assemblages are related to differences in chemical compositon of the parent rock units. Figures 49 and 50, and Table 9, show that the greenschist layers form a group that is chemically distinct from the blueschists. With few exceptions, the blueschist variants are relatively enriched in $Na_2O$, as compared to the greenschists.

On a world-wide basis, intercalated sequences of blueschists and greenschists only occur within terranes which belong to the high-temperature subdividion of the blueschist facies, with the diagnostic absence of low-temperature-high pressure phases such as aragonite, jadeite and lawsonite. When pressures and temperatures approach the boundary between the blueschist and greenschist facies, the chemical composition of the original protolith is critical in determining whether chlorite-albite, or sodic amphibole bearing assemblages will recrystallize. Only those parental rocks containing sodium concentrations greater than three weight percent produced metamorphic mineral assemblages with crossite.

The origin of the sodium-rich crossite layers is somewhat problematical. The parental material for the metabasites was a basaltic rock with tholeiitic affinities, although it is unlikely that the rocks were submarine flows because there is no evidence for relict pillow structures. The progenitors for these schists were most likely distal tuffaceous units as suggested by the characteristic layering. The association of such rocks with cherts, shales, carbonates and other ocean floor lithologies, indicate that they were deposited in a submarine aquagene environment, on an abyssal ocean floor. As each tuff layer was deposited, the upper few centimeters underwent spilitic degradation which enriched the layer in $Na_2O$ and $SiO_2$ and depleted it in respect to MgO and CaO by means of low-temperature hydrous readjustment, as discussed by Vallance (1965), Cann and Vine (1966), Melson and van Andel (1966) and Cann (1969). These trends are expressed in the bar diagram shown as Figure 47.

Spilitization is not a new idea for the generation of blueschists. It was proposed by Coleman and Lee (1963) who stated that some of the glaucophane-bearing basalts in the Franciscan Complex of California may have originally had compositions that would qualify them as spilites. In this particular case, however, it is clear that sodium enrichment occurred before metamorphism, and not during recrystallization.

Subsequent to the spilitization process, the Seldovia-Kodiak Islands schists were subducted and metamorphosed under boundary P-T conditions between the blueschists and greenschists facies, and accreted to the continental margin before Early Jurassic time.

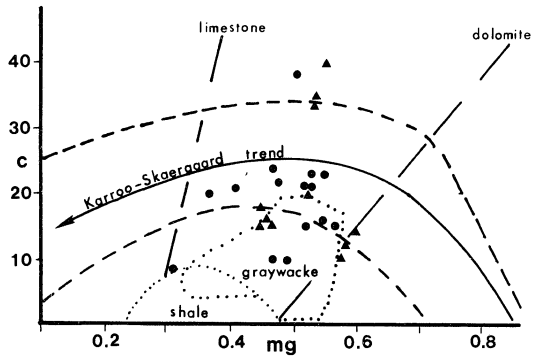


Figure 53. Niggli mg vs. c for the Seldovia-Kodiak Islands area. Symbols conform to usage in Fig. 50. After Leake (1964).

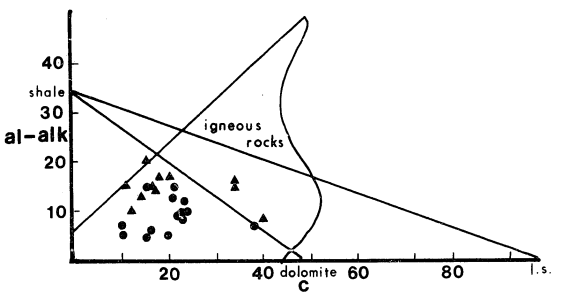


Figure 54. Niggli c vs. Al-Alk for Seldovia-Kodiak Islands area. Symbols conform to usage in Fig. 50. After van de Kamp (1969).

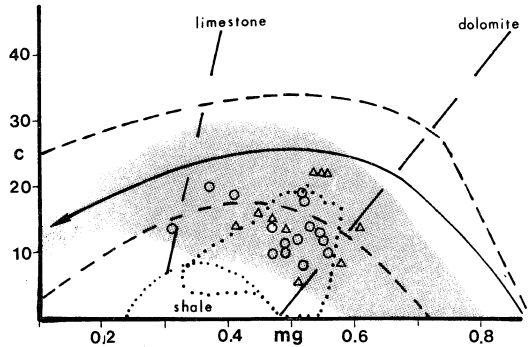


Figure 55. Niggli mg. vs. c for Seldovia-Kodiak Islands area. Symbols conform to usage in Fig. 49. Shaded area is field of 90 spillites.

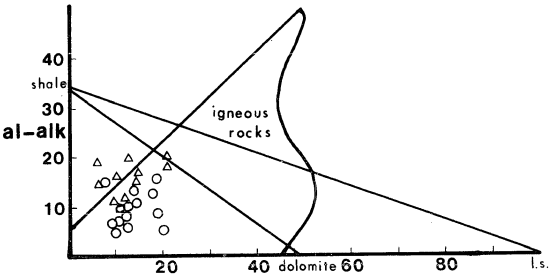


Figure 56. Niggli c vs. al-alk for Seldovia-Kodiak Islands area. Symbols conform to usage in Fig. 49. After van de Kamp (1969).

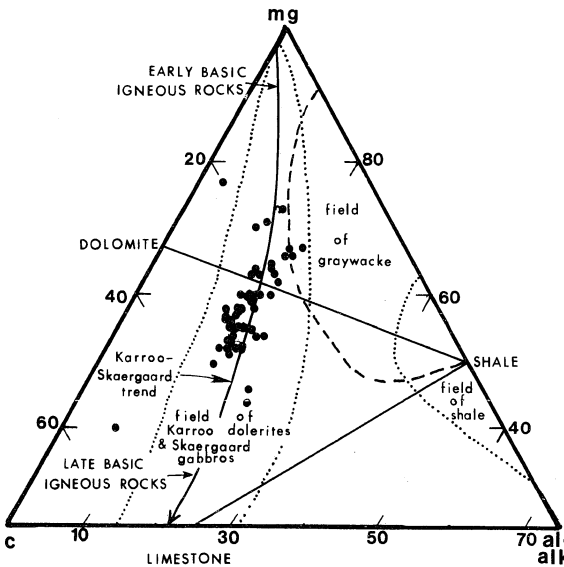


Figure 57. Ternary variation diagram of Niggli al-alk, c, 100 mg for Brooks Range metabasites presented in Table 8. Trend lines for Karroo-Skaergaard were modified after Leak (1964) with data from Wager and Brown (1967). Shale field from Leake (1964) and graywacke field compiled from Rivalenti and Sighinolfi (1969).

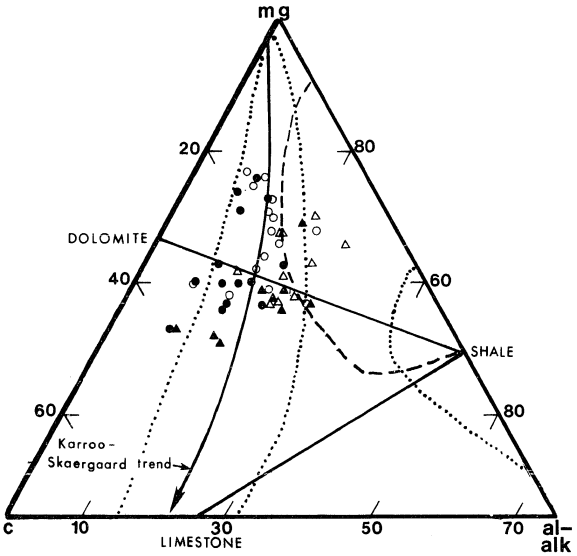


Figure 58. Ternary variation diagram of Niggli al-alk, c, 100 mg for Seldovia-Kodiak Islands metabasites presented in Table 9. Symbols conform to usage in Figures 49 and 50. Trend lines for Karroo-Skaergaard were modified after Leake (1964) with data from Wager and Brown (1967). Shale field from Leake (1964) and graywacke field compiled from Rivalenti and Sighinolfi (1969).

## SUMMARY AND CONCLUSIONS

Blueschist facies rocks are formed in zones of plate convergence under conditions of high pressure and relatively low temperature. Wherever rocks containing the high-pressure mineral assemblage characteristic of the blueschist facies are found, the metamorphic belt may be considered to mark the position of a former plate suture zone. Rocks which recrystallized in the higher temperature subdivision of this facies are commonly intercalated with rocks containing greenschist facies mineral assemblages which supposedly form at different pressure-temperature conditions.

Although several authors have noted the close relationship of these two diverse rock types, there has been no detailed geochemical, petrologic and geochronologic study of their space-time association. The object of this study was to investigate two metamorphic terranes in Alaska of differing tectonic style where these assemblages are in close association.

### SELDOVIA - KODIAK ISLANDS BELT

At the outset of this study, the only known occurrence of blueschist facies rocks on the southern Alaska margin was at Seldovia Bay, located on the southeast Kenai Peninsula. This study has shown, based on lithologic and geochronologic

considerations, that the blueschists discovered near Uyak Bay and at other localities on the northwest coast of the Kodiak Islands are correlative with those at Seldovia Bay; this belt has been named the Seldovia-Kodiak Islands metamorphic belt.

The Seldovia-Kodiak Islands metamorphic belt is bounded on the southeast by a dismembered ophiolite sequence and Cretaceous turbidites which have been metamorphosed to the prehnite-pumpellyite facies. On the northwest, the blueschists are in fault contact with sedimentary rocks of forearc affinities which have been intruded in some places by quartz-diorite plutons.

The metamorphic belt contains quartz-mica schist, marble, epidote-amphibolite, metachert and intercalated blueschist-greenschist facies lithologies. The blueschists are typically composed of crossite, epidote, chlorite, albite sphene $\pm$, with rare occurrences of lawsonite near Uyak Bay, on Kodiak Island.

K-Ar dating of mineral phases from the Seldovia and Kodiak Islands schist terranes has produced correlative mineral ages, including a characteristic age discordance between muscovite-actinolitic hornblende and crossite ages.

The cooling ages indicate that these rocks were accreted to the continental margin some time prior to 190 m.y. ago. This subduction episode is consistent with independently

determined age estimates based on (1) biostratigraphy of the associated forearc basin deposits and (2) K-Ar ages from the associated plutonic arc on the Alaska Peninsula. Similarities in rock types, mineral ages and tectonic setting indicate that the Kodiak Islands schist terrane is the southwestern extension of the Seldovia schists of the Kenai Peninsula.

On Kodiak and Afognak Islands, plutons adjacent to the metamorphic belt yield concordant Late Triassic-Early Jurassic K-Ar mineral ages. This has raised a question as to whether or not these plutons have reset the K-Ar ages of the minerals in the Seldovia-Kodiak belt, or whether the mineral ages in the schist terrane date the time of cooling to Ar-retention temperatures following metamorphic recrystallization in a subduction zone, with the Afognak and related plutons representing a late synkinematic plutonic event. The latter hypothesis is favored for the following reasons. 1) No plutons occur adjacent to the schist belt at Seldovia-Port Graham, yet K-Ar ages there are essentially identical to those from the extension of this belt on the Kodiak Islands, even to the crossite-white mica discordance. 2) Although Early Jurassic plutons do occur at the western tip of the Kenai Peninsula, they are more than 11 km from the nearest schist outcrop. The thick, intervening section of

Triassic sediments shows no effect of thermal metamorphism other than local contact effects adjacent to the small plutons. 3) There is no evidence for arc-related plutonism or forearc sedimentation on the Alaska Peninsula compatable with a subduction event much earlier than Late Triassic time.

Oxygen isotope analyses were performed on coexisting minerals from the Seldovia-Kodiak Islands and the Brooks Range metamorphic terranes by J. O'Neil of the U.S. Geological Survey. The data indicate that schists from the Kodiak segment of the belt have undergone a lower recrystallization temperature ($\bar{x}$ = 289° C) than the Seldovia segment of the same belt ($\bar{x}$ = 406° C). The oxygen isotope composition of hydrous minerals indicates that there was very little if any exchange of fluid phases between lithologic units during metamorphism. Therefore, the hypothesis that selective sodium metasomatism might produce the intercalated crossite versus chlorite-albite assemblages is rejected.

Pressure constraints imposed by sodic amphibole compositions (average crossite compositions = $Gl_{50}$) indicate that these blueschists were recrystallized under a minimum confining pressure of 5.5 kb.

Whole rock chemical compositions as determined for selected blueschists and greenschists by the U.S. Geological Survey Rapid Rock Analysis Lab, indicate that the protolith

for the metabasites from the Seldovia-Kodiak Islands terrane was a tholeiitic basalt. Multivariate discriminant analyses of the chemically analyzed metabasite population indicates that of eight possible parental groups, the metabasites have the greatest probability of having a spilitic parent vs. other alternatives. These data coupled with field observations suggest that the intercalated blueschist-greenschist sequence was most likely a series of tholeiitic tuff eruptions that were deposited on an abyssal ocean floor, or on the flank of a oceanic ridge. Subsequent to the emplacement of each layer, the upper few centimeters of the tuff blanket underwent spilitic degradation which enriched the layer in $Na_2O$ and $SiO_2$, while depleting it with respect to MgO and CaO through the process of low temperature hydrous readjustment. Metaspilitic layers with a $Na_2O$ content above about 3 percent produced crossite, and those layers containing lesser amounts of $Na_2O$ produced chlorite-albite assemblages.

The Seldovia-Kodiak Islands schist belt is a deeply subducted remnant of an accretionary complex which was emplaced by Early Jurassic time. Its relationship with other schist terranes along the southern Alaska margin such as the Knik River schist terrane, the blueschist terrane near Chitina, Alaska, the Hubbard Glacier locality and the blueschist localities on western Chichagof Island will have to remain uncertain until more data are collected. However,

the above terranes have several factors in common, including: (1) metamorphic grade increasing toward the continental block, (2) association with ophiolite and/or melange type rocks, (3) location on the continental side of the Border Ranges Fault and younger turbidite sequences, and (4) with the exception of the Knik River schist terrance, all contain similar high-temperature blueschist mineral assemblages. If these terranes have the same Early Jurassic crystallization ages as the Seldovia-Kodiak schist belt, they may all have participated in a common early Mesozoic subduction and continental accretion episode.

## BROOKS RANGE METAMORPHIC BELT

Massive, pod-like lenses of glaucophane-bearing metabasite crop out discontinuously along the south flank of the Brooks Range schist belt from Chandalar Lake to an area just north of Kiana. The Brooks Range schist belt is probably a Precambrian basement complex which has had overlying Devonian rocks stripped away by erosion, exposing a 550 km long polymetamorphic core now flanked on both the north and south sides by remnants of younger Devonian rocks. The Devonian fossils found in at least one locality within the schist terrane possibly represent an infolded bit of younger Devonian carbonates.

The Brooks Range metamorphic belt is dominantly composed of pelitic schists that contain lens-like bodies of marble, metapsammite, and metavolcanic rocks. The pelitic schists are composed of quartz, mica, albite and chlorite with biotite absent in most of the section with the exception of contact zones with intercalated feldspathic schists. The absence of biotite in metapelites that contain both muscovite and chlorite suggests that these rocks recrystallized at temperatures below the biotite isograd.

Some marbles contain biaxial calcite with anomalous optic angles averaging 20 degrees which suggests that the carbonate grains were formerly aragonite that has inverted to calcite.

Both felsic and mafic metavolcanic rocks occur on Ruby Ridge. The most obvious difference between the two rock types, in addition to color difference, is that the metabasites are completely composed of metamorphic minerals and no relict igneous mineral phases are present. Furthermore, the metamorphic minerals show strong evidence of polymetamorphism as characterized by mineral zonation, retrograde textures, overgrowths, and cross-cutting foliations. Conversely, the metafelsites have a blastoporphyritic texture including relict igneous phases and show no evidence of polymetamorphism. This suggests that the metabasites are older than the metafelsites and that the metafelsites were

probably metamorphosed subsequent to the blueschist facies metamorphic event.

At the outset of the study, it was believed that calcic amphibole-bearing metabasites occurred together in time as well as space with the glaucophane metabasites. This study has shown, however, that there is a continual gradation in mineralogy and texture between the two end members due to a strong regional metamorphic event that upgraded some of the blueschist facies metabasites to the greenschist facies. This event was isochemical, with no addition or subtraction of elements to form the greenschist facies assemblages. From geochronologic studies (Turner and Forbes, 1978), it is clear that although the glaucophane and actinolite are spatially related, in most cases their age relations are discordant as separated by a blueschist vs. greenschist interval of approximately 500 million years. However, actinolite and hornblende was formed during the earlier blueschist episode and some was unaffected by the later episode of Cretaceous metamorphism.

Seven Late Precambrian glaucophane, actinolite, hornblende and muscovite K-Ar ages indicate that the blueschist facies culminated at this time. There is some suggestion from scattered occurrences of partially amphibolized eclogite that an early eclogite facies event may have preceded the blueschist event. However, due to the rarity of the eclogite

occurrences, little is known about the genesis or age of these rocks.

Fossil aragonite, relict jadeite and evidence of former lawsonite attest that the Late Precambrian blueschist event was of the low-temperature type. There is additional evidence that temperatures increased during the later stages of the blueschist event, which upgraded the initial mineral assemblage to that of the high-temperature subdividion of the blueschist facies. There is no conclusive evidence to support a second blueschist facies event subsequent to the Late Precambrian episode of metamorphism.

The Cretaceous disturbance which culminated about 115 m.y. ago, was a lower greenschist facies event which exceeded temperatures of the biotite isograd in pelitic rocks north of the Walker Lake fault. This same greenschist event caused: (1) actinolization of glaucophane, (2) chloritization of garnet, (3) inversion of aragonite, (4) epidote to be rimmed by clinozoisite and (5) resetting of almost all white mica K-Ar ages. It is possible that some of this initial retrogradation may have taken place during the late stages of the Precambrian event. The Mesozoic orogeny was accompanied by the emplacement of a synkinematic belt of east-west trending gneissose plutons, that intruded rocks on the north margin of the schist belt. Similar plutons core the Devonian rocks in the Cosmos Hills to the south.

Temperatures of recrystallization for the blueschist facies metabasites could not be determined from oxygen isotope studies because of the polymetamorphic history. The quartz that was analyzed had re-equilibrated with coexisting micas, which had in turn recrystallized during the Late Cretaceous metamorphic event. However, initial temperatures of recrystallization are inferred to have been between 200-325°C from the stability relations of coexisting mineral assemblages recrystallized during the early part of the blueschist event. During the later portion of the Late Precambrian blueschist episode a new re-equilibrated high-temperature assemblage of blueschist minerals became stable at temperatures between 400-500°C.

Pressure constraints implied by sodic amphibole composition and jadeite + quartz assemblages indicate that recrystallization occurred at a minimum pressure of 6.5 kb.

Normative mineral compositions calculated for whole rock chemical analyses of metabasites indicate that the protolith was tholeiitic basalt. When metabasite compositions are plotted on a conventional AMF diagram, the rocks lie directly on the classic Karroo-Skaergaard continental tholeiitic trend, and there is no evidence that the blueschists are more enriched in alkalis than greenschist metabasites. Some of the cores of the large pod-like masses

of blueschist contain what appears to be a relict igneous fabric, similar to that of coarse-grained diabase or gabbro. However, the original igneous phases have been obliterated and are replaced by metamorphic minerals. Furthermore, the metabasites have oxidation ratios indicative of an intrusive origin. Cumulatively, these data indicate that the parent mafic rocks were intruded as small plutons or dikes and sills.

Although a consuming plate margin is a convenient model for the generation of blueschist facies pressure-temperature conditions, the blueschists that occur in the Brooks Range schist belt do not seem to fit the classic subduction model. There does not appear to be any evidence for a fossil subduction zone for the generation of these blueschists, as there are no ophiolites, paired metamorphic belts or identifiable trench lithologies. With further work other alternatives will have to be explored to explain the generation of the Late Precambrian blueschists of the Brooks Range.

## RECOMMENDATIONS FOR FURTHER STUDY

Of prime importance to the understanding of the tectonics of southern Alaska is the dating of other schist terranes mentioned in this study that occur along the southern Alaska margin. The dating of these terranes is not only vital to correlation and tectonic understanding, but also may shed light on the hypothesis that the nearby plutons have reset the recrystallization ages. If the schists dated in other terranes are not close to intrusive bodies, yet yield similar ages as the Seldovia-Kodiak Islands belt, then the hypothesis that the ages of these schists were reset may be discarded.

Another approach which may be used to determine if the schist ages have been reset, would be a study to determine if temperatures high enough to reset actinolite K-Ar ages would appreciably affect $\delta_O 18$. If proven, then it is unlikely that these rocks have been reset because the temperatures of recrystallization as determined by oxygen isotope studies are compatible with the stability field for the coexisting lime-alumino silicates and what is known about the stability field of blueschist facies rocks in other terranes throughout the world.

Furthermore, much additional field work is needed to tie in the gaps between terranes that contain blueschist facies assemblages. Although it is doubtful that blue-

schists crop out between the tip of the Kenai Peninsula and Anchorage, there is a good chance that terranes containing sodic amphibole assemblages occur between Anchorage and Chitina. A particularly interesting study would be a detailed petrographic study of the Knik River schist terrane to determine if blueschist facies assemblages occur there.

Other topics related to the blueschists of southern Alaska which may warrant study are: (1) a follow-up study of the relationship and possible correlation of the Early Jurassic blueschists of the Kamchatkan Peninsula, 2) the nature and tectonic significance of the "near trench" Afognak pluton and similar plutons on the Kenai Peninsula and 3) chemical studies of other intercalated blueschist-greenschist terranes to determine if they yield similar chemical differences between layers as outlined in this study.

There are several topics of interest which may justify further study that are related to the Brooks Range schist belt. One important follow-up study is the inter-relationship of the Brooks Range schist belt and the coarse-grained Precambrian blueschist terranes on the Seward Peninsula. A study of this nature would test the hypothesis of whether it is feasible that the rocks of the Brooks Range schist belt have undergone a syntaxial bend under Kotzebue Sound and are correlative to those found on the Seward Peninsula.

A natural follow-up to this work would be a study of the temperatures that accompanied recrystallization for the different metamorphic episodes of the schist belt. Since the oxygen isotope studies were not conclusive, another approach would have to be taken, perhaps trace element partitioning of coexisting mineral phases as related to temperature of recrystallization.

Another topic of vital importance, is a study to determine whether the Precambrian K-Ar ages determined for minerals of the schist belt are real. A study of this type might utilize an incremental heating method to determine if the Late Precambrian ages are anomously old.

Finally, if the Precambrian ages determined for minerals in the Brooks Range schist belt are real, what is the tectonic significance of these ages? It is fairly clear that the basaltic protolith for the blueschist facies metabasites was a continental tholeiite, and a classic subduction model does not seem to be appropriate. Although it is difficult to reconstruct Precambrian history, a study of the generation mechanism for blueschist facies rocks is necessary.

# APPENDIX 1

Chemical analyses, CIPW norms, and Niggli values of selected rocks from the Brooks Range metamorphic belt.

| Sample | Blueschist 1 | 2 | 3 | 4 | 5 | 6 | 7 | 8 |
|---|---|---|---|---|---|---|---|---|
| | Chemical Analyses (Weight Percent) | | | | | | | |
| $SiO_2$ | 49.2 | 47.6 | 46.9 | 47.0 | 47.8 | 50.2 | 48.5 | 44.8 |
| $TiO_2$ | 1.2 | 1.3 | 1.2 | 1.1 | 1.7 | 1.4 | 2.2 | 1.7 |
| $Al_2O_3$ | 13.3 | 15.4 | 17.0 | 14.6 | 16.0 | 14.0 | 15.3 | 14.4 |
| $Fe_2O_3$ | 2.7 | 3.7 | 3.8 | 2.7 | 1.8 | 3.2 | 2.6 | 2.6 |
| FeO | 9.2 | 6.6 | 5.9 | 10.4 | 14.1 | 10.2 | 10.2 | 8.0 |
| MnO | 0.17 | 0.13 | 0.03 | 0.17 | 0.17 | 0.13 | 0.16 | 0.12 |
| MgO | 8.1 | 7.5 | 6.7 | 10.1 | 7.2 | 6.8 | 6.3 | 11.5 |
| CaO | 11.4 | 15.7 | 14.9 | 8.6 | 3.7 | 8.8 | 9.3 | 5.2 |
| $Na_2O$ | 1.9 | 0.97 | 1.5 | 1.7 | 3.7 | 3.0 | 3.0 | 3.4 |
| $K_2O$ | 0.63 | 0.61 | 0.14 | 0.78 | 0.72 | 0.43 | 0.20 | 0.16 |
| $P_2O_5$ | 0.1 | 0.2 | 0.12 | 0.1 | 0.07 | 0.1 | 0.18 | 0.29 |
| $H_2O^+$ | 1.3 | 0.96 | 1.0 | 2.8 | 1.9 | 0.86 | 1.9 | 5.6 |
| $H_2O^-$ | 0.09 | 0.04 | 0.06 | 0.11 | 0.17 | 0.09 | 0.12 | 0.19 |
| $CO_2$ | 0.10 | 0.08 | 0.02 | 0.03 | 0.62 | 0.02 | 0.39 | 2.30 |
| Total | 99.39 | 100.77 | 99.27 | 100.19 | 99.65 | 99.23 | 100.35 | 100.26 |
| | CIPW Norm | | | | | | | |
| Qz | 0.20 | 0.92 | 0.75 | 0.00 | 0.00 | 0.25 | 0.00 | 0.00 |
| Or | 3.84 | 3.67 | 0.85 | 4.76 | 4.38 | 2.62 | 1.22 | 0.97 |
| Ab | 17.60 | 8.87 | 13.87 | 15.76 | 34.19 | 27.74 | 27.72 | 31.48 |
| An | 26.73 | 36.52 | 40.42 | 30.87 | 14.39 | 24.17 | 28.50 | 9.66 |
| Ne | 0.00 | 0.00 | 0.00 | 0.00 | 0.00 | 0.00 | 0.00 | 0.00 |
| Di | 24.24 | 32.86 | 27.83 | 9.84 | 0.00 | 16.00 | 12.19 | 0.00 |
| Hy | 22.27 | 10.80 | 10.15 | 24.18 | 27.18 | 23.51 | 22.17 | 36.41 |
| Ol | 0.00 | 0.00 | 0.00 | 9.80 | 9.23 | 0.00 | 0.85 | 3.75 |
| Mt | 2.91 | 3.94 | 4.09 | 2.91 | 1.94 | 3.45 | 2.80 | 2.80 |
| Il | 1.72 | 1.84 | 1.72 | 1.58 | 2.44 | 2.01 | 3.15 | 2.44 |
| Ap | 0.22 | 0.38 | 0.26 | 0.22 | 0.15 | 0.22 | 0.39 | 0.63 |
| Cc | 0.26 | 0.21 | 0.05 | 0.08 | 1.61 | 0.05 | 1.01 | 6.00 |
| | Niggli Values | | | | | | | |
| si | 111.2 | 101.6 | 103.4 | 102.3 | 115.3 | 119.4 | 115.4 | 103.2 |
| al | 17.7 | 19.3 | 22.1 | 18.7 | 22.7 | 19.6 | 21.4 | 19.5 |
| fm | 49.7 | 41.9 | 39.4 | 56.6 | 58.0 | 50.4 | 47.7 | 59.8 |
| c | 27.6 | 35.9 | 35.2 | 20.1 | 9.6 | 22.4 | 23.7 | 12.8 |
| alk | 5.1 | 2.8 | 3.4 | 4.7 | 9.8 | 7.6 | 7.2 | 7.8 |
| mg | 0.55 | 0.57 | 0.56 | 0.58 | 0.45 | 0.48 | 0.47 | 0.66 |
| ti | 2.0 | 2.1 | 2.0 | 1.8 | 3.1 | 2.5 | 3.9 | 2.9 |

Appendix 1 (continued)

| Sample | 9 | 10 | 11 | Blueschist 12 | 13 | 14 | 15 | 16 |
|---|---|---|---|---|---|---|---|---|
| | | | | Chemical Analyses (Weight Percent) | | | | |
| $SiO_2$ | 50.2 | 47.8 | 48.4 | 49.6 | 50.7 | 38.2 | 48.1 | 47.7 |
| $TiO_2$ | 1.4 | 1.6 | 1.6 | 1.4 | 1.5 | 0.95 | 2.1 | 2.3 |
| $Al_2O_3$ | 15.0 | 14.9 | 15.6 | 12.0 | 13.9 | 8.3 | 16.3 | 16.4 |
| $Fe_2O_3$ | 3.1 | 3.0 | 3.4 | 4.6 | 4.0 | 2.4 | 2.6 | 2.5 |
| FeO | 8.8 | 9.6 | 9.6 | 5.9 | 10.5 | 6.6 | 8.3 | 8.1 |
| MnO | 0.14 | 0.19 | 0.21 | 0.10 | 0.13 | 0.17 | 0.12 | 0.13 |
| MgO | 7.4 | 6.0 | 5.6 | 7.9 | 6.1 | 3.2 | 6.7 | 6.5 |
| CaO | 7.8 | 8.8 | 8.9 | 5.7 | 3.6 | 19.1 | 8.2 | 8.3 |
| $Na_2O$ | 4.0 | 4.1 | 3.9 | 6.3 | 2.2 | 1.5 | 3.8 | 3.8 |
| $K_2O$ | 0.15 | 0.03 | 0.04 | 0.22 | 2.60 | 0.79 | 0.29 | 0.44 |
| $P_2O_5$ | 0.15 | 0.22 | 0.15 | 0.38 | 0.16 | 0.07 | 0.25 | 0.31 |
| $H_2O^+$ | 2.0 | 2.4 | 2.2 | 3.1 | 4.0 | 2.9 | 2.2 | 2.2 |
| $H_2O^-$ | 0.13 | 0.14 | 0.14 | 0.19 | 0.15 | 0.35 | 0.15 | 0.17 |
| $CO_2$ | 0.02 | 1.30 | 0.80 | 2.20 | 0.55 | 15.10 | 0.02 | 0.02 |
| Total | 100.29 | 100.08 | 100.54 | 99.59 | 100.09 | 99.63 | 99.13 | 98.87 |
| | | | | CIPW Norms | | | | |
| Qz | 0.00 | 0.00 | 0.00 | 0.00 | 6.74 | 17.11 | 0.00 | 0.00 |
| Qr | 0.90 | 0.18 | 0.24 | 1.31 | 16.33 | 4.75 | 1.77 | 2.69 |
| Ab | 36.50 | 37.73 | 35.85 | 57.09 | 21.01 | 13.72 | 35.21 | 35.31 |
| An | 22.90 | 22.72 | 25.54 | 3.85 | 14.19 | -1.18 | 27.41 | 27.32 |
| Ne | 0.00 | 0.00 | 0.00 | 0.00 | 0.00 | 0.00 | 0.00 | 0.00 |
| Di | 12.24 | 9.71 | 10.79 | 6.52 | 0.00 | 0.00 | 10.20 | 10.46 |
| Hy | 13.57 | 11.50 | 13.22 | 3.16 | 30.24 | 16.63 | 8.31 | 5.64 |
| Ol | 8.23 | 8.81 | 6.05 | 14.83 | 0.00 | 0.00 | 10.69 | 11.84 |
| Mt | 3.29 | 3.21 | 3.64 | 4.85 | 4.45 | 2.56 | 2.80 | 2.70 |
| Il | 1.98 | 2.28 | 2.28 | 1.97 | 2.22 | 1.35 | 3.02 | 3.32 |
| Ap | 0.32 | 0.47 | 0.32 | 0.80 | 0.36 | 0.15 | 0.54 | 0.67 |
| Cc | 0.05 | 3.37 | 2.07 | 5.62 | 1.48 | 38.90 | 0.05 | 0.05 |
| | | | | Niggli Values | | | | |
| si | 119.5 | 114.9 | 116.2 | 124.9 | 137.7 | 96.6 | 116.6 | 116.4 |
| al | 21.0 | 21.1 | 22.0 | 17.8 | 22.2 | 12.4 | 23.2 | 23.5 |
| fm | 49.7 | 46.7 | 45.9 | 51.1 | 57.0 | 31.0 | 46.1 | 45.1 |
| c | 19.9 | 22.7 | 22.9 | 15.4 | 10.5 | 51.8 | 21.3 | 21.7 |
| alk | 9.4 | 9.6 | 9.1 | 15.7 | 10.3 | 5.0 | 9.4 | 9.7 |
| mg | 0.53 | 0.46 | 0.44 | 0.58 | 0.44 | 0.39 | 0.53 | 0.53 |
| ti | 2.5 | 2.9 | 2.9 | 2.6 | 3.1 | 1.8 | 3.8 | 4.2 |

Appendix 1 (continued)

| | Blueschist | | | | | | | |
|---|---|---|---|---|---|---|---|---|
| Sample | 17 | 18 | 19 | 20 | 21 | 22 | 23 | 24 |
| | Chemical Analyses (Weight Percent) | | | | | | | |
| $SiO_2$ | 47.6 | 50.2 | 47.1 | 47.1 | 58.2 | 49.7 | 49.6 | 59.1 |
| $TiO_2$ | 1.4 | 1.6 | 1.4 | 1.8 | 1.5 | 1.5 | 3.7 | 1.5 |
| $Al_2O_3$ | 15.8 | 15.6 | 14.7 | 15.1 | 11.9 | 14.1 | 13.5 | 11.5 |
| $Fe_2O_3$ | 1.7 | 2.0 | 2.9 | 2.8 | 5.0 | 5.7 | 3.3 | 5.0 |
| FeO | 9.9 | 8.9 | 13.6 | 12.2 | 11.4 | 9.0 | 12.2 | 11.4 |
| MnO | 0.15 | 0.14 | 0.36 | 0.17 | 0.22 | 0.20 | 0.21 | 0.25 |
| MgO | 8.3 | 7.5 | 6.8 | 6.3 | 0.96 | 6.3 | 5.5 | 0.87 |
| CaO | 6.9 | 6.7 | 8.8 | 6.2 | 5.1 | 8.5 | 6.7 | 5.1 |
| $Na_2O$ | 2.5 | 3.7 | 2.4 | 3.5 | 2.6 | 1.3 | 2.5 | 2.8 |
| $K_2O$ | 0.24 | 0.27 | 0.11 | 0.38 | 0.35 | 1.40 | 0.06 | 0.35 |
| $P_2O_5$ | 0.21 | 0.23 | 0.17 | 0.1 | 0.41 | 0.16 | 0.39 | 0.43 |
| $H_2O^+$ | 3.3 | 2.3 | 0.84 | 3.6 | 0.96 | 1.0 | 1.7 | 0.75 |
| $H_2O^-$ | 0.10 | 0.13 | 0.11 | 0.15 | 0.15 | 0.07 | 0.09 | 0.13 |
| $CO_2$ | 1.00 | 0.12 | 0.02 | 0.02 | 0.02 | 0.37 | 0.56 | 0.02 |
| Total | 99.10 | 99.39 | 99.31 | 99.42 | 98.77 | 99.30 | 100.01 | 99.20 |
| | CIPW Norms | | | | | | | |
| Qz | 1.54 | 0.00 | 0.00 | 0.00 | 24.57 | 8.20 | 8.70 | 24.69 |
| Or | 1.48 | 1.64 | 0.68 | 2.37 | 2.24 | 8.68 | 0.37 | 2.23 |
| Ab | 23.43 | 34.13 | 22.40 | 33.23 | 25.31 | 12.25 | 23.63 | 27.06 |
| An | 27.71 | 25.85 | 30.16 | 25.77 | 21.43 | 29.92 | 26.79 | 19.14 |
| Ne | 0.00 | 0.00 | 0.00 | 0.00 | 0.00 | 0.00 | 0.00 | 0.00 |
| Di | 0.00 | 4.78 | 11.15 | 4.74 | 2.37 | 8.63 | 1.44 | 3.95 |
| Hy | 36.91 | 24.74 | 23.14 | 16.76 | 15.17 | 22.54 | 27.66 | 14.04 |
| Ol | 0.00 | 3.61 | 6.87 | 11.10 | 0.00 | 0.00 | 0.00 | 0.00 |
| Mt | 1.86 | 2.15 | 3.15 | 3.09 | 5.67 | 6.25 | 3.63 | 5.63 |
| Il | 2.04 | 2.29 | 2.03 | 2.65 | 2.27 | 2.19 | 5.43 | 2.25 |
| Ap | 0.46 | 0.49 | 0.37 | 0.22 | 0.93 | 0.35 | 0.86 | 0.97 |
| Cc | 2.64 | 0.31 | 0.05 | 0.05 | 0.05 | 0.98 | 1.49 | 0.05 |
| | Niggli Values | | | | | | | |
| si | 115.1 | 124.3 | 105.9 | 114.8 | 193.5 | 121.4 | 128.3 | 197.5 |
| al | 22.5 | 22.7 | 19.4 | 21.7 | 23.3 | 20.3 | 20.6 | 22.6 |
| fm | 53.4 | 50.2 | 54.0 | 53.3 | 49.5 | 52.3 | 54.5 | 49.3 |
| c | 17.9 | 17.8 | 21.2 | 16.2 | 18.2 | 22.2 | 18.6 | 18.3 |
| alk | 6.2 | 9.3 | 5.4 | 8.9 | 9.1 | 5.3 | 6.4 | 9.8 |
| mg | 0.56 | 0.56 | 0.43 | 0.43 | 0.10 | 0.44 | 0.39 | 0.09 |
| ti | 2.5 | 3.0 | 2.4 | 3.3 | 3.7 | 3.7 | 7.2 | 3.8 |

Appendix 1 (continued)

| Blueschist | Greenschist | | | | | |
|---|---|---|---|---|---|---|
| Sample | 25 | 26 | 27 | 28 | 29 | 30 | 31 |
| | Chemical Analyses (Weight Percent) | | | | | | |
| $SiO_2$ | 46.9 | 46.9 | 49.8 | 43.4 | 46.6 | 47.6 | 46.6 |
| $TiO_2$ | 1.8 | 2.0 | 1.4 | 2.1 | 2.3 | 1.7 | 3.0 |
| $Al_2O_3$ | 14.3 | 14.0 | 14.1 | 16.1 | 14.8 | 14.3 | 13.5 |
| $Fe_2O_3$ | 2.4 | 3.2 | 2.5 | 1.8 | 3.0 | 2.0 | 3.3 |
| FeO | 9.4 | 9.4 | 9.7 | 9.3 | 9.4 | 10.0 | 10.2 |
| MnO | 0.14 | 0.18 | 0.16 | 0.13 | 0.16 | 0.14 | 0.16 |
| MgO | 7.6 | 7.3 | 7.5 | 6.7 | 6.6 | 8.1 | 2.9 |
| CaO | 7.1 | 11.9 | 9.7 | 8.7 | 11.2 | 7.9 | 8.7 |
| $Na_2O$ | 4.0 | 1.6 | 1.5 | 3.3 | 1.8 | 2.9 | 2.6 |
| $K_2O$ | 0.04 | 0.10 | 0.05 | 0.14 | 0.34 | 0.23 | 0.38 |
| $P_2O_5$ | 0.21 | 0.32 | 0.16 | 0.28 | 0.31 | 0.13 | 0.4 |
| $H_2O^+$ | 2.6 | 2.1 | 2.5 | 3.0 | 2.4 | 3.8 | 3.3 |
| $H_2O^-$ | 0.07 | 0.06 | 0.06 | 0.11 | 0.08 | 0.11 | 0.21 |
| $CO_2$ | 2.30 | 0.02 | 0.02 | 4.30 | 0.02 | 0.20 | 1.20 |
| Total | 98.86 | 99.08 | 99.15 | 99.36 | 99.01 | 99.11 | 98.75 |
| | | CIPW Norms | | | | | |
| Qz | 0.00 | 2.07 | 6.34 | 1.84 | 1.53 | 0.00 | 4.77 |
| Or | 0.24 | 0.62 | 0.31 | 0.85 | 2.12 | 1.43 | 2.41 |
| Ab | 36.95 | 15.13 | 14.21 | 30.41 | 17.09 | 27.41 | 25.08 |
| An | 19.87 | 32.37 | 33.35 | 14.52 | 33.11 | 26.66 | 25.84 |
| Ne | 0.00 | 0.00 | 0.00 | 0.00 | 0.00 | 0.00 | 0.00 |
| Di | 0.00 | 22.00 | 12.97 | 0.00 | 18.71 | 9.90 | 7.67 |
| Hy | 25.21 | 20.59 | 27.60 | 29.69 | 19.99 | 22.79 | 21.88 |
| Ol | 5.46 | 0.00 | 0.00 | 0.00 | 0.00 | 6.29 | 0.00 |
| Mt | 2.58 | 3.52 | 2.76 | 1.93 | 3.32 | 2.20 | 3.71 |
| Il | 2.58 | 2.94 | 2.06 | 3.00 | 3.39 | 2.49 | 4.49 |
| Ap | 0.45 | 0.70 | 0.35 | 0.60 | 0.69 | 0.29 | 0.90 |
| Cc | 5.98 | 0.05 | 0.05 | 11.16 | 0.05 | 0.53 | 3.26 |
| | | Niggli Values | | | | | |
| si | 114.2 | 106.8 | 120.0 | 105.0 | 108.9 | 113.5 | 119.7 |
| al | 20.5 | 18.8 | 20.0 | 22.9 | 20.4 | 20.1 | 20.4 |
| fm | 51.5 | 48.6 | 51.4 | 46.6 | 47.0 | 52.7 | 48.6 |
| c | 18.5 | 29.0 | 25.0 | 22.6 | 28.1 | 20.2 | 24.0 |
| alk | 9.5 | 3.7 | 3.6 | 7.9 | 4.6 | 7.0 | 7.1 |
| mg | 0.54 | 0.51 | 0.53 | 0.52 | 0.49 | 0.55 | 0.41 |
| ti | 3.3 | 3.4 | 2.5 | 3.8 | 4.0 | 3.0 | 5.8 |

Appendix 1 (continued)

| Sample | Greenschist 32 | 33 | 34 | 35 | 36 | 37 | 38 | 39 |
|---|---|---|---|---|---|---|---|---|
| | Chemical Analyses (Weight Percent) | | | | | | | |
| $SiO_2$ | 48.9 | 48.5 | 47.4 | 47.8 | 48.4 | 45.5 | 44.7 | 49.4 |
| $TiO_2$ | 3.7 | 1.5 | 1.7 | 1.5 | 2.5 | 3.6 | 3.1 | 2.4 |
| $Al_2O_3$ | 13.5 | 13.5 | 16.0 | 15.7 | 16.7 | 12.0 | 14.4 | 12.7 |
| $Fe_2O_3$ | 2.2 | 3.6 | 1.9 | 1.7 | 3.4 | 2.6 | 2.9 | 2.5 |
| FeO | 13.3 | 9.5 | 9.4 | 9.8 | 8.8 | 15.6 | 11.2 | 10.9 |
| MnO | 0.19 | 0.18 | 0.14 | 0.12 | 0.15 | 0.31 | 0.18 | 0.16 |
| MgO | 5.5 | 6.5 | 7.1 | 7.6 | 4.5 | 6.3 | 6.7 | 6.5 |
| CaO | 5.1 | 8.9 | 8.1 | 6.8 | 10.7 | 9.5 | 9.2 | 8.1 |
| $Na_2O$ | 1.8 | 3.1 | 3.3 | 3.4 | 2.6 | 1.8 | 2.6 | 2.9 |
| $K_2O$ | 0.17 | 0.09 | 0.12 | 0.20 | 0.05 | 0.14 | 0.38 | 0.28 |
| $P_2O_5$ | 0.68 | 0.17 | 0.23 | 0.23 | 0.06 | 0.00 | 0.33 | 0.26 |
| $H_2O^+$ | 3.0 | 1.7 | 3.2 | 3.1 | 1.8 | 1.6 | 3.0 | 2.9 |
| $H_2O^-$ | 0.18 | 0.09 | 0.18 | 0.19 | 0.08 | 0.06 | 0.20 | 0.22 |
| $CO_2$ | 1.30 | 2.10 | 1.00 | 0.67 | 0.04 | 0.02 | 0.02 | 0.02 |
| Total | 99.52 | 99.43 | 99.77 | 98.81 | 99.78 | 99.03 | 98.91 | 99.24 |
| | CIPW Norms | | | | | | | |
| Qz | 16.41 | 3.34 | 0.00 | 0.00 | 3.32 | 0.09 | 0.00 | 2.44 |
| Or | 1.08 | 0.55 | 0.73 | 1.23 | 0.31 | 0.89 | 2.39 | 1.75 |
| Ab | 17.41 | 28.70 | 30.67 | 31.82 | 24.38 | 17.30 | 24.86 | 27.59 |
| An | 13.62 | 23.37 | 29.49 | 28.14 | 35.25 | 25.96 | 28.23 | 22.05 |
| Ne | 0.00 | 0.00 | 0.00 | 0.00 | 0.00 | 0.00 | 0.00 | 0.00 |
| Di | 0.00 | 5.87 | 3.20 | 0.84 | 15.61 | 19.48 | 14.37 | 14.88 |
| Hy | 31.66 | 26.30 | 22.63 | 24.51 | 13.54 | 27.95 | 12.52 | 24.35 |
| Ol | 0.00 | 0.00 | 5.65 | 7.17 | 0.00 | 0.00 | 9.02 | 0.00 |
| Mt | 2.48 | 3.88 | 2.06 | 1.85 | 3.71 | 2.91 | 3.23 | 2.77 |
| Il | 5.55 | 2.15 | 2.45 | 2.18 | 3.64 | 5.37 | 4.60 | 3.54 |
| Ap | 1.53 | 0.37 | 0.50 | 0.50 | 0.13 | 0.00 | 0.73 | 0.58 |
| Cc | 3.54 | 5.48 | 2.62 | 1.77 | 0.11 | 0.05 | 0.05 | 0.05 |
| | Niggli Values | | | | | | | |
| si | 134.3 | 118.1 | 114.5 | 116.9 | 119.2 | 104.1 | 104.5 | 123.6 |
| al | 21.8 | 19.3 | 22.7 | 22.6 | 24.2 | 16.1 | 19.8 | 18.7 |
| fm | 58.1 | 50.0 | 48.4 | 51.2 | 41.3 | 56.4 | 50.7 | 52.1 |
| c | 15.0 | 23.2 | 21.0 | 17.8 | 28.3 | 23.3 | 23.0 | 21.7 |
| alk | 5.1 | 7.5 | 7.9 | 8.4 | 6.3 | 4.2 | 6.5 | 7.5 |
| mg | 0.39 | 0.48 | 0.53 | 0.54 | 0.40 | 0.38 | 0.46 | 0.47 |
| ti | 7.6 | 2.7 | 3.1 | 2.7 | 4.6 | 6.2 | 5.4 | 4.5 |

Appendix 1 (continued)

| | Greenschist | | | | | | | |
|---|---|---|---|---|---|---|---|---|
| Sample | 40 | 41 | 42 | 43 | 44 | 45 | 46 | 47 |
| | Chemical Analyses (Weight Percent) | | | | | | | |
| $SiO_2$ | 44.2 | 47.7 | 49.2 | 48.6 | 49.9 | 45.6 | 46.4 | 46.5 |
| $TiO_2$ | 1.7 | 3.5 | 1.7 | 1.8 | 1.2 | 2.0 | 1.6 | 1.5 |
| $Al_2O_3$ | 16.8 | 11.9 | 16.2 | 15.4 | 14.7 | 14.7 | 14.5 | 16.0 |
| $Fe_2O_3$ | 1.2 | 1.4 | 3.5 | 1.9 | 2.2 | 3.2 | 3.5 | 1.5 |
| FeO | 10.8 | 15.7 | 6.8 | 9.6 | 8.2 | 8.7 | 10.6 | 10.0 |
| MnO | 0.10 | 0.26 | 0.22 | 0.26 | 0.27 | 0.28 | 0.21 | 0.15 |
| MgO | 7.1 | 3.6 | 6.2 | 6.8 | 7.0 | 6.3 | 6.7 | 9.4 |
| CaO | 4.9 | 6.9 | 8.3 | 5.8 | 11.6 | 14.4 | 11.0 | 10.2 |
| $Na_2O$ | 5.3 | 2.2 | 3.4 | 4.1 | 1.8 | 1.7 | 2.1 | 2.2 |
| $K_2O$ | 0.03 | 0.11 | 0.77 | 0.32 | 0.43 | 0.20 | 0.15 | 0.16 |
| $P_2O_5$ | 0.38 | 0.41 | 0.32 | 0.25 | 0.15 | 0.29 | 0.3 | 0.15 |
| $H_2O^+$ | 5.0 | 3.1 | 2.6 | 3.1 | 1.2 | 2.1 | 2.1 | 2.9 |
| $H_2O^-$ | 0.23 | 0.18 | 0.13 | 0.20 | 0.10 | 0.12 | 0.19 | 0.06 |
| $CO_2$ | 2.40 | 3.80 | 0.13 | 1.00 | 0.27 | 0.01 | 0.02 | 0.05 |
| Total | 100.14 | 100.76 | 99.47 | 99.13 | 99.02 | 99.60 | 99.37 | 100.77 |
| | CIPW Norms | | | | | | | |
| Qz | 0.00 | 15.45 | 0.00 | 0.00 | 3.36 | 0.00 | 0.00 | 0.00 |
| Qr | 0.18 | 0.69 | 4.71 | 1.96 | 2.63 | 1.24 | 0.93 | 0.97 |
| Ab | 48.91 | 21.02 | 31.62 | 38.19 | 16.74 | 16.00 | 19.83 | 20.18 |
| An | 6.84 | 8.01 | 27.63 | 21.60 | 31.86 | 33.44 | 31.23 | 34.03 |
| Ne | 0.00 | 0.00 | 0.00 | 0.00 | 0.00 | 0.00 | 0.00 | 0.00 |
| Di | 0.00 | 0.00 | 9.61 | 0.00 | 19.97 | 31.53 | 19.17 | 13.07 |
| Hy | 5.33 | 30.67 | 18.96 | 24.51 | 20.30 | 7.37 | 20.05 | 11.80 |
| Ol | 21.67 | 0.00 | 0.19 | 5.13 | 0.00 | 3.33 | 1.89 | 15.78 |
| Mt | 1.29 | 1.56 | 3.79 | 2.06 | 2.38 | 3.51 | 3.85 | 1.60 |
| Il | 2.43 | 5.19 | 2.45 | 2.60 | 1.73 | 2.92 | 2.34 | 2.13 |
| Ap | 0.82 | 0.91 | 0.69 | 0.54 | 0.32 | 0.64 | 0.66 | 0.32 |
| Cc | 6.24 | 10.23 | 0.34 | 2.62 | 0.71 | 0.03 | 0.55 | 0.13 |
| | Niggli Values | | | | | | | |
| si | 108.0 | 131.2 | 123.1 | 123.7 | 118.0 | 100.9 | 105.2 | 100.5 |
| al | 24.2 | 19.3 | 23.8 | 23.1 | 20.4 | 19.1 | 19.3 | 20.4 |
| fm | 50.4 | 54.4 | 44.5 | 50.5 | 45.4 | 42.8 | 49.1 | 51.2 |
| c | 12.8 | 20.3 | 22.2 | 15.8 | 29.4 | 34.1 | 26.7 | 23.6 |
| alk | 12.6 | 6.1 | 9.5 | 10.6 | 4.8 | 3.9 | 4.8 | 4.8 |
| mg | 0.52 | 0.27 | 0.52 | 0.51 | 0.55 | 0.49 | 0.46 | 0.60 |
| ti | 3.1 | 7.2 | 3.2 | 3.4 | 2.1 | 3.3 | 2.7 | 2.4 |

Appendix 1 (continued)

| Sample | Greenschist 48 | 49 | 50 | 51 | 52 | 53 | 54 | 55 |
|---|---|---|---|---|---|---|---|---|
| | Chemical Analyses (Weight Percent) | | | | | | | |
| $SiO_2$ | 45.9 | 45.1 | 42.3 | 40.7 | 49.9 | 49.4 | 50.2 | 49.4 |
| $TiO_2$ | 1.5 | 1.1 | 0.87 | 1.1 | 1.1 | 1.0 | 1.1 | 1.2 |
| $Al_2O_3$ | 13.2 | 12.1 | 10.6 | 12.2 | 14.9 | 15.3 | 16.6 | 14.7 |
| $Fe_2O_3$ | 1.3 | 0.6 | 0.7 | 3.3 | 2.9 | 3.8 | 2.6 | 2.7 |
| FeO | 11.4 | 10.9 | 11.8 | 12.0 | 7.3 | 5.6 | 6.9 | 8.3 |
| MnO | 0.16 | 0.12 | 0.14 | 0.18 | 0.10 | 0.09 | 0.08 | 0.14 |
| MgO | 5.9 | 11.8 | 16.8 | 16.1 | 8.5 | 6.9 | 7.3 | 7.7 |
| CaO | 10.1 | 6.7 | 9.3 | 7.8 | 10.9 | 14.0 | 9.6 | 12.1 |
| $Na_2O$ | 1.6 | 0.26 | 0.36 | 1.3 | 2.6 | 2.2 | 2.9 | 2.1 |
| $K_2O$ | 0.62 | 0.09 | 0.07 | 0.11 | 0.65 | 0.16 | 0.38 | 0.56 |
| $P_2O_5$ | 0.1 | 0.17 | 0.1 | 0.13 | 0.1 | 0.1 | 0.08 | 0.1 |
| $H_2O^+$ | 2.4 | 6.5 | 5.9 | 5.9 | 1.9 | 1.2 | 2.1 | 1.5 |
| $H_2O^-$ | 0.15 | 0.12 | 0.08 | 0.06 | 0.15 | 0.05 | 0.07 | 0.08 |
| $CO_2$ | 6.40 | 4.60 | 2.30 | 0.11 | 0.02 | 0.02 | 0.02 | 0.02 |
| Total | 100.73 | 100.16 | 101.32 | 100.99 | 101.02 | 99.82 | 99.93 | 100.60 |
| | CIPW Norms | | | | | | | |
| Qz | 12.78 | 15.91 | 0.00 | 0.00 | 0.00 | 1.43 | 0.09 | 0.00 |
| Or | 3.75 | 0.56 | 0.43 | 0.68 | 3.88 | 0.97 | 2.29 | 3.37 |
| Ab | 14.69 | 2.48 | 3.32 | 12.13 | 23.56 | 20.18 | 26.58 | 19.20 |
| An | 9.20 | 3.24 | 27.88 | 28.21 | 27.32 | 32.09 | 31.81 | 29.56 |
| Ne | 0.00 | 0.00 | 0.00 | 0.00 | 0.00 | 0.00 | 0.00 | 0.00 |
| Di | 0.00 | 0.00 | 3.16 | 8.34 | 21.18 | 30.47 | 12.92 | 24.61 |
| Hy | 31.92 | 50.66 | 37.84 | 6.53 | 13.58 | 9.11 | 21.74 | 16.61 |
| Ol | 0.00 | 0.00 | 19.17 | 38.37 | 5.63 | 0.00 | 0.00 | 1.82 |
| Mt | 1.39 | 0.67 | 0.75 | 3.59 | 3.06 | 4.06 | 2.77 | 2.87 |
| Il | 2.14 | 1.63 | 1.25 | 1.59 | 1.55 | 1.42 | 1.56 | 1.70 |
| Ap | 0.21 | 0.38 | 0.22 | 0.28 | 0.21 | 0.21 | 0.17 | 0.21 |
| Cc | 16.55 | 12.35 | 5.98 | 0.29 | 0.05 | 0.05 | 0.05 | 0.05 |
| | Niggli Values | | | | | | | |
| si | 114.8 | 107.5 | 80.9 | 75.9 | 112.2 | 111.8 | 120.1 | 110.7 |
| al | 19.4 | 17.0 | 11.9 | 13.4 | 19.7 | 20.4 | 23.4 | 19.4 |
| fm | 48.7 | 65.2 | 68.3 | 68.6 | 47.4 | 40.6 | 44.8 | 46.2 |
| c | 27.1 | 17.1 | 19.1 | 15.6 | 26.3 | 34.0 | 24.6 | 29.1 |
| alk | 4.9 | 0.7 | 0.8 | 2.5 | 6.6 | 5.1 | 7.3 | 5.4 |
| mg | 0.46 | 0.65 | 0.71 | 0.66 | 0.60 | 0.58 | 0.59 | 0.56 |
| ti | 2.8 | 2.0 | 1.3 | 1.5 | 1.9 | 1.7 | 2.0 | 2.0 |

Appendix 1 (continued)

| Sample | 56 | 57 | 58 | 59 | 60 | 61 | 62 |
|---|---|---|---|---|---|---|---|
| | Quartz-Mica Schist | | | | | | |
| | Chemical Analyses (Weight Percent) | | | | | | |
| $SiO_2$ | 76.2 | 74.9 | 64.6 | 70.3 | 64.3 | 72.1 | 71.9 |
| $TiO_2$ | 0.92 | 0.5 | 0.92 | 0.52 | 0.6 | 0.42 | 0.5 |
| $Al_2O_3$ | 11.8 | 13.3 | 15.5 | 13.5 | 10.9 | 14.0 | 12.7 |
| $Fe_2O_3$ | 0.6 | 0.88 | 1.3 | 1.4 | 0.93 | 0.68 | 1.2 |
| FeO | 2.6 | 0.56 | 6.2 | 2.4 | 2.6 | 0.84 | 1.1 |
| MnO | 0.00 | 0.07 | 0.06 | 0.02 | 0.04 | 0.00 | 0.01 |
| MgO | 2.1 | 0.28 | 2.6 | 2.5 | 3.6 | 0.67 | 1.1 |
| CaO | 0.63 | 0.00 | 0.4 | 0.23 | 6.5 | 0.51 | 0.24 |
| $Na_2O$ | 3.0 | 1.7 | 1.3 | 1.2 | 0.04 | 1.1 | 1.0 |
| $K_2O$ | 0.24 | 6.90 | 2.10 | 5.90 | 2.50 | 7.00 | 7.60 |
| $P_2O_5$ | 0.12 | 0.08 | 0.15 | 0.15 | 0.18 | 0.09 | 0.1 |
| $H_2O^+$ | 2.0 | 0.64 | 3.4 | 1.6 | 2.4 | 0.97 | 1.1 |
| $H_2O^-$ | 0.06 | 0.10 | 0.07 | 0.11 | 0.08 | 0.09 | 0.07 |
| Total | 100.27 | 99.91 | 98.60 | 99.83 | 94.67 | 98.47 | 98.62 |
| | CIPW Norms | | | | | | |
| Qz | 50.68 | 36.68 | 40.88 | 34.58 | 37.64 | 35.93 | 34.11 |
| Qr | 1.48 | 42.03 | 13.47 | 36.31 | 16.57 | 43.43 | 47.21 |
| Ab | 28.11 | 15.47 | 12.68 | 11.23 | 0.40 | 10.37 | 9.44 |
| An | 2.44 | -0.54 | 1.09 | 0.17 | 24.88 | 2.04 | 0.56 |
| Ne | 0.00 | 0.00 | 0.00 | 0.00 | 0.00 | 0.00 | 0.00 |
| Di | 0.00 | 0.00 | 0.00 | 0.00 | 7.98 | 0.00 | 0.00 |
| Hy | 8.48 | 0.80 | 15.96 | 9.33 | 10.08 | 2.20 | 3.39 |
| Ol | 0.00 | 0.00 | 0.00 | 0.00 | 0.00 | 0.00 | 0.00 |
| Mt | 0.65 | 0.43 | 1.48 | 1.52 | 1.09 | 0.75 | 1.32 |
| Il | 1.34 | 0.72 | 1.39 | 0.75 | 0.94 | 0.61 | 0.73 |
| Ap | 0.26 | 0.17 | 0.34 | 0.33 | 0.42 | 0.20 | 0.22 |
| Cc | 0.00 | 0.00 | 0.00 | 0.00 | 0.00 | 0.00 | 0.00 |

# APPENDIX 2

Chemical analyses, CIPW norms, and Niggli values of selected rocks from the Seldovia-Kodiak Islands schist terrane.

| Sample | Blueschist 1 | 1a | 2 | 2a | 3 | 3a | 4 | 4a |
|---|---|---|---|---|---|---|---|---|
| | Chemical Analyses (Weight Percent) | | | | | | | |
| $SiO_2$ | 48.2 | 51.9 | 49.4 | 50.5 | 56.4 | 58.2 | 45.2 | 49.0 |
| $TiO_2$ | 1.7 | 1.8 | 2.3 | 2.4 | 1.7 | 1.8 | 2.2 | 2.4 |
| $Al_2O_3$ | 14.8 | 15.9 | 14.7 | 15.0 | 12.0 | 12.4 | 14.9 | 16.2 |
| $Fe_2O_3$ | 4.2 | 4.5 | 6.9 | 7.1 | 3.2 | 3.3 | 5.4 | 5.9 |
| FeO | 4.3 | 4.6 | 3.9 | 4.0 | 5.2 | 5.4 | 5.2 | 5.6 |
| MnO | 0.11 | 0.10 | 0.12 | 0.10 | 0.07 | 0.10 | 0.12 | 0.10 |
| MgO | 5.6 | 6.0 | 6.4 | 6.5 | 6.0 | 6.2 | 5.4 | 5.9 |
| CaO | 8.3 | 4.3 | 7.8 | 6.6 | 4.8 | 3.1 | 8.4 | 4.1 |
| $Na_2O$ | 5.1 | 5.5 | 3.6 | 3.7 | 5.6 | 5.8 | 3.6 | 3.9 |
| $K_2O$ | 1.00 | 1.10 | 0.10 | 0.10 | 0.29 | 0.30 | 2.50 | 2.70 |
| $P_2O_5$ | 0.26 | 0.3 | 0.39 | 0.4 | 0.31 | 0.3 | 0.28 | 0.3 |
| $H_2O^+$ | 2.4 | 2.6 | 2.9 | 3.0 | 2.0 | 2.1 | 2.9 | 3.1 |
| $H_2O^-$ | 0.22 | 0.20 | 0.18 | 0.20 | 0.00 | 0.00 | 0.14 | 0.20 |
| $CO_2$ | 3.10 | 0.00 | 0.96 | 0.00 | 1.30 | 0.00 | 3.40 | 0.00 |
| Total | 99.29 | 98.80 | 99.65 | 99.60 | 98.87 | 99.00 | 99.64 | 99.40 |
| | CIPW Norms | | | | | | | |
| Qz | 0.00 | 0.00 | 6.69 | 6.99 | 7.04 | 7.26 | 0.00 | 0.00 |
| Or | 5.98 | 6.67 | 0.62 | 0.62 | 1.75 | 1.81 | 15.18 | 16.63 |
| Ab | 46.37 | 50.69 | 33.67 | 34.77 | 51.22 | 53.20 | 33.23 | 36.51 |
| An | 14.72 | 15.86 | 24.64 | 25.15 | 6.88 | 7.06 | 17.6 | 19.17 |
| Ne | 0.00 | 0.00 | 0.00 | 0.00 | 0.00 | 0.00 | 0.00 | 0.00 |
| Di | 4.33 | 3.22 | 5.35 | 5.11 | 5.56 | 5.32 | 1.02 | 0.00 |
| Hy | 7.91 | 10.80 | 15.73 | 16.23 | 17.73 | 18.62 | 9.50 | 12.65 |
| Ol | 5.35 | 4.70 | 0.00 | 0.00 | 0.00 | 0.00 | 5.08 | 4.33 |
| Mt | 4.45 | 4.83 | 4.73 | 4.73 | 3.41 | 3.52 | 5.80 | 6.43 |
| Il | 2.40 | 2.57 | 3.34 | 3.50 | 2.41 | 2.56 | 3.15 | 3.49 |
| Ap | 0.55 | 0.64 | 0.85 | 0.88 | 0.66 | 0.64 | 0.60 | 0.65 |
| Cc | 7.95 | 0.00 | 2.53 | 0.00 | 3.35 | 0.00 | 8.84 | 0.00 |
| | Niggli Values | | | | | | | |
| si | 125.5 | 143.1 | 127.7 | 132.8 | 167.9 | 177.6 | 114.6 | 130.9 |
| al | 22.7 | 25.8 | 22.4 | 23.2 | 21.0 | 22.3 | 22.2 | 25.4 |
| fm | 39.7 | 44.9 | 46.9 | 48.6 | 47.0 | 49.9 | 42.1 | 48.1 |
| c | 23.2 | 12.7 | 21.6 | 18.6 | 15.3 | 10.1 | 22.8 | 11.7 |
| alk | 14.5 | 16.6 | 9.2 | 9.6 | 16.7 | 17.7 | 12.9 | 14.7 |
| mg | 0.55 | 0.55 | 0.53 | 0.53 | 0.57 | 0.57 | 0.49 | 0.49 |
| ti | 3.3 | 3.7 | 4.5 | 4.7 | 3.8 | 4.1 | 4.2 | 4.8 |

Appendix 2 (continued)

| Sample | 5 | 5a | 6* | 6a | 7* | 7a | 8* | 8a |
|---|---|---|---|---|---|---|---|---|
| | Blueschist | | | | | | | |
| | Chemical Analyses (Weight Percent) | | | | | | | |
| $SiO_2$ | 57.6 | 57.6 | 44.5 | 47.8 | 46.7 | 50.0 | 50.0 | 50.8 |
| $TiO_2$ | 2.6 | 2.6 | 2.3 | 2.5 | 1.8 | 1.9 | 2.3 | 2.3 |
| $Al_2O_3$ | 12.5 | 12.5 | 15.1 | 16.2 | 15.7 | 16.8 | 15.9 | 16.2 |
| $Fe_2O_3$ | 4.5 | 4.5 | 5.0 | 5.4 | 3.6 | 3.9 | 6.8 | 6.9 |
| FeO | 5.2 | 5.2 | 5.3 | 5.7 | 4.4 | 4.7 | 3.6 | 3.7 |
| MnO | 0.07 | 0.07 | 0.08 | 0.10 | 0.08 | 0.10 | 0.09 | 0.10 |
| MgO | 5.0 | 5.0 | 5.0 | 5.4 | 5.0 | 5.4 | 5.9 | 6.0 |
| CaO | 3.0 | 3.0 | 9.0 | 5.2 | 8.1 | 4.7 | 7.7 | 6.8 |
| $Na_2O$ | 5.7 | 5.7 | 3.5 | 3.8 | 5.0 | 5.4 | 3.3 | 3.4 |
| $K_2O$ | 0.59 | 0.59 | 2.40 | 2.60 | 0.10 | 0.10 | 0.04 | 0.00 |
| $P_2O_5$ | 0.37 | 0.37 | 0.17 | 0.2 | 0.17 | 0.2 | 0.34 | 0.3 |
| $H_2O^+$ | 2.2 | 2.2 | 2.1 | 2.3 | 1.3 | 1.4 | 3.0 | 3.0 |
| $H_2O^-$ | 0.23 | 0.23 | 0.13 | 0.10 | 0.12 | 0.10 | 0.10 | 0.10 |
| $CO_2$ | 0.02 | 0.00 | 3.0 | 0.00 | 2.70 | 0.00 | 0.70 | 0.00 |
| Total | 99.58 | 101.63 | 97.58 | 97.30 | 94.77 | 94.70 | 99.77 | 99.60 |
| | CIPW Norms | | | | | | | |
| Qz | 9.39 | 9.36 | 0.00 | 0.00 | 0.00 | 0.00 | 8.60 | 8.70 |
| Or | 3.59 | 3.59 | 14.72 | 16.23 | 0.62 | 0.63 | 0.25 | 0.00 |
| Ab | 52.68 | 52.69 | 32.62 | 36.06 | 47.15 | 51.31 | 30.94 | 31.98 |
| An | 6.98 | 6.98 | 19.11 | 20.58 | 21.11 | 22.55 | 29.71 | 30.32 |
| Ne | 0.00 | 0.00 | 0.00 | 0.00 | 0.00 | 0.00 | 0.00 | 0.00 |
| Di | 4.58 | 4.68 | 3.02 | 4.25 | 1.60 | 0.60 | 2.59 | 2.37 |
| Hy | 13.37 | 13.32 | 6.37 | 4.76 | 14.36 | 16.44 | 15.71 | 16.17 |
| Ol | 0.00 | 0.00 | 6.12 | 8.03 | 1.02 | 0.93 | 0.00 | 0.00 |
| Mt | 4.84 | 4.84 | 5.43 | 5.97 | 3.95 | 4.31 | 3.94 | 4.22 |
| Il | 3.73 | 3.73 | 3.33 | 3.68 | 2.63 | 2.80 | 3.35 | 3.36 |
| Ap | 0.80 | 0.80 | 0.37 | 0.44 | 0.37 | 0.44 | 0.74 | 0.66 |
| Cc | 0.05 | 0.00 | 8.93 | 0.00 | 7.17 | 0.00 | 1.85 | 0.00 |
| | Niggli Values | | | | | | | |
| si | 181.6 | 181.6 | 113.6 | 127.7 | 127.1 | 141.9 | 132.1 | 135.7 |
| al | 23.2 | 23.2 | 22.7 | 25.5 | 25.1 | 28.1 | 24.7 | 25.5 |
| fm | 48.1 | 48.1 | 40.2 | 45.4 | 37.9 | 42.7 | 45.0 | 46.3 |
| c | 10.1 | 10.1 | 24.6 | 14.9 | 23.6 | 14.3 | 21.8 | 19.5 |
| alk | 18.6 | 18.5 | 12.6 | 14.3 | 13.3 | 15.0 | 8.5 | 8.8 |
| mg | 0.49 | 0.49 | 0.48 | 0.48 | 0.54 | 0.54 | 0.52 | 0.52 |
| ti | 6.2 | 6.2 | 4.4 | 5.0 | 3.7 | 4.0 | 4.6 | 4.6 |

Appendix 2 (continued)

| Sample | 9* | 9a | 10* | 10a | 11 | 11a | 12 | 12a |
|---|---|---|---|---|---|---|---|---|
| | Blueschist | | | | | | | |
| | Chemical Analyses (Weight Percent) | | | | | | | |
| $SiO_2$ | 56.7 | 58.2 | 56.7 | 56.7 | 40.7 | 50.9 | 46.63 | 49.0 |
| $TiO_2$ | 1.7 | 1.7 | 2.5 | 2.5 | 1.6 | 2.0 | 0.93 | 1.0 |
| $Al_2O_3$ | 12.8 | 13.1 | 13.8 | 13.8 | 12.46 | 15.6 | 19.47 | 20.4 |
| $Fe_2O_3$ | 3.2 | 3.3 | 4.7 | 4.7 | 4.64 | 5.8 | 3.86 | 4.1 |
| FeO | 5.1 | 5.2 | 4.8 | 4.8 | 4.34 | 5.4 | 6.58 | 6.9 |
| MnO | 0.03 | 0.00 | 0.02 | 0.02 | 0.16 | 0.20 | 0.09 | 0.10 |
| MgO | 5.6 | 5.7 | 4.6 | 4.6 | 5.19 | 6.5 | 6.22 | 6.5 |
| CaO | 5.1 | 3.7 | 3.0 | 3.0 | 15.64 | 4.3 | 5.88 | 3.2 |
| $Na_2O$ | 5.5 | 5.6 | 5.7 | 5.7 | 4.0 | 5.0 | 5.07 | 5.3 |
| $K_2O$ | 0.43 | 0.40 | 0.60 | 0.60 | 0.65 | 0.80 | 0.90 | 0.90 |
| $P_2O_5$ | 0.17 | 0.2 | 0.34 | 0.34 | 0.25 | 0.3 | 0.25 | 0.3 |
| $H_2O^+$ | 1.7 | 1.7 | 1.9 | 1.9 | 2.07 | 2.6 | 2.46 | 2.6 |
| $H_2O^-$ | 0.09 | 0.10 | 0.14 | 0.14 | 0.10 | 0.10 | 0.15 | 0.20 |
| $CO_2$ | 1.10 | 0.00 | 0.20 | 0.00 | 8.87 | 0.00 | 2.11 | 0.00 |
| Total | 99.22 | 98.90 | 99.00 | 98.80 | 100.67 | 99.50 | 100.60 | 100.50 |
| | CIPW Norms | | | | | | | |
| Qz | 6.81 | 7.62 | 8.89 | 8.65 | 0.00 | 0.05 | 0.00 | 0.00 |
| Qr | 2.58 | 2.41 | 3.65 | 3.66 | 3.80 | 4.85 | 5.30 | 5.34 |
| Ab | 50.10 | 51.34 | 52.70 | 52.83 | 35.50 | 46.12 | 45.34 | 47.78 |
| An | 9.10 | 9.63 | 10.60 | 10.63 | 13.96 | 18.25 | 14.14 | 13.97 |
| Ne | 0.00 | 0.00 | 0.00 | 0.00 | 0.00 | 0.00 | 0.00 | 0.00 |
| Di | 6.71 | 6.23 | 0.91 | 1.95 | 4.55 | 1.32 | 0.00 | 0.00 |
| Hy | 15.73 | 16.41 | 13.35 | 12.87 | 9.90 | 19.67 | 4.48 | 7.79 |
| Ol | 0.00 | 0.00 | 0.00 | 0.00 | 2.61 | 0.00 | 14.21 | 12.64 |
| Mt | 3.39 | 3.52 | 5.06 | 5.07 | 4.79 | 6.23 | 4.02 | 4.30 |
| Il | 2.40 | 2.42 | 3.59 | 3.60 | 2.20 | 2.86 | 1.29 | 1.40 |
| Ap | 0.36 | 0.43 | 0.73 | 0.73 | 0.52 | 0.64 | 0.52 | 0.63 |
| Cc | 2.82 | 0.00 | 0.52 | 0.00 | 22.17 | 0.00 | 5.31 | 0.00 |
| | Niggli Values | | | | | | | |
| si | 168.4 | 177.9 | 179.0 | 179.0 | 93.8 | 134.3 | 113.7 | 123.1 |
| al | 22.4 | 23.6 | 25.6 | 25.6 | 16.9 | 24.2 | 27.9 | 30.2 |
| fm | 44.8 | 47.0 | 45.6 | 45.6 | 34.6 | 49.5 | 43.4 | 46.9 |
| c | 16.2 | 12.1 | 10.2 | 10.2 | 38.6 | 12.2 | 15.4 | 8.6 |
| alk | 16.6 | 17.4 | 18.6 | 18.6 | 9.9 | 14.1 | 13.4 | 14.3 |
| mg | 0.56 | 0.56 | 0.48 | 0.48 | 0.52 | 0.52 | 0.53 | 0.52 |
| ti | 3.8 | 3.9 | 5.9 | 5.9 | 2.8 | 4.0 | 1.7 | 1.9 |

Appendix 2 (continued)

| Sample | Blueschist 13 | 13a | 14 | 14a | 15 | 15a |
|---|---|---|---|---|---|---|
| | Chemical Analyses (Weight Percent) | | | | | |
| $SiO_2$ | 53.2 | 53.2 | 47.5 | 47.5 | 47.1 | 48.0 |
| $TiO_2$ | 0.11 | 0.11 | 2.9 | 2.9 | 2.9 | 3.0 |
| $Al_2O_3$ | 6.2 | 6.2 | 12.8 | 12.8 | 12.6 | 12.8 |
| $Fe_2O_3$ | 11.4 | 11.4 | 8.1 | 8.1 | 3.6 | 3.7 |
| FeO | 13.2 | 13.2 | 4.9 | 4.9 | 9.6 | 9.8 |
| MnO | 0.19 | 0.19 | 0.16 | 0.16 | 0.17 | 0.20 |
| MgO | 6.0 | 6.0 | 4.1 | 4.1 | 5.1 | 5.2 |
| CaO | 3.4 | 3.3 | 7.0 | 6.9 | 8.0 | 7.0 |
| $Na_2O$ | 4.6 | 4.6 | 5.4 | 5.4 | 3.5 | 3.6 |
| $K_2O$ | 0.38 | 0.38 | 1.20 | 1.20 | 0.77 | 0.80 |
| $P_2O_5$ | 0.01 | 0.01 | 0.35 | 0.35 | 0.35 | 0.4 |
| $H_2O^+$ | 1.5 | 1.5 | 2.0 | 2.0 | 2.7 | 2.8 |
| $H_2O^-$ | 0.20 | 0.20 | 0.20 | 0.20 | 0.20 | 0.20 |
| $CO_2$ | 0.10 | 0.00 | 0.10 | 0.00 | 0.80 | 0.00 |
| Total | 100.49 | 100.29 | 96.71 | 96.51 | 97.39 | 97.50 |
| | CIPW Norms | | | | | |
| Qz | 6.61 | 6.60 | 0.00 | 0.00 | 1.03 | 1.05 |
| Qr | 2.36 | 2.37 | 7.57 | 7.58 | 4.89 | 5.10 |
| Ab | 33.28 | 33.60 | 45.25 | 44.80 | 33.81 | 34.87 |
| An | 0.00 | 0.00 | 7.63 | 7.64 | 17.64 | 17.70 |
| Ne | 0.00 | 0.00 | 3.91 | 4.21 | 0.00 | 0.00 |
| Di | 13.63 | 13.78 | 21.07 | 21.64 | 13.73 | 13.56 |
| Hy | 26.00 | 26.01 | 0.00 | 0.00 | 17.53 | 18.14 |
| Ol | 0.00 | 0.00 | 1.16 | 0.96 | 0.00 | 0.00 |
| Mt | 9.49 | 9.51 | 6.09 | 6.10 | 4.05 | 4.17 |
| Il | 0.16 | 0.16 | 4.31 | 4.32 | 4.35 | 4.51 |
| Ap | 0.02 | 0.02 | 0.78 | 0.78 | 0.79 | 0.90 |
| Cc | 0.27 | 0.00 | 0.27 | 0.00 | 2.18 | 0.00 |
| | Niggli Values | | | | | |
| si | 130.7 | 131.1 | 126.8 | 126.8 | 122.8 | 126.5 |
| al | 9.0 | 9.0 | 20.1 | 20.1 | 19.3 | 19.9 |
| fm | 70.6 | 70.7 | 43.9 | 43.9 | 48.2 | 49.9 |
| c | 9.0 | 8.7 | 20.0 | 20.0 | 22.4 | 19.8 |
| alk | 11.5 | 11.6 | 16.0 | 16.0 | 10.1 | 10.5 |
| mg | 0.31 | 0.31 | 0.37 | 0.37 | 0.41 | 0.41 |
| ti | 0.2 | 0.2 | 5.8 | 5.8 | 5.7 | 5.9 |

Appendix 2 (continued)

| Sample | Greenschist | | | | | | | |
|---|---|---|---|---|---|---|---|---|
| | 16* | 16a | 17* | 17a | 18* | 18a | 19* | 19a |
| | Chemical Analyses (Weight Percent) | | | | | | | |
| $SiO_2$ | 53.4 | 53.4 | 44.7 | 49.2 | 44.7 | 44.7 | 48.5 | 49.3 |
| $TiO_2$ | 2.3 | 2.3 | 3.4 | 4.7 | 3.0 | 3.0 | 3.0 | 3.0 |
| $Al_2O_3$ | 17.0 | 17.0 | 15.1 | 16.6 | 17.2 | 17.2 | 17.8 | 18.1 |
| $Fe_2O_3$ | 8.5 | 8.5 | 1.7 | 1.9 | 5.1 | 5.1 | 4.9 | 5.0 |
| FeO | 2.0 | 2.0 | 9.3 | 10.2 | 5.4 | 5.4 | 6.0 | 6.1 |
| MnO | 0.11 | 0.11 | 0.13 | 0.10 | 0.04 | 0.04 | 0.13 | 0.10 |
| MgO | 4.9 | 4.9 | 6.7 | 7.4 | 8.8 | 8.8 | 4.9 | 5.0 |
| CaO | 4.9 | 4.9 | 7.3 | 2.2 | 5.7 | 5.7 | 6.3 | 5.4 |
| $Na_2O$ | 2.6 | 2.6 | 0.61 | 0.7 | 3.2 | 3.2 | 3.7 | 3.8 |
| $K_2O$ | 0.96 | 0.96 | 2.86 | 3.10 | 2.30 | 2.30 | 0.76 | 0.80 |
| $P_2O_5$ | 0.26 | 0.26 | 0.52 | 0.6 | 0.52 | 0.52 | 0.34 | 0.3 |
| $H_2O^+$ | 3.1 | 3.1 | 3.8 | 4.2 | 2.8 | 2.8 | 3.22 | 3.3 |
| $H_2O^-$ | 0.11 | 0.11 | 0.29 | 0.30 | 0.21 | 0.21 | 0.14 | 0.10 |
| $CO_2$ | 0.20 | 0.00 | 4.00 | 0.00 | 0.20 | 0.00 | 0.68 | 0.00 |
| Total | 100.34 | 100.14 | 100.41 | 100.20 | 99.17 | 98.97 | 100.37 | 100.30 |
| | CIPW Norms | | | | | | | |
| Qz | 17.61 | 17.13 | 11.95 | 13.98 | 0.00 | 0.00 | 4.86 | 4.73 |
| Qr | 5.97 | 5.98 | 17.75 | 19.62 | 14.01 | 14.05 | 4.66 | 4.92 |
| Ab | 24.56 | 24.62 | 5.75 | 6.73 | 29.63 | 29.21 | 34.50 | 35.52 |
| An | 22.46 | 23.85 | 7.91 | 7.49 | 24.36 | 25.73 | 25.69 | 25.85 |
| Ne | 0.00 | 0.00 | 0.00 | 0.00 | 0.00 | 0.30 | 0.00 | 0.00 |
| Di | 0.00 | 0.00 | 0.00 | 0.00 | 0.00 | 0.00 | 0.00 | 0.00 |
| Hy | 14.23 | 14.27 | 28.57 | 32.04 | 1.29 | 0.00 | 16.03 | 16.39 |
| Ol | 0.00 | 0.00 | 0.00 | 0.00 | 18.36 | 19.38 | 0.00 | 0.00 |
| Mt | 0.11 | 0.11 | 1.87 | 2.13 | 5.50 | 5.51 | 5.32 | 5.44 |
| Il | 3.37 | 3.38 | 4.98 | 5.52 | 4.31 | 4.32 | 4.34 | 4.35 |
| Ap | 0.57 | 0.57 | 1.14 | 1.34 | 1.12 | 1.12 | 0.74 | 0.65 |
| Cc | 0.53 | 0.00 | 10.63 | 0.00 | 0.52 | 0.00 | 1.79 | 0.00 |
| | Niggli Values | | | | | | | |
| si | 157.7 | 157.7 | 116.7 | 137.1 | 105.6 | 105.6 | 129.6 | 133.1 |
| al | 29.5 | 29.5 | 23.2 | 27.2 | 23.9 | 23.9 | 28.0 | 28.8 |
| fm | 45.7 | 45.7 | 50.1 | 58.8 | 50.9 | 50.9 | 43.1 | 44.3 |
| c | 15.5 | 15.5 | 20.4 | 6.6 | 14.4 | 14.4 | 18.0 | 15.6 |
| alk | 9.2 | 9.2 | 6.3 | 7.4 | 10.8 | 10.8 | 10.9 | 11.3 |
| mg | 0.48 | 0.48 | 0.52 | 0.53 | 0.61 | 0.61 | 0.46 | 0.46 |
| ti | 5.1 | 5.1 | 6.7 | 7.7 | 5.3 | 5.3 | 6.0 | 6.1 |

Appendix 2 (continued)

| Sample | 20* | 20a | 21* | 21a | 22* | 22a | 23 | 23a |
|---|---|---|---|---|---|---|---|---|
| | Greenschist | | | | | | | |
| | Chemical Analyses (Weight Percent) | | | | | | | |
| $SiO_2$ | 44.4 | 49.5 | 51.3 | 53.0 | 44.5 | 51.7 | 47.5 | 48.2 |
| $TiO_2$ | 1.7 | 1.9 | 2.2 | 2.3 | 1.7 | 2.0 | 2.9 | 2.9 |
| $Al_2O_3$ | 17.6 | 19.6 | 15.1 | 15.6 | 12.1 | 14.0 | 15.7 | 15.9 |
| $Fe_2O_3$ | 5.1 | 5.7 | 3.1 | 3.2 | 2.9 | 3.4 | 3.7 | 3.8 |
| FeO | 2.1 | 2.3 | 7.9 | 8.2 | 5.2 | 6.0 | 8.1 | 8.2 |
| MnO | 0.08 | 0.10 | 0.15 | 0.20 | 0.05 | 0.10 | 0.15 | 0.20 |
| MgO | 4.5 | 5.0 | 5.1 | 5.3 | 5.5 | 6.4 | 9.0 | 9.1 |
| CaO | 13.0 | 7.3 | 5.1 | 3.3 | 15.7 | 8.0 | 3.9 | 3.1 |
| $Na_2O$ | 3.2 | 3.6 | 3.4 | 3.5 | 3.5 | 4.1 | 1.4 | 1.4 |
| $K_2O$ | 0.81 | 0.90 | 0.36 | 0.40 | 0.12 | 0.10 | 2.80 | 2.80 |
| $P_2O_5$ | 0.13 | 0.1 | 0.26 | 0.3 | 0.17 | 0.2 | 0.25 | 0.3 |
| $H_2O^+$ | 2.0 | 2.2 | 3.9 | 4.0 | 1.3 | 1.5 | 4.4 | 4.5 |
| $H_2O^-$ | 0.06 | 0.10 | 0.10 | 0.10 | 0.05 | 0.10 | 0.20 | 0.20 |
| $CO_2$ | 4.50 | 0.00 | 1.40 | 0.00 | 6.00 | 0.00 | 0.60 | 0.00 |
| Total | 99.18 | 98.30 | 99.37 | 99.40 | 98.79 | 97.60 | 100.60 | 100.60 |
| | CIPW Norms | | | | | | | |
| Qz | 1.53 | 2.40 | 12.01 | 12.70 | 1.32 | 3.00 | 5.73 | 6.41 |
| Or | 4.86 | 5.53 | 2.25 | 2.51 | 0.72 | 0.61 | 17.38 | 17.44 |
| Ab | 29.21 | 33.62 | 32.29 | 33.42 | 31.74 | 38.32 | 13.20 | 13.25 |
| An | 31.79 | 36.06 | 15.61 | 15.33 | 17.12 | 20.30 | 14.63 | 14.15 |
| Ne | 0.00 | 0.00 | 0.00 | 0.00 | 0.00 | 0.00 | 0.00 | 0.00 |
| Di | 3.20 | 0.75 | 0.00 | 0.00 | 17.69 | 15.72 | 0.00 | 0.00 |
| Hy | 11.03 | 13.98 | 22.56 | 23.62 | 10.72 | 15.00 | 32.58 | 33.15 |
| Ol | 0.00 | 0.00 | 0.00 | 0.00 | 0.00 | 0.00 | 0.00 | 0.00 |
| Mt | 1.54 | 1.67 | 3.43 | 3.56 | 3.06 | 3.70 | 4.06 | 4.19 |
| Il | 2.41 | 2.75 | 3.24 | 3.41 | 2.39 | 2.90 | 4.24 | 4.26 |
| Ap | 0.28 | 0.22 | 0.58 | 0.67 | 0.36 | 0.44 | 0.55 | 0.66 |
| Cc | 11.57 | 0.00 | 3.75 | 0.00 | 15.32 | 0.00 | 1.59 | 0.00 |
| | Niggli Values | | | | | | | |
| si | 110.2 | 133.1 | 148.5 | 157.2 | 105.4 | 135.8 | 119.6 | 122.6 |
| al | 25.7 | 31.0 | 25.7 | 27.2 | 16.9 | 21.6 | 23.3 | 23.8 |
| fm | 30.8 | 37.1 | 48.3 | 51.5 | 35.1 | 45.3 | 58.3 | 59.8 |
| c | 34.6 | 21.0 | 15.8 | 10.5 | 39.9 | 22.5 | 10.5 | 8.5 |
| alk | 9.0 | 10.9 | 10.2 | 10.8 | 8.2 | 10.6 | 7.9 | 8.0 |
| mg | 0.55 | 0.54 | 0.46 | 0.46 | 0.56 | 0.56 | 0.58 | 0.58 |
| ti | 3.2 | 3.8 | 4.8 | 5.1 | 3.0 | 3.9 | 5.5 | 5.5 |

Appendix 2 (continued)

| | Greenschist | | | | | |
|---|---|---|---|---|---|---|
| Sample | 24 | 24a | 25 | 25a | 26 | 26a |
| | Chemical Analyses (Weight Percent) | | | | | |
| $SiO_2$ | 46.2 | 46.2 | 47.2 | 48.4 | 42.9 | 47.4 |
| $TiO_2$ | 1.7 | 1.7 | 2.8 | 2.9 | 1.4 | 1.5 |
| $Al_2O_3$ | 14.9 | 14.9 | 15.8 | 16.2 | 16.6 | 18.3 |
| $Fe_2O_3$ | 3.6 | 3.6 | 5.4 | 5.5 | 5.5 | 6.1 |
| FeO | 10.6 | 10.6 | 6.2 | 6.4 | 2.3 | 2.5 |
| MnO | 0.17 | 0.17 | 0.14 | 0.10 | 0.12 | 0.10 |
| MgO | 7.8 | 7.8 | 5.3 | 5.4 | 4.8 | 5.3 |
| CaO | 4.9 | 4.9 | 6.2 | 4.8 | 12.9 | 7.7 |
| $Na_2O$ | 3.9 | 3.9 | 3.8 | 3.9 | 3.2 | 3.5 |
| $K_2O$ | 0.92 | 0.92 | 0.65 | 0.70 | 0.71 | 0.80 |
| $P_2O_5$ | 0.1 | 0.1 | 0.49 | 0.5 | 0.24 | 0.3 |
| $H_2O^+$ | 3.4 | 3.4 | 3.9 | 4.0 | 2.7 | 3.0 |
| $H_2O^-$ | 0.20 | 0.20 | 0.17 | 0.20 | 0.13 | 0.10 |
| $CO_2$ | 0.10 | 0.00 | 1.10 | 0.00 | 1.40 | 0.00 |
| Total | 98.49 | 98.39 | 99.15 | 99.00 | 94.90 | 96.60 |
| | CIPW Norms | | | | | |
| Qz | 0.00 | 0.00 | 4.56 | 4.86 | 0.00 | 1.36 |
| Or | 5.72 | 5.73 | 4.07 | 4.41 | 4.53 | 5.05 |
| Ab | 36.85 | 36.90 | 36.13 | 37.32 | 24.86 | 33.57 |
| An | 21.51 | 21.54 | 21.82 | 21.90 | 31.17 | 34.04 |
| Ne | 0.00 | 0.00 | 0.00 | 0.00 | 3.72 | 0.00 |
| Di | 2.18 | 2.72 | 0.00 | 0.00 | 21.40 | 3.74 |
| Hy | 5.18 | 4.39 | 17.79 | 18.23 | 0.00 | 13.76 |
| Ol | 21.62 | 22.05 | 0.00 | 0.00 | 2.72 | 0.00 |
| Mt | 3.96 | 3.97 | 5.98 | 6.13 | 2.92 | 3.11 |
| Il | 2.49 | 2.50 | 4.13 | 4.30 | 2.11 | 2.23 |
| Ap | 0.22 | 0.22 | 1.09 | 1.11 | 0.54 | 0.67 |
| Cc | 0.27 | 0.00 | 2.95 | 0.00 | 3.83 | 0.00 |
| | Niggli Values | | | | | |
| si | 110.7 | 110.7 | 126.5 | 132.5 | 106.0 | 126.1 |
| al | 21.0 | 21.0 | 24.9 | 26.1 | 24.1 | 28.6 |
| fm | 56.0 | 56.0 | 46.3 | 48.3 | 33.0 | 39.1 |
| c | 12.6 | 12.6 | 17.8 | 14.1 | 34.2 | 21.9 |
| alk | 10.5 | 10.5 | 11.0 | 11.6 | 8.8 | 10.4 |
| mg | 0.50 | 0.50 | 0.46 | 0.46 | 0.54 | 0.54 |
| ti | 3.1 | 3.1 | 5.6 | 6.0 | 2.6 | 3.0 |

# APPENDIX 3

## Calculation of Niggli Numbers

(wt. % SiO ÷ 60) X 1000 + SI

(wt. % $Al_2O_3$ ÷ 102) X 1000 = AL

(wt. % $Fe_2O_3$ ÷ 160) X 1000 = FA

(wt. % FeO ÷ 72) X 1000 = FB  zfm = FA+FB+MN+MG

(wt. % MnO ÷ 71) X 1000 = MN  zalk = NA+KO

(wt. % MgO ÷ 40) X 1000 = MG  SUM = zfm+AL+CA+zalk

(wt, % CaO ÷ 56) X 1000 = CA

(wt. % $Na_2O$ ÷ 62) X 1000 = NA

(wt. % $K_2O$ ÷ 94) X 1000 = KO

(wt. % $TiO_2$ ÷ 80) X 1000 = TI

(wt. % $P_2O_5$ ÷ 142) X 1000 = PO

Niggli si = SI X 100/SUM

Niggli ti = TI X 100/SUM  Niggli c = CA X 100/SUM

Niggli p = PO X 100/SUM  Niggli alk = zalk X 100/SUM

Niggli al = AL X 100/SUM  Niggli k = KO/CA

Niggli fm = zfm X 100/SUM  Niggli mg = MG/zfm

For a full discussion of these calculations see Niggli, 1954.

BIBLIOGRAPHY

Anonymous, 1972, Ophiolites: Geotimes, v. 17, p. 24-25.

Armbrustmacher, T.J. and Simons, F.S., 1977, Geochemistry of amphibolites from the central Beartooth Mountains, Montana-Wyoming: Jour. Res. U. S. Geol. Survey, v. 5, p. 53-60.

Aumento, F., 1968, The mid-Atlantic ridge near 45° N II: basalts from the area of Confederation Peak: Canadian Jour. Earth Sci., v. 5, p. 1-21.

Aumento, F., 1969, Diorites from the mid-Atlantic ridge at 45° N: Science, v. 165, p. 112.

Aumento, F. and Loncarevic, B.D., 1969, The mid-Atlantic ridge near 45° N III: Bald Mountain: Canadian Jour. Earth Sci., v. 6, p. 11-23.

Bandy, M.C., 1937, Geology and petrology of Easter Island: Geol. Soc. Am. Bull., v. 48, p. 1589-1610.

Banno, S., 1958, Glaucophane schists and associated rocks in the Omi district, Japan: Japanese Jour. Geol. and Geog., v. 29, p. 29-44.

Barnes, F.F. and Payne, T.G., 1956, The Wishbone Hill district, Matanuska Valley coal field, Alaska: U. S. Geol. Survey Bull. 1016, 46 p.

Barth, T.F.W., 1956, Geology and petrology of the Priblof Islands, Alaska: U. S. Geol. Survey Bull. 1028-F, p. 110-160.

Birch, F. and LeComte, P., 1960, Temperature-pressure plane for albite composition: Am. Jour. Sci., v. 258, p. 209-217.

Bloxam, T.W., 1958, Pumpellyite from south Ayrshire: Mineralogy Mag., v. 31, p. 811-813.

Boettcher, A.L. and Wyllie, P.J., 1967, Revision of the calcite-aragonite transition, with the location of a triple point between calcite I, calcite II, and aragonite: Nature, v. 213, p. 792-793.

Boettcher, A.L. and Wyllie, P.J., 1968a, Calcite-aragonite transition measured in the system $CaO-CO_2-H_2O$: Jour. Geol., v. 76, p. 314-330.

Boettcher, A.L. and Wyllie, P.J., 1968b, Jadeite stability measured in the presence of silicate liquids in the system $NaAlSiO_4-SiO_2-H_2O$: Geochim. et Cosmochim. Acta, v. 32, p. 999-1012.

Borg, I.Y., 1967, Optical properties and cell parameters in the glaucophane-riebeckite series: Contr. Mineral. and Petrol., v. 15, p. 67-92.

Bottinga, Y. and Javoy, M., 1973, Comments on oxygen isotope geothermometry: Earth and Planetary Sci. Letters, v. 20, p. 250-265.

Brosge, W.P. and Pessel, G.H., 1977, Geologic map of the Survey Pass quadrangle, Alaska: U. S. Geol. Survey Open-file Rept.

Brothers, R.N., 1954, Glaucophane schists from the north Berkeley Hills, California: Am. Jour. Sci., v. 252, p. 614-626.

Brotzu, P., Morbidelli, L., Piccirillo, E.M., and Travusa, A., 1974, Petrological features of Boseti Mountains, a complex volcanic system in axial portion of the Ethiopian rift: Bull. Volcanologique, v. 38, p. 206-233.

Burk, C.A., 1965, Geology of the Alaska Peninsula island arc and continental margin: Geol. Soc. Am. Mem. 99, 250 p.

Calderwood, K.W. and Fackler, W.C., 1972, Proposed stratigraphic nomenclature for Kenai Group, Cook Inlet Basin, Alaska: Am. Assoc. Petroleum Geologists Bull., v. 56, p. 739-754.

Cann, J.R., 1969, Spilites from the Carlsberg Ridge, Indian Ocean: Jour. of Petrology, v. 10, p. 1-19.

Cann, J.R. and Vine, F.J., 1966, An area on the crest of the Carlsberg Ridge - petrology and magnetic survey: Roy. Soc. Lond. Phil. Trans., ser. A, v. 259, p. 198-217.

Capps, S.R., 1937, Kodiak and adjacent islands, Alaska: U. S. Geol. Survey Bull. 880-C, p. 111-160.

Carden, J.R., Connelly, Wm., Forbes, R.B., and Turner, D.L., 1977a, Blueschists of the Kodiak Islands, Alaska: an extension of the Seldovia schist terrane: Geol. Soc. Am. Abs. with programs, v. 9, p. 397.

Carden, J.R., Connelly, Wm., Forbes, R.B., and Turner, D.L., 1977b, Blueschists of the Kodiak Islands, Alaska: an extension of the Seldovia schist terrane: Geology, v. 5, p. 529-533.

Carden, J.R. and Decker, J.E., 1977, Tectonic significance of the Knik River schist terrane, south-central Alaska: Alaska Div. Geol. and Geophys. Surveys Geol. Rept., 55, p. 7-9.

Carden, J.R. and Forbes, R.B., 1976, Discovery of blueschists on Kodiak Island: Alaska Div. Geol. and Geophys. Surveys Geol. Rept. 51, p. 19-22.

Carmichael, I.S.E., 1964, The petrology of Thingmuli: A Tertiary volcano in eastern Iceland: Jour. of Petrology, v. 5, p. 435-460.

Carmichael, I.S.E., Turner, F.J., and Verhoogen, J., 1974, Igneous petrology, McGraw-Hill, New York, 739 p.

Chayes, F., 1964, Variance-covariance relations in some published Harker diagrams of volcanic suites: Jour. of Petrology, v. 5, p. 219.

Chayes, F. and Velde, D., 1965, On distinquishing basaltic lavas of circumoceanic and oceanic-island type by means of discriminant functions: Am. Jour. Sci., v. 263, p. 206.

Chinner, G.A., 1960, Pelitic gneisses with varying ferrous/ferric ratios from Glen Cove, Angus, Scotland: Jour. of Petrology, v. 1, p. 178-217.

Clardy, B.I., 1974, Origin of the lower and middle Tertiary Wishbone and Tsadaka Formations, Matanuska Valley, Alaska: Unpublished M.S. thesis, Univ. of Alaska, Fairbanks, Alaska, 74 p.

Clark, S.H.B., 1972a, Reconnaissance bedrock geologic map of the Chugach Mountains near Anchorage, Alaska: U. S. Geol. Survey Misc. Field Studies Map, MF-350.

Clark, S.H.B., 1972b, The Wolverine Complex, a newly discovered layered ultramafic body in the western Chugach Mountains, Alaska: U. S. Geol. Survey Open-file Rept., 72-70, 10 p.

Clark, S.H.B., 1973, The McHugh Complex of south-central Alaska: U. S. Geol. Survey Bull. 1372-D, p. D1-D11.

Clark, S.P., Jr., 1957, A note on calcite-aragonite equilibrium: Am. Mineralogist, v. 42, p. 564-566.

Coleman, R.G., 1971, Plate tectonic emplacement of upper mantle peridotites along continental edges: Jour. Geophys. Res., v. 76, p. 1212-1222.

Coleman, R.G. and Lanphere, M.A., 1971, Distribution and age of high-grade blueschists, associated eclogites, and amphibolites from Oregon and California: Geol. Soc. Am. Bull., v. 82, p. 2397-2412.

Coleman, R.G. and Lee, D.E., 1963, Glaucophane-bearing metamorphic rock types of the Cazadero area, California: Jour. of Petrology, v. 4, p. 260-301.

Coleman, R.G. and Papike, J.J., 1968, Alkali amphiboles from the blueschists of Cazadero, California: Jour. of Petrology, v. 9, p. 105-122.

Connelly, Wm., 1976, Mesozoic geology of the Kodiak Islands and its bearing on the tectonics of southern Alaska: Unpublished Ph.D. thesis, Univ. of California, Santa Cruz, California, 197 p.

Connelly, Wm., Hill, M., Hill B.B., and Moore, J.C., 1976, The Uyak Formation, Kodiak Islands, Alaska: an early Mesozoic subduction zone complex: Geol. Soc. Am. Abs. with Programs, v. 8, p. 364.

Connelly, Wm. and Moore, J.C., 1977, Geologic map of the northwest side of Kodiak Islands, Alaska: U. S. Geol. Survey Open-file Map, 77-382.

Coombs, D.S., Horodyski, R.J., and Naylor, R.S., 1970, Occurrence of prehnite-pumpellyite facies metamorphism in northern Maine: Am. Jour. Sci., v. 268, p. 142-156.

Cortesogno, L., Ernst, W.G., Galli, M., Messiga, B., Pedemonte, G.M., and Piccardo, G.B., 1977, Chemical petrology of eclogitic lenses in serpeninite, Gruppo de Voltri, Ligurian Alps: Jour. Geol., v. 85, p. 255-277.

Cowan, D.S. and Boss, R.F., 1977, Tectonic framework of the southwestern Kenai Peninsula, Alaska: Geol. Soc. Am. Bull., (in press).

Crawford, W.A. and Fyfe, W.S., 1964, Calcite-aragonite equilibrium at 100° C: Science, v. 144, p. 1569-1570.

Crawford, W.A. and Fyfe, W.S., 1965, Lawsonite equilibria: Am. Jour. Sci., v. 263, p. 262-270.

Crawford, W.A. and Hoersch, A.L., 1972, Calcite-aragonite equilibrium from 50° C to 150° C: Am. Mineralogist, v. 57, p. 995-998.

Crittenden, M.D., Jr., 1951, Geology of the San Jose-Mount Hamilton area, California: California Div. Mines Bull., v. 157, p. 1-74.

Dalrymple, G.B. and Lanphere, M.A., 1969, Potassium-argon dating: W. H. Freeman, San Franciso, California, 258 p.

Daly, R.A., 1933, Igneous rocks and the depths of the earth: McGraw-Hill, New York, 598 p.

Davis, B.L. and Adams, L.H., 1965, Kinetics of the calcite-aragonite transformation: Jour. Geophys. Res., v. 70, p. 433-441.

Detterman, R.L. and Hartsock, J.K., 1966, Geology of the Inukin-Tuxedni region, Alaska: U. S. Geol. Survey Prof. Paper 512, 78 p.

Detterman, R.L. and Jones. D.L., 1974, Mesozoic fossils from Augustine Island, Cook Inlet, Alaska: Am. Assoc. Petroleum Geologists Bull., v. 58, p. 868-876.

Devereux, I., 1968, Oxygen isotope ratios of minerals from regionally metamorphosed schists of Otago, New Zealand: New Zealand Jour. Sci., v. 11, p. 526-548.

Dewey, J.F. and Bird, J.M., 1970, Mountain belts and the new global tectonics: Jour. Geophys. Res., v. 75, p. 2625-2647.

Dixon, W.J., 1970, BMD biomedical computer programs, University of California publications in automatic computation no. 2: University of California Press, Los Angeles, California, 600p.

Dobretsov, N.L., 1975, Metamorphic belts of the northwestern circum-Pacific region, in Forbes, R.B., ed., Contributions to the geology of the Bering Sea Basin and adjacent regions: Geol. Soc. Am. Special Paper 151, p. 133-144.

El-Hinnawi, E.E., 1973, Remarks on "biaxial calcite": Contr. Mineral. and Petrol., v. 38, p. 339-341.

Engel, A.E.J. and Engel, C.G., 1964a, Composition of basalts from the mid-Atlantic Ridge: Science, v. 144, p. 1330-1333.

Engel, A.E.J. and Engel, C.G., 1964b, Igneous rocks of the East Pacific Rise: Science, v. 146, p. 477-485.

Engel, A.E.J., Engel, C.G., and Havens, R.G., 1965, Chemical characteristics of oceanic basalts and the upper mantle: Geol. Soc. Am. Bull., v. 76, p. 719-734.

Engel, C.G. and Engel, A.E.J., 1963, Basalts dredged from the northeastern Pacific Ocean: Science, v. 140, p. 1321-1324.

Engel, C.G. and Engel, A.E.J., 1966, Volcanic rocks dredged southwest of the Hawaiian Islands: U. S. Geol. Survey Prof. Paper 550-D, p. D104-D108.

Engels, J.C. and Ingamells, C.O., 1970, Effect of sample inhomogeneity in K-Ar dating: Geochim. et Cosmochim. Acta, v. 34, p. 1007-1017.

Epstein, S., 1959, The variations of the $O^{18}/O^{16}$ ratio in nature and some geologic applications, in Abelson, P.H., ed., Researches in geochemistry: John Wiley, New York, p. 217-240.

Ernst, W.G., 1961, Stability relations of glaucophane: Am. Jour. Sci., v. 259, p. 735-765.

Ernst, W.G., 1963a, Petrogenesis of glaucophane schists: Jour. of Petrology, v. 4, p. 1-30.

Ernst, W.G., 1963b, Polymorphism in alkali amphiboles: Am. Mineralogist, v. 48, p. 241-260.

Ernst, W.G., 1964, Petrochemical study of coexisting minerals from low-grade schists, eastern Shikoku, Japan: Geochim. et Cosmochim. Acta, v. 28, p. 1631-1668.

Ernst, W.G., 1971a, Metamorphic zonation on presumably subducted lithospheric plates from Japan, California, and the Alps: Contr. Mineral. and Petrol., v. 34, p. 43-59.

Ernst, W.G., 1971b, Do mineral parageneses reflect unusually high-pressure conditions of Franciscan metamorphism?: Am. Jour. Sci., v. 270, p. 81-108.

Ernst, W.G., 1972a, Ca-amphibole paragenesis in the Shirataki district, central Shikoku, Japan: Geol. Soc. Am. Mem., v. 135, p. 74-94.

Ernst, W.G., 1972b, Occurrence and mineralogic evolution of blueschist belts with time: Am. Jour. Sci., v. 272, p. 657-668.

Ernst, W.G., 1973a, Blueschist metamorphism and P-T regimes in active subduction zones: Tectonophysics, v. 17, p. 252-272.

Ernst, W.G., 1973b, Interpretive synthesis of metamorphism in the Alps: Geol. Soc. Am. Bull., v. 84, p. 2053-2078.

Ernst, W.G. and Seki, Y., 1967, Petrologic comparison of the Franciscan and Sanbagawa metamorphic terranes: Tectonophysics, v. 4, p. 463-478.

Escola, P., 1929, Om mineralfacies: Geol. Foren. Stockholm Forh. 51, p. 157-172.

Essene, E.J., Fyfe, W.S., and Turner, F.J., 1965, Petrogenesis of Franciscan glaucophane schists and associated metamorphic rocks, California: Beitrage zur Mineralogie and Petrographie, v. 11, p. 695-704.

Folk, R.L., 1974, The natural history of crystalline calcium carbonate effect of Mg content and salinity: Jour. of Sed. Petrology, v. 44, p. 40-53.

Forbes, R.B., Carden, J.R., and Connelly, Wm., 1976, The Kodiak-Chugach-Chichagof terranes--A newly defined Alaskan blueschist belt: Trans. Am. Geophys. Union, v. 57, p. 351, (abs.).

Forbes, R.B., Carden, J.R., Turner, D.L., and Connelly, Wm., 1977, Tectonic implications of Alaskan blueschist terranes: Alaska Geol. Soc. Symposium Proceedings.

Forbes, R.B., Dugdale, R.C., Katsura, T., Matsumato, H., and Haramura, H., 1969, Dredged basalt from Giacomini seamount: Nature, v. 221, p. 849-850.

Forbes, R.B., Hamilton, T., Tailleur, I.L., Miller, T.P., and Patton, W.W., 1971, Tectonic implications of blueschist facies metamorphic terranes in Alaska: Nature (Phys. Sci.), v., 234, p. 106-108.

Forbes, R.B. and Hoskin, C.M., 1969, Dredged trachyte and basalt from Kodiak seamount and the adjacent Aleutian trench, Alaska: Science, v. 166, p. 502-504.

Forbes, R.B. and Lanphere, M.A., 1973, Tectonic significance of mineral ages of blueschists near Seldovia, Alaska: Jour. Geophys. Res., v. 78, p. 1383-1386.

Forbes, R.B. and Turner, D.L., 1974, The comparative petrology and geochronology of Alaskan blueschists; Part 1: The Baird Mountains-Survey Pass and Seldovia terranes: A University of Alaska Geophysical Institute research proposal to the National Science Foundation.

Forbes, R.B., Turner, D.L., Gilbert, W.G., and Carden, J.R., 1974, Ruby Ridge traverse, southwestern Brooks Range: Alaska Div. Geol. and Geophys. Surveys Annual Rept. 1975, p. 34-36.

Fritts, C.E., 1969, Geology and geochemistry in the southeastern part of the Cosmos Hills, Shungnak D-2 quadrangle, Alaska: Alaska Div. of Mines and Geol., Geol. Rept. 37, 35 p.

Fritts, C.E., 1970a, Geology and geochemistry of the Cosmos Hills, Ambler River, and Shungnak quadrangles, Alaska: Alaska Div. of Mines and Geol., Geol. Rept. 39, 69 p.

Fritts, C.E., 1970b, Geology and geochemistry of the Angayucham Mountains, western Alaska: Alaska Div. Geol. and Geophys. Surveys Annual Rept. 1971, p. 8-9.

Fritts, C.E., 1972, Geology and geochemistry near Walker Lake, southern Survey Pass quadrangle, Arctic Alaska: Alaska Div. Geol. and Geophys. Surveys Annual Rept. 1972, p. 19-26.

Ghent, E.D., 1965, Glaucophane-schist facies metamorphism in the Black Butte area, northern Coast Ranges, California: Am. Jour. Sci., v. 263, p. 385-400.

Gilbert, W.G., Wiltse, M.A., Carden, J.R., Forbes, R.B., and Hackett, S.W., 1977, Geology of Ruby Ridge, southwestern Brooks Range, Alaska: Alaska Div. Geol. and Geophys. Surveys Geol. Rept., (in press).

Gresens, R.L., 1969, Blueschist alteration during serpentization: Contr. Mineral. and Petrol., v. 24, p. 93-113.

Grow, J.A. and Atwater, T., 1970, Mid-Tertiary tectonic transition in the Aleutian arc: Geol. Soc. Am. Bull., v. 81, p. 3715-3722.

Halferdahl, L.B., 1961, Chloritoid: Its composition, x-ray and optical properties, stability, and occurrence: Jour. of Petrology, v. 2, p. 49-135.

Hamilton, W., 1970, The Uralides and the motion of the Russian and Siberian platforms: Geol. Soc. Am. Bull., v. 81, p. 2553-2576.

Harker, A., 1932, Metamorphism: a study of the transformation of rock masses: Chapman and Hall, London, 362 p.

Hasabe, K., Fujii, N., and Uyeda, S., 1970, Thermal processes under island arcs: Tectonophysics, v. 10, p. 335-355.

Hawkins, J.W., 1967, Prehnite-pumpellyite facies metamorphism of a graywacke-shale series, Mt. Olympus, Washington: Am. Jour. Sci., v. 265, p. 798-818.

Hawley, C.C., 1976, Exploration and distribution of stratiform sulfide deposits in Alaska, in Recent and ancient sedimentary enviroments in Alaska: Alaska Geol. Soc. Symposium Proceedings, p. T1-T23.

Hayase, I. and Ishizaka, K., 1967, Rb-Sr dating on the rocks in Japan: Japanese Assoc. Mineral. Petrol. and Economic Geol. Jour., v. 58, p. 201-211.

Hertz, N. and Banerjee, S., 1973, Amphiboles of the Lafaiete, Minas, Gerais, and the Serra do Navio manganese deposits, Brazil: Economic Geol., v. 68, p. 1289-1296.

Hess, H.H., Bowin, C.O., Donnelly, J.V., Whetten, J.T., and Oxburgh, E.R., 1966, Caribbean geological investigations: Geol. Soc. Am. Mem. 98, p. 1-10.

Hess, H. and Poldervaart, A., 1967, Basalts, vol. 2: Wiley Interscience, New York, p. 483-862.

Hill, M.D. and Gill, J.B., 1976, Mesozoic greenstones of diverse ages from the Kodiak Islands, Alaska: Trans. Am. Geophys. Union, v. 57, p. 1021, (abs.).

Himmelberg, G.R. and Papike, J.J., 1969, Coexisting amphiboles from blueschist facies metamoprhic rocks: Jour. of Petrology, v. 10, p. 102-114.

Hopkins, D.M., Scholl, D.W., Addicott, W.O., Pierce, R.L., Smith, P.B., Wolfe, J.A., Grershanovich, D., Kotenev, B., Lochman, K.E., Lipps, J.H., and Obradivich, J., 1969, Cretaceous, Tertiary, and early Pleistocene rocks from the continental margin in the Bering Sea: Geol. Soc. Am. Bull., v. 80, p. 1471-1480.

Hormann, P.K. and Raith, M., 1973, Bildungsbedingungen von Al-Fe(III)-epidoten: Contr. Mineral. Petrol., v. 38, p. 307-320.

Horsfield, W.T., 1972, Glaucophane schists of Caledonian age from Spitsburgen: Geol. Mag., v. 109, p. 29-36.

Ingamells, C.O., 1970, Lithium metaborate flux in silicate analysis: Anal. Chim. Acta, v. 52, p. 323.

Isacks, B., Oliver, J., and Sykes, L.R., 1968, Seismology and the new global tectonics: Jour. Geophys. Res., v. 73, p. 5855-5899.

Iwasaki, M., 1963, Metamorphic rocks of the Kotu-Bizan area, eastern Shikoku: Tokyo Univ. Fac. Sci. Jour., v. 15, p. 1-90.

Jamieson, J.C., 1953, Phase equilibria in the system calcite-aragonite: Jour. Chem. Physics, v. 21, p. 1385-1390.

Johannes, W. and Puhan, D., 1971, The calcite-aragonite transition, reinvestigated: Contr. Mineral. and Petrol., v. 31, p. 28-38.

Jones, D.L. and Clark, S.H.B., 1975, Upper Cretaceous (Maestrichtian) fossils from the Kenai-Chugach Mountains, Kodiak and Shumagin Islands, southern Alaska: Jour. Res. U. S. Geol. Survey, v. 1, p. 125-136.

Jones, J.G., 1969, Pillow lavas as depth indications: Am. Jour. Sci., v. 267, p. 181-195.

Joplin, G.A., 1963, Chemical analysis of Australian rocks, Part 1: Igneous and metamorphic: Commonwealth of Australia Bull. No. 65, Dept. of National Development, Bureau of Mineral Resources, Geology, and Geophysics, p. 177-252.

Kaaden, G.V.D., 1966, The significance and distribution of glaucophane rocks in Turkey: Bull. of Mineral Resources and Exploration Institute of Turkey, No. 67, p. 36-67.

Kirschner, C.E. and Lyon, C.A., 1973, Stratigraphic and tectonic development of Cook Inlet petroleum province, in Pitcher, M.G., ed., Arctic geology: Am. Assoc. Petroleum Geologists Mem. 19, p. 396-407.

Kuno, H., 1950, Petrology of Hakone volcano and the adjacent areas, Japan: Geol. Soc. Am. Bull., v. 61, p. 957-1020.

Kuno, H., 1960, High-alumina basalt: Jour. of Petrology, v. 1, p. 121-145.

Kuno, H., 1966, Lateral variation of basaltic magma type across continental margins and island arcs: Bull. Volcanologique, v. 29, p. 195-222.

Laughlin, A.W., Manzer, G.K., and Carden, J.R., 1974, Feldspar megacrysts in alkali basalts: Geol. Soc. Am. Bull., v. 85, p. 413-416.

Le Pichon, X., 1968, Sea-floor spreading and continental drift: Jour. Geophys. Res., v. 73, p. 3661-3697.

Lidiak, E.G., 1965, Petrology of andesitic spilitic and keratophyric flow rock, north-central Puerto Rico: Geol. Soc. Am. Bull., v. 76, p. 57-88.

Liou, J.G., 1971, P-T stabilities of laumontite, wairakite, lawsonite, and related minerals in a system $CaAl_2Si_2O_8$-$SiO_2$-$H_2O$: Jour. of Petrology, v. 12, p. 379-411.

Liou, J.G., Ho C.O., and Yen, T.P., 1975, Petrology of some glaucophane schists and related rocks from Taiwan: Jour. of Petrology, v. 16, p. 80-109.

Loney, R.A., Brew, D.A., Muffler, L.J.P., and Pomeroy, J.S., 1975, Reconnaissance geology of Chichagof, Baranof, and Kruzof Islands, southeastern Alaska: U. S. Geol. Survey Prof. Paper 792, 105 p.

Luepke, G., 1975, Heavy-mineral trends in the Beaufort Sea: U. S. Geol. Survey Open-file Rept., 75-667, 29 p.

MacDonald, G.A., 1944, Petrography of the Samoan Islands; Geol. Soc. Am. Bull., v. 55, p. 1333-1362.

MacDonald, G.A., 1949, Hawaiian petrographic province: Geol. Soc. Am. Bull., v. 60, p. 1541-1596.

MacDonald, G.A., 1960, Dissimilarity of continental and oceanic rock types: Jour. of Petrology, v. 1, p. 172-177.

MacDonald, G.A. and Katsura, T., 1964, Chemical composition of Hawaiian lavas: Jour. of Petrology, v. 5, p. 82-133.

MacKevett, E.M., Jr. and Plafker, G., 1974, The Border Ranges fault in south-central Alaska: Jour. Res. U. S. Geol. Survey, v. 2, p. 323-329.

Maddren, A.G., 1917, The beach placers of the west coast of Kodiak Island, Alaska: U. S. Geol. Survey Bull. 692, p. 299-303.

Magoon, L.B., Adkison, W.L., Wolfe, J.A., Kelley, J.S., and Jones, D.L., 1976, Geologic framework of lower Cook Inlet, Alaska, with emphasis to onshore geology: Am. Assoc. Petroleum Geologists Abs. with Programs, Pacific section, p. 12-13.

Marshak, S.R. and Karig, D.E., 1977, Triple junctions as a cause for anomalously near-trench igneous activity between the trench and volcanic arc: Geology, v. 5, p. 233-236.

Martin, G.C., 1912, Mineral deposits of Kodiak and the neighboring islands: U. S. Geol. Survey Bull. 542, p. 125-131.

Martin, G.C., 1915, The western part of the Kenai Peninsula: U. S. Geol. Survey Bull. 587, p. 41-112.

Martin, G.C., Johnson, B.L., and Grant, U.S., 1915, Geology and mineral resources of Kenai Peninsula, Alaska: U. S. Geol. Survey Bull. 587, 242 p.

McBirney, A.R., ed., 1969, Proceedings of the andesite conference, in International upper mantle project science report no. 16: State of Oregon, Dept. Geol. and Mineral Industries Bull. 65, 193 p.

Melson, W.G. and van Andel, T.H., 1966, Metamorphism in the mid-Atlantic Ridge, 22° N. latitude: Marine Geol., v. 4, p. 165-186.

Mendenhall, W.C., 1901, Reconnaissances in the Cape Nome and Norton Bay regions, Alaska, in 1900: U. S. Geol. Survey Special Paper, 222 p.

Mertie, J.B., Jr., 1936, Mineral deposits of the Ruby-Kuskokwim region, Alaska: U.S. Geol. Survey Bull. 864-C, p. 115-245.

Metz, P.A., 1975, Geology of the central portion of the Valdez C-2 quadrangle, Alaska: Unpublished M.S. thesis, Univ. of Alaska, Fairbanks, Alaska, 65 p.

Metz, P.A., 1976, Occurrences of sodic amphibole-bearing rocks in the Valdez C-2 quadrangle: Alaska Div. of Geol. and Geophys. Surveys Geol. Rept. 51, p. 27-28.

Misch, P. 1966, Tectonic evolution of the northern Cascades of Washington state, in Gunning, H.C., ed., Tectonic history and mineral deposits of the western Cordillera: Canadian Institute of Mining and Metallurgy, v. 8, p. 108-148.

Miyashiro, A., 1957, The chemistry, optics, and genesis of the alkali-amphiboles: Tokyo Univ. Fac. Sci. Jour., v. 11, p. 57-83.

Miyashiro, A., 1961, Evolution of metamorphic belts: Jour. of Petrology, v. 2, p. 277-311.

Miyashiro, A., 1967, Aspects of metamorphism in the circum-Pacific region: Tectonophysics, v. 4, p. 519-521.

Miyashiro, A., 1972, Metamorphism amd related magmatism in plate tectonics: Am. Jour. Sci., v. 272, p. 629-656.

Miyashiro, A., 1973a, Metamorphism and metamorphic belts: John Wiley and Son, New York, 492 p.

Miyashiro, A., 1973b, Paired and unpaired metamorphic belts: Tectonophysics, v. 17, p. 241-254.

Miyashiro, A., 1974, Volcanic rock series in island arcs and active continental margins: Am. Jour. Sci., v. 274, p. 321-355.

Miyashiro, A. and Banno, S., 1958, Nature of glaucophanitic metamorphism: Am. Jour. Sci., v. 256, p. 97-110.

Miyashiro, A. and Seki, Y., 1958, Enlargement of the composition field of epidote and piemontite with rising temperature: Am. Jour. Sci., v. 256, p. 423-430.

Miyashiro, A., Shido, F., and Ewing, M., 1969, Diversity and origin of abyssal tholeiite from the mid-Atlantic ridge near 24° and 30° north latitude: Contr. Mineral. and Petrol., v. 23, p. 38-52.

Moffit, F.H., 1913, Geology of the Nome and Grand Central quadrangles, Alaska: U. S. Geol. Survey Bull. 533, 140 p.

Moore, G.W., 1967, Preliminary geologic map of Kodiak Island and vicinity, Alaska: U. S. Geol. Survey Open-file Rept. 271.

Moore, G.W., 1969, New formations on Kodiak and adjacent Islands, Alaska: U. S. Geol. Survey Bull. 1247-A, p. A28-A35.

Moore, J.C., 1972, Uplifted trench sediments: southwestern Alaska--Bering shelf edge: Science, v. 175, p. 1103-1105.

Moore, J.C., 1973a, Complex deformation of Cretaceous trench deposits, southwestern Alaska: Geol. Soc. Am. Bull., v. 84, p. 2005-2020.

Moore, J.C., 1973b, Cretaceous continental margin sedimentation, southwestern Alaska: Geol. Soc. Am. Bull., v. 84, p. 595-614.

Moore, J.C., 1974, The ancient continental margin of Alaska, in Burk, C.A. and Drake, C.L., eds., The geology of continental margins: Springer-Verlag, New York, p. 811-815.

Moore, J.C., 1975, Selective subduction: Geology, v. 3, p. 530-532.

Moore, J.C. and Connelly, Wm., 1976, Subduction, arc volcanism, and forearc sedimentation during the early Mesozoic, southwest Alaska: Geol. Soc. Am. Abs. with Programs (Cordilleran Sec.), v. 8, p. 397-398.

Moore, J.G., 1965, Petrology of deep-sea basalts near Hawaii: Am. Jour. Sci., v. 263, p. 40-52.

Morgan, W.J., 1968, Rises, trenches, great faults, and crustal rocks: Jour. Geophys. Res., v. 73, p. 1959-1965.

Morgan, W.J., 1971, Convection plumes in the lower mantle: Nature, v. 230, p. 42-43.

Muir, I.D. and Tilley, C.E., 1964, Basalts from the northern part of the rift zone of the mid-Atlantic ridge: Jour. of Petrology, v. 5, p. 409-434.

Nelson, A.E., 1969, Origin of some amphibolites in western North Carolina: U. S. Geol. Survey Prof. Paper 650-B, p. B1-B7.

Newton, R.C., Goldsmith, J.R., and Smith, J.V., 1969, Aragonite recrystallization from strained calcite at reduced pressures and its bearing on aragonite in low-grade metamorphism: Contr. Mineral. and Petrol., v. 22, p. 335-348.

Newton, R.C. and Kennedy, G.C., 1963, Some equilibrium reactions in the join $CaAl_2Si_2O_8$-$H_2O$: Jour. Geophys. Res., v. 68, p. 2967-2983.

Newton, R.C. and Kennedy, G.C., 1968, Jadeite, analcite, nepheline, and albite at high temperatures and pressures: Am. Jour. Sci., v. 266, p. 728-735.

Niggli, P., 1954, Rocks and mineral deposits: W.H. Freeman and Co., San Franciso, California, 559 p.

Nitsch, K.H., 1968, Die stabilitat von lawsonit: Naturwissenschaften, v. 55, p. 388.

O'Neil, J.R. and Ghent, E.D., 1975, Stable isotope study of coexisting metamorphic minerals from Esplanade Range, British Columbia: Geol. Soc. Am. Bull., v. 86, p. 1708-1712.

Oxburgh, E.R. and Turcotte, D.L., 1971, Origin of paired metamorphic belts and crustal dilation in island arc regions: Jour. Geophys. Res., v. 76, p. 1315-1327.

Payne, T.G., 1955, Mesozoic and Cenozoic tectonic elements of Alaska: U. S. Geol. Survey Misc. Geol. Investigations Map I-84.

Pearce, J.A. and Cann, J.R., 1971, Ophiolite origin investigated by discriminate analysis using Ti, Zr, and Y: Earth and Planetary Sci. Letters, v. 12, p. 339-349.

Pearce, T.H., Gorman, B.E., and Birkett, T.C., 1975, The $TiO_2$-$K_2O$-$P_2O_5$ diagram: A method of discriminating between oceanic and non-oceanic basalts: Earth and Planetary Sci. Letters, v. 24, p. 419-426.

Pessel, G.H. and Brosge, W.P., 1977, Preliminary reconnaissance geologic map of Ambler River quadrangle, Alaska: U. S. Geol. Survey Open-file Rept. 77-28.

Pessel, G.H., Eakins, G.R., and Garland, R.E., 1973a, Geology and geochemistry of the southeastern Ambler River quadrangle: Alaska Div. Geol. and Geophys. Surveys Annual Rept., 1972, p. 7-10.

Plafker, G., 1972, Alaskan earthquake of 1964 and Chilean earthquake of 1960: implications for arc tectonics: Jour. Geophys. Res., v. 77, p. 901-925.

Plas, L. van der and Tobi, A.C., 1965, A chart for judging the reliability of point counting results: Am. Jour. Sci., v. 263, p. 87-90.

Preto, V.A.G., 1970, Amphibolites from the Grand Forks quadrangle of British Columbia, Canada: Geol. Soc. Am. Bull., v. 81, p. 763-782.

Ramberg, H., 1973, The origin of metamorphic and metasomatic rocks: Univ. of Chicago Press, Chicago, Ill., 317 p.

Ray, D.K., 1967, Geochemistry and petrology of the Mt. Trident andesites, Katmai National Monument, Alaska: Unpublished Ph.D. thesis, Univ. of Alaska, Fairbanks, Alaska, 198 p.

Reed, B.L. and Lanphere, M.A., 1973, Alaska-Aleutian Range batholith: Geochronology, chemistry, and relation to circum-Pacific plutonism: Geol. Soc. Am. Bull., v. 84, p. 2583-2610.

Reed, B.L. and Lanphere, M.A., 1974, Chemistry variations across the Alaskan-Aleutian Range batholith: Jour. Res. U. S. Geol. Survey, v. 2, p. 343-352.

Reed, J.C. and Coats, R.R., 1941, Geology and ore deposits of the Chichagof mining district, Alaska: U. S. Geol. Survey Bull. 929, 148 p.

Rivalenti, G. and Sighinolfi, G.P., 1969, Geochemical study of graywackes as a possible starting material of para-amphibolites: Contr. Mineral. and Petrol., v. 23, p. 173-188.

Roever, W.P., de and Beunk, F.F., 1976, Blue amphibole-albite-chlorite assemblages from Fuscaldo (S. Italy) and the role of glaucophane in metamorphism: Contr. Mineral. and Petrol., v. 58, p. 221-234.

Roever, W.P., de and Nijhnis, H.J., 1963, Plurifacial alpine metamorphism in the eastern Betic Cordilleras, southeast Spain, with special reference to the genesis of the glaucophane: Geol. Rundschau., v. 53, p. 324-336.

Roubault, M., La Roche, H. de, and Govindaraju, K., 1968, Report (1966-1968) on geochemical standards: granites GR, GA, GH; basalt BR; ferriferous biotite mica-Fe; phlogopite mica-Mg: Sciences De La Terre, v. 13, p. 379-404.

Sainsbury, C.L., Coleman, R.G., and Kachadoorian, R., 1970, Blueschist and related greenschist facies rocks of the Seward Peninsula, Alaska: U. S. Geol. Survey Prof. Paper 700-B, p. B33-B42.

Sainsbury, C.L., Dutro, J.T., Jr., and Churkin, M., Jr., 1971, The Ordovician-Silurian boundary in the York Mountains, western Seward Peninsula, Alaska: U. S. Geol. Survey Prof. Paper 750-C, p. C52-C57.

Schilling, J.G., 1973, Afar mantle plume: Rare earth evidence: Nature, v. 242, p.2.

Scholl, D.W., Buffington, E.C., and Marlow, M.S., 1975, Plate tectonics and the structural evolution of the Aleutian-Bering Sea region, in Forbes, R.B., ed., Contributions to the geology of the Bering Sea basin and adjacent regions: Geol. Soc. Am. Special Paper 151, p. 1-31.

Shido, F., Miyashiro, A., and Ewing, M., 1971, Crystallization of abyssal tholeiites: Contr. Mineral. and Petrol., v. 31, p. 251-266.

Smith, J.P., 1906, The paragenesis of the minerals in the glaucophane-bearing rocks of California: Am. Philos. Proc., v. 45, p. 183-242.

Smith, P.S., 1910, Geology and mineral resources of the Solomon and Casadepage quadrangles, Seward Peninsula, Alaska: U. S. Geol. Survey Bull. 433, 234 p.

Smith, R.E., 1968, Redistribution of major elements in the alteration of some basic lavas during burial metamorphism: Jour. of Petrology, v. 9, p. 191-219.

Steinmann, G., 1927, Die ophiolitischem zonen in dem Mediterranean Kettengebirgen: Int. Geol. Congress, v. 14, p. 636-667.

Stewart, R.J., 1976, Turbidites of the Aleutian abyssal plain: mineralogy, provenance, and constraints for Cenozoic motion of the Pacific plate: Geol. Soc. Am. Bull., v. 87, p. 793-808.

Suhr, N.H. and Ingamells, C.O., 1966, Solution technigues for analysis of silicates: Anal. Chemistry, v. 38, p. 730-748.

Suppe, J. and Armstrong, R.L., 1972, Potassium-argon dating of Franciscan metamorphic rocks: Am. Jour. Sci., v. 272, p. 217-233.

Takeuchi, H. and Uyeda, S., 1965, A possibility of present-day regional metamorphism: Tectonophysics, v. 2, p. 59-68.

Taliaferro, N.L., 1943, Franciscan-Knoxville problem: Am. Assoc. Petroleum Geologists Bull., v. 27, p. 109-219.

Taylor, H.P., Jr., Albee, A.L., and Epstein, S., 1963, $O^{18}/O^{16}$ ratios of coexisting minerals in three assemblages of Kyanite-zone pelitic schist: Jour. Geol., v. 71, p. 513-522.

Taylor, H.P., Jr. and Coleman, R.G., 1968, $O^{18}/O^{16}$ ratios of coexisting minerals in glaucophane-bearing metamorphic rocks: Geol. Soc. Am. Bull., v. 79, p. 1727-1756.

Thompson, G., Shido, F., and Miyashiro, A., 1972, Three element distributions in fractionated oceanic basalts: Chem. Geol., v. 9, p. 89.

Toksoz, M.N., Minear, J.W., and Julian, B.R., 1971, Temperature field and geophysical effects of a downgoing slab: Jour. Geophys. Res., v. 76, p. 1113-1138.

Turner, D.L., 1978, Early Jurassic plutonism in the western Kenai Peninslua: An extension of the Kodiak-Afognak-Barren Islands plutonic trend: Alaska Div. Geol. and Geophys. Surveys Geol. Rept., (in press).

Turner, D.L. and Forbes, R.B., 1978, Geochronology of the southwestern Brooks Range: Alaska Geol. Society Symposium Proceedings.

Turner, D.L., Forbes, R.B., and Mayfield, C., 1978, K-Ar geochronology of the Survey Pass, Ambler River, and eastern Baird Mountains quadrangles, southwestern Brooks Range, Alaska: U. S. Geolvey Open-file Rept., (in press).

Turner, F.J., 1968, Metamorphic petrology: McGraw-Hill, New York, 403 p.

Turner, F.J. and Verhoogen, J., 1960, Igneous and metamorphic petrology, 2nd Ed.: McGraw-Hill, New York, 694 p.

Ulrich, E.O., 1904, Fossils and age of the Yakutat formation: Harriman Alaska Expedition, v. 4, p. 125-146.

Vallance, T.G., 1960, Concerning spilites: Proceedings of the Linnean Society of New South Wales, v. 85, p. 8-52.

Vallance, T.G., 1965, On the chemistry of pillow lavas and the origin of spilites: Mineral. Mag., v. 34, p. 471-481.

Vallance, T.G., 1969, Spilites again: some consequences of the degradation of basalts: Proceedings of the Linnean Society of New South Wales, v. 94, p. 8-51.

Vallance, T.G., 1974, Spilitic degradation of a tholeiitic basalt: Jour. of Petrology, v. 15, p. 79-96.

van Alstine, R.E., 1971, Amphibolites near Salida, Colorado: U. S. Geol. Survey Prof. Paper 750-B, p. B74-B81.

Vance, J.A., 1968, Metamorphic aragonite in prehnite-pumpellyite facies, northwest Washington: Am. Jour. Sci., v. 266, p. 299-315.

van de Kamp, P.C., 1969, Origin of amphibolites in the Beartooth Mountains, Wyoming and Montana--New data and interpretation: Geol. Soc. Am. Bull., v. 80, p. 1127-1136.

Vereschagrin, V.N., Kinasov, V.P., Paraketsov, K.V., and Terekhova, G.P., 1965, Polevoi Atlas, Melovoi fauni Servo-Vostoka U.S.S.R.: Magadan, Gosudarst Proizvodst. Geol. Dom. RSFSR, Servero-Vostoch Geol. Upravlenie, 66 p.

Von Huene, R., 1972, Structure of the continental margin and tectonism at the eastern Aleutian trench: Geol. Soc. Am. Bull., v. 83, p. 3613-3626.

Wager, L.R. and Brown, G.M., 1967, Layered igneous rocks: W.H. Freeman and Co., San Francisco, California, 588 p.

Wager, L.R. and Deer, W.A., 1939, Geological investigations in east Greenland, Part III: The petrology of the Skaergaard intrusion, Kangerdlugssuag, east Greenland: Medd. om Gronland, v. 105, 352 p.

Wahlstrom, E.E., 1969, Optical crystallography, 4th Ed.: John Wiley and Son, New York, 489 p.

Washington, H.S., 1901, A chemical study of the glaucophane schists: Am. Jour. Sci., v. 11, p. 35-59.

Wilkinson, J.F.G., 1974, The mineralogy and petrography of alkali basaltic rocks, in Sørensen, H., ed., The alkaline rocks: John Wiley and Son, New York, p. 67-95.

Williams, H., 1935, Newberry volcano of central Oregon: Geol. Soc. Am. Bull., v. 46, p. 253-304.

Wiltse, M.A., 1975, Geology of the Arctic Camp prospect, Ambler River quadrangle, Alaska: Alaska Div. Geol. and Geophys. Surveys Open-file Rept. 60, 41 p.

Winkler, H.G.F., 1967, Petrogenesis of metamorphic rocks, 2nd Ed.: Springer-Verlag, New York, 237 p.

Yen, T.P., 1966, Glaucophane schist of Taiwan: Geol. Soc. China Proc., v. 9, p. 70-73.

Yoder, H.S. and Tilley, C.E., 1962, Origin of basalt magmas; An experimental study of natural and synthetic rock systems: Jour. of Petrology, v. 3, p. 342-532.

Zimmermann, H.D., 1971, Equilibrium conditions of the calcite/aragonite reaction between 150° C and 350° C: Nature (Phys. Sci.), v. 231, p. 203-204.